VOL. 258 OCTOBER 1960 No. 8

American Journal of Science

Established in 1818 by Benjamin Silliman

EDITORS
JOHN RODGERS—JOSEPH T. GREGORY

ASSOCIATE EDITORS

GEORGE GAYLORD SIMPSON, CAMBRIDGE, MASS.
A. F. BUDDINGTON, PRINCETON, N. J.
CARL O. DUNBAR
HENRY MARGENAU
HORACE WINCHELL
EDWARD S. DEEVEY, JR.
MATT WALTON
RICHARD F. FLINT
HAROLD G. CASSIDY
G. EVELYN HUTCHINSON
NEW HAVEN, CONN.
WILMOT H. BRADLEY, PHILIP H. ABELSON
WASHINGTON, D. C.
LEASON H. ADAMS, LOS ANGELES, CALIF.
HOWEL WILLIAMS, BERKELEY, CALIF.
C. R. LONGWELL, PALO ALTO, CALIF.
ADOLPH KNOPF, STANFORD, CALIF.
FREDERICK J. ALCOCK, OTTAWA, CANADA
CECIL E. TILLEY, CAMBRIDGE, ENGLAND

STERLING TOWER
YALE UNIVERSITY
NEW HAVEN, CONNECTICUT

Published 10 times a year. Ten dollars a year. One dollar twenty-five cents a copy.
Foreign, ten dollars sixty cents. Canada, ten dollars thirty-five cents.

AMERICAN JOURNAL OF SCIENCE

Established in 1818 by Benjamin Silliman

THE FIRST SCIENTIFIC JOURNAL IN THE UNITED STATES

DEVOTED TO THE GEOLOGICAL SCIENCES AND TO RELATED FIELDS

Editors: JOHN ROGERS—JOSEPH T. GREGORY
Managing Editor: BETH A. BROMBERT

Entered as second-class matter at the Post Office at New Haven, Conn., under the Act of March 3, 1879. Published monthly, except July and September, at Sterling Tower, Yale University, New Haven, Conn.

Subscription rate $10 per year ($1.25 a number). Student rate $5 per year (application blanks available on request). Postage prepaid to the United States; 35 cents per year to Canada; 60 cents per year elsewhere.

The JOURNAL completed its *first* series of 50 volumes in 1845, its *second* series of 50 volumes in 1870, its *third* series of 50 volumes in 1895, its *fourth* series of 50 volumes in 1920, its *fifth* series of 36 volumes in 1938. Since 1938 the numbering by series has been discontinued, and volumes are annual and bear the whole numbers as of 1818, that for 1939 being volume 237.

Back numbers and volumes, also cumulative indices of all series, may with few exceptions be obtained from the office of the AMERICAN JOURNAL OF SCIENCE, Sterling Tower, New Haven, Conn. Positive microfilm copies of each complete volume may be purchased by subscribers to the paper edition from *University Microfilms*, 313 N. First St., Ann Arbor, Michigan. Regular subscribers may purchase each past year in microcard form, from *The Microcard Foundation*, Wesleyan University, Middletown, Connecticut.

INSTRUCTIONS TO CONTRIBUTORS

Typescripts of articles submitted should be double-spaced, should follow the recommendations in the pamphlet *Suggestions to Authors*, 5th ed. (see below), and should be preceded by brief abstracts. They should be checked with special care before being submitted, to avoid changes in proof other than printer's errors.

References to literature should be listed alphabetically by authors at the end of the article; all references should be complete. For articles in journals or other serial publications, the reference should give in order: Author's name, year of publication, full title; name of periodical or series, volume number, inclusive pages. For books or other unnumbered publications, it should give: Author's name, years of publication, full title; place of publication, publisher. This form follows the recommendations in the pamphlet "Abbreviations used in publications of the U. S. Geological Survey", which is also the standard used for abbreviating names of periodicals, etc. Citations within an article should be to author and year, with specific pages wherever appropriate.

Plates (photographs), *figures* (line drawings), and *footnotes* should each be numbered consecutively through each article, using arabic numerals. If two photographs form one plate, they are figures 1 and 2 of that plate.

Illustrations should be neat and legible and should include explanations of symbols used. Copy that cannot be reproduced cannot be accepted. Plates and figures should be capable of reduction to not more than 4 by 7 inches, all lettering being at least 1/16th inch high after reduction. When necessary, one large map or table can be accepted, if it will not exceed 7 inches in width after reduction. Line drawings should be in black India ink on white drawing board, tracing cloth, or coordinate paper printed in blue. Photographs should be positive glossy prints. Photostatic and typewritten material cannot be accepted as copy for illustrations.

Reprints. Thirty separate copies of each article will be furnished to the author free of cost and without previous notice from him; these will be without a cover. Additional copies will be furnished at cost, which will of course be greater if the article is accompanied by plates involving unusual expense. Copies will be furnished with a printed cover giving the title, author, volume, page, and year, when specially ordered.

Suggestions to Authors of the Reports of the United States Geological Survey. 5th ed. Washington, D. C., 1938 (Government Printing Office, $1.75).

[American Journal of Science, Vol. 258, October 1960, P. 529-547]

American Journal of Science

OCTOBER 1960

REGRESSIONS OF PHYSICAL PROPERTIES ON THE COMPOSITIONS OF CLINOPYROXENES
I. LATTICE CONSTANTS

HORACE WINCHELL and ROBERT TILLING

Department of Geology, Yale University, New Haven, Connecticut

ABSTRACT. The compositions of clinopyroxenes are represented by nine variables that may be referred to the formula ABC_2O_6, as follows: $x_1 = (Si)_c$, $x_2 = (Al, Fe''', Ti)_b$, $x_3 = (Mg)_b$, $x_4 = (Fe, Mn)_a$, $x_5 = (Ca)_a$, $x_6 = (Al, Fe''')_c$, $x_7 = (Fe, Mn)_b$, $x_8 = (Mg)_a$, $x_9 = (Na, K)_a$; among these the last four (x_6 . . x_9) are considered dependent upon the others by reasons of space-availability and valence. Regressions of the lattice constants a, b, c, and β have been calculated by least squares for 12 specimens of clinopyroxene covering the system diopside-hedenbergite-clinoenstatite-clinohypersthene-pigeonite-augite-jadeite, published by various authors between 1949 and 1956. The maximum difference between observed and calculated values of the linear constants is 0.011 angstrom; of the angular constant, 18 minutes of arc. The standard errors for these regressions are 0.0085, 0.0098, 0.0083 A. for a, b, and c, and 12 minutes for β, respectively. More data are needed to test those regressions and improve them, but the evidence suggests that the entire clinopyroxene system can be represented by such linear regressions.

INTRODUCTION

Graphical methods are well established in the mineralogical literature dealing with the relations between chemical composition and physical properties such as lattice and optical constants, and specific gravity, but few attempts have been made to elucidate such relations in generalized systems where more than two or three independent variables can be considered. Variation diagrams relating optical properties and chemical composition are very well known. Troeger (1956) and Winchell and Winchell (1951) gave extended summaries of such diagrams, and more are being published every year. Similar diagrams may be used to relate lattice constants to composition; a few are given by Winchell and Winchell, and more of this type also are being published every year (e.g., Donnay, et al., 1959).

Attempts to include more than two independent variables of composition in graphical solutions have had varying success, especially for systems involving few physical constants and more chemical variables; in such instances it may be convenient to plot the physical measurements along the coordinate axes and show the overlapping fields representing chemical compositions that correspond to given sets of physical constants (Ford, 1915; Winchell, 1958). Mertie (1949) described methods for charting five or six variables in the bounding tetrahedra and triangles of an n-dimensional hypertetrahedron, but we know of no published example of the use of his methods.

ACKNOWLEDGMENTS

We acknowledge with sincere thanks the work of members of the advanced mineralogy class of 1958-59 at Yale University, for their efforts in

collecting and checking data. The aid of Professor Alan T. James of the Department of Mathematics has been invaluable to us in interpretation of the results and in their discussion. One of us (R.T.) spent many hours with a desk computer early in 1959; later computation was carried out, and all results were checked, through the courtesy and cooperation of the Yale University Computing Center, using a program written by Harold Watts for the IBM 650 digital computer. To all these our thanks. We are indebted to Dr. G. M. Brown of Oxford University for calling our attention to analysis 326, and to Professor H. H. Hess of Princeton University for some significant improvements in the discussion.

REGRESSION THEORY

Many physical properties that are commonly used in mineralogical and petrological studies are related simply to the chemical variations within mineral systems. The most useful relations are given by linear formulas such as the following:

$$y = a + b_1x_1 + b_2x_2 + \ldots, \text{etc.}, \pm s$$

which may be written more compactly thus:

$$y = \Sigma\, b_ix_i \pm s$$

where b_0 is the constant term a of the first equation, ($x_0 = 1$, a "pseudo-variable"), the remaining b_i and x_i are respectively the partial regression coefficients, and the independent variables, i in general designating which chemical element or group of elements is concerned with each term of the summation, and s is the standard error of regression. If we are interested in several dependent variables, as the several lattice constants, refractive indices, etc., we may designate these by y_p, and the entire set of equations is represented by the following:

$$y_p = \Sigma\, b_{ip}x_i \pm s_p\,.$$

The x_i are usually expressed as relative numbers (not weights) of the different kinds of atoms of type i, but number percentages and weight percentages are also occasionally used. Terms in x_i^2 or in x_ix_j, or in x_i^3, etc., may be needed if there is curvature in the relation of y_p to x_i, but for many minerals the range of y is small, and the coefficients of these higher powers of x_i are also very small, and empirically valid results may be obtained without such higher powers of x.

Henriques (1958b) calculated 22 regression coefficients for 2V and for each of the three refractive indices of ordinary clinopyroxene, using 11 chemical variables and their squares as the 22 independent variables; only 8 or 9 of the 22 parameters for each refractive index-regression, and only two for the regression of 2V, turned out to be larger than their respective standard deviations. Part of the reason for this unsatisfactory result may be his use of 39 samples covering only the "ordinary" clinopyroxenes without much alkali-metal content, but part may be due to an intrinsically small departure of the relations from linearity.

"Least-squares" procedures for obtaining the particular set of b_{ip} that minimizes the sum of the squared residuals, $\Sigma(y_{obs.}-y_{calc.})^2$, are well known (Fisher, 1958; Acton, 1959; and many other references on statistics). Esti-

mates s_{ip} of the standard deviations of the regression coefficients b_{ip} are also available; the "multiple coefficient of determination," R^2, as well as other statistics can be used for measuring the general significance of the regression: qualitatively, $0 \leqslant R^2 \leqslant 1$, and the closer it is to unity, the better the regression can be considered.

TABLE 1

Analyses of clinopyroxenes, ABC_2O_6, recast as atoms per 6000 oxygen, showing assignment to formula-positions A, B, C, and symbols x_i used in computation

Symbol	Element (position)	Analysis number 186	266	242	250	247	244	283	245	181	292	326	293	294
x_1	Si(C)	1988	1990	1851	1930	1903	1911	1986	1906	1956	2000	1902	1990	2000*
	Al(C)	12	10	149	33	28	89	14	94	18	0	98	10	0
	Fe'''(C)	0	0	0	37	69	0	0	0	26	0	0	0	0
x_2	Al(B)	3	40	65	0	0	5	3	19	0	0	49	942	0
	Fe'''(B)	47	14	22	76	37	27	11	18	5	0	41**	13	8
	Ti(B)	2	2	11	19	21	22	1	7	7	0	13	3	0
x_3	Mg(B)	64	334	827	905	942	917	932	956	988	1000	897	42	60
	Fe"(B)	788	610	75	0	0	29	53	0	0	0	0	0	34
	Mn(B)	96	0	0	0	0	0	0	0	0	0	0	0	898
	Mg(A)	0	0	0	4	1	0	0	23	317	1000	31	12	0
x_4	Fe"(A)	0	0	108	760	576	179	19	425	522	0	113	7	0
	Mn(A)	35	6	0	80	25	7	5	14	18	0	4	2	50
x_5	Ca(A)	938	961	903	132	392	794	971	574	160	0	807	55	976
	Na(A)	12	14	13	0	28	22	4	0	13	0	26	882	0
	K(A)	0	0		0	5	9	2	0	0	0	1	27	0
	Sum	3985	3981	4024	3976	4027	4011	4001	4036	4030	4000	3982	3985	4026

* Author states that impurities were present; analysis recast on basis of 2000 Si instead of the usual 6000 Oxygen atoms;
** Includes 26 Cr.

Sources: 186, Hedenbergite, Herault, Calif. (Hess, 1949, no. 18; Kuno and Hess, 1953, no. 6); 266, Ferrosalite, Whiteface Anorthosite, Adirondacks, N. Y. (Hess, 1949, no. 16; Kuno and Hess, 1953, no. 5); 242, Salite, Taga Volcano, Japan (H. Kuno, 1955, no. 1); 250, Ferropigeonite, Hakone Volcano, Japan (Kuno, 1955, no. 15); 247, Subcalcic Augite, Mihara-yama Crater, O-sima, Japan (Kuno, 1955, no. 9); 244, Augite, Hakone Volcano, Japan (Kuno, 1955, no. 5); 283, Diopside, Colton, St. Lawrence Co., N.Y. (Hess, 1949, no. 35; Kuno, 1955, table 6); 245, Pigeonitic Augite, Taga Volcano, Japan (Kuno, 1955, no. 6); 181, Pigeonite, Hakone Volcano, Japan (Kuno and Nagashima, 1952, no. 3; Kuno and Hess, 1953, no. 2); 292, Clinoenstatite, synthetic, "from [W. R.] Foster" (Kuno and Hess, 1953, no. 1); 326, Diopside, Rhum, Inner Hebrides (Brown, 1956); 293, Jadeite, Cloverdale, Calif. (Wolfe, 1955); 294, Johannsenite, Monte Civillina, Vicenza, Italy (Schiavinato, 1953).

REGRESSIONS IN MINERAL SYSTEMS

Hey (1956) described the use of partial regression equations in relating the physical properties of mineral systems to their chemical compositions, and illustrated the work by means of a set of selected superior data on the antho-

phyllite series (orthoamphibole). Hori (1954; 1956) and Henriques (1958a, b, c) used the method for a study of the optical properties of ortho-, and clinopyroxenes. This method, or some other algebraic-analytical method, seems to be the only practical way of elucidating the relationships between physical and chemical properties in complex systems. As Hey pointed out, the least-squares regressions of physical on chemical data are not particularly well adapted for predicting the composition that would most likely give an observed set of physical data. Such purpose is approached, however, if we use for comparison a set of known observational data fairly close to those of the unknown material, and find the changes in physical data that would be expected from postulated changes in the chemical data. This is likely to be necessary anyway, because there are usually many more chemical than physical variables, which means that there would be, in principle, a few equations having more than a few chemical variables—an indeterminate situation indeed.

The limitation in applicability of the regressions may be explained using a simplified example: Consider a system with two variates x and y. If y is treated as dependent upon x, we obtain a formula expressing the "regression of y on x," $y = a + bx \pm s_y$, where a and b are constants that define a line in the x-y plane, and s_y is the standard deviation of the calculated y, measured by, and expressing, the y-component of the scatter of the plotted points (x,y) about that line. The proper equation for finding the most probable value of x from a given observation of y is the "regression of x on y," $x = c + dy \pm s_x$, wherein the standard-deviation term shows the x-component instead of the y-component of scatter. The two lines $y = a + bx$ and $x = c + dy$ both pass through the point $(\bar{x},\bar{y})$ of our graph corresponding to the means of all the observed values of x and of y, but with different slopes because each treats the deviation of the dependent variable from its own mean as due only in part to the deviation of the other variable from its mean: the other part (s) is due to random "statistical" variations of the dependent variable. Thus the two lines $y = a + bx$, and $x = c + dy$, are identical and coincident only if $s_y = s_x = 0$. The regression of y on x treats all errors as belonging to y; that of x on y conversely. Unfortunately the arithmetic of treating the data as if both x and y contain errors is considerably more involved. For the present problem we therefore treat the errors in x (chemical variables) as if they were negligible in comparison with those in y (physical variables); this treatment secures a further arithmetical advantage because there are more chemical than physical variables, even after the rather drastic simplifications that we make in combining certain minor elements with more abundant ones that presumably have similar effects on the physical properties.

In mineralogical and petrological work there is ordinarily external evidence such as paragenesis, metamorphic facies, etc., on which to base a preliminary estimate of the chemical variables x, so that calculated values of the physical variables y can be determined *a priori* for comparison with the observed ones. Individual regression coefficients can properly be used in making that comparison.

The failure of regression theory to fit the mineralogical facts in the assumption that the independent variables are free of significant error should be

considered later on the basis of more data.

The assumption of normal distribution of the variables about their respective means, required in regression theory, is perhaps not valid for mineralogical systems, but this seems to be not very critical (Acton, 1959, chapter 2).

DATA AND RESULTS

There appear to be only 11 analyzed specimens of ordinary clinopyroxene, plus one jadeite and one johannsenite, that have been studied by x-ray methods to determine with assurance the unit cell constants of the actually analyzed material. Optical data for these are also available. A few others have been rejected because of doubtful identity of the material analyzed with that studied physically. The 13 specimens thus selected are listed in table 1, together with their analyses, recast in the form of numbers of metal atoms relative to 6000 oxygen. These relative numbers of atoms are distributed according to the order of increasing ionic radius in the positions C, B, and A, of the pyroxene formula ABC_2O_6. We thus assume a completely ordered distribution of the elements in these positions even though that is known to be partially untrue for pyroxenes crystallized at high temperatures. It is another of our simplifying assumptions that need further data for investigation.

For calculating regression constants it is necessary to have "independent" variables x that are not linearly related to one another. In the present system some of the chemical variables are obviously so related. Thus the sum of the atoms in position C is exactly 2; that for position B is 1, and that for A should be 1 but in fact is not; moreover, the sum of the valences of all atoms A, B, and C, is exactly 12 to balance the assumed 6 oxygens. Because the sum of $Si)_C + Al)_C + Fe''')_C$ is limited to two by the crystal structure expressed in the formula ABC_2O_6, we must reject one of these components as dependent upon the others. Also, ferric iron and Ti are minor components, and because their sizes and charge are nearly the same as those of Al, they are grouped with Al in table 1; similarly, several others of the fifteen composition-components in the same table have been grouped, reducing the number to 9. Five of these may be selected in several ways as the independent variables to be used in the regressions. The five actually selected are designated by the x_i (x_1, x_2, etc.) in the left column of table 1. Except for a small error introduced by grouping tetravalent Ti with trivalent $(Al,Fe)_b$, the number of B and C spaces available plus the requirement of electrical neutrality plus the numerical values of the x_i may be combined to determine uniquely the amounts of each cation-group shown in brackets in table 1. The error due to tetravalent Ti grouped with trivalent elements would be smaller if some of the Ti is actually trivalent. This error and the deviation from 2, of the total number of atoms in A, are disregarded.

The physical constants y_p of the same specimens are given in table 2, and the regression coefficients b_{ip} relating the lattice constants y_p to the chemical components x_i are given, together with standard deviations s_{ip} of b_{ip}, and s_p of the regressions, and certain statistics for evaluating reliability, in tables 3, 4, and 5. The ordinary lattice constants $abc\beta$ given in table 2 were used to

TABLE 2

Physical properties of analysed specimens in table 1

	Analysis number												
	186	266	242	250	247	244	283	245	181	292	326	293	294
$y_1 = a$	9.854	9.804	9.742	9.712	9.716	9.744	9.750	9.722	9.692	9.618	9.734	9.50	9.81
$y_2 = b$	9.024	8.980	8.901	8.959	8.944	8.909	8.930	8.925	8.917	8.828	8.907	8.61	9.02
$y_3 = c$	5.263	5.259	5.268	5.251	5.242	5.260	5.249	5.242	5.239	5.186	5.246	5.24	5.26
$y_4 = a'[101]$	9.956	9.833	9.607	9.458	9.537	9.667	9.731	9.597	9.438	9.380	9.698	9.37	9.86
$y_5 = \beta$	75°40′	74°46′	73°55′	71°27′	72°20′	73°28′	74°10′	72°57′	71°27′	71°38½′	73°51′	72°34′	75°
$y_6 = \beta'$	73 32	74 09	77 00	76 47	76 05	75 05	74 34	75 35	76 48	76 42	74 36	75 12	74
G_{obs}	3.535	3.413					3.281				(3.33)	3.245	3.45
G_{calc}			3.361	3.58	3.517	3.358		3.429	3.524	3.19	3.341		
n_x	1.7225	1.7080	1.690	1.713	1.711	1.690	1.6718	1.691	1.695	1.651	1.6820	1.640	1.710
n_y	1.7300	1.7140	1.696	1.713	1.713	1.696	1.6785	1.697	1.698	1.652	1.6870	1.645	1.719
n_z	1.7505	1.7360	1.715	(*)	1.739	1.716	1.7013	1.718	1.722	1.661	1.7092	1.652	1.738
$2V_x$	62.5°	59.75°	59°	11°	25°	51°	56.5°	44°	14°**	35°**	51°	67°	70°
Z:c	47.5°	43°***	3°			5°	39.5°	10°	42°	22°		40°	48°

Notes. *About 1.734 (graphical estimate); **X = b for nos. 181, 292 only, all others have Y = b; ***original says "43°?".

TABLE 3

Regression constants for unit cells of 11 ordinary clinopyroxenes Chemical formula ABC_2O_6; regression equation $y_p = \Sigma a_{ip}x_i \pm s_p$

	i	0	1	2	3	4	5			
	x_i	constant	Si)$_c$	Al $+Fe'''$ $+Ti$)$_b$	Mg)$_b$	Fe'' $+Mn$)$_a$	Ca)$_a$	(5 variables, 5 degrees of freedom)		
	$\bar{x}$	1.000	1.938	0.053	0.797	0.263	0.603			
	s_x	0.000	.486	.035	.305	.291	.370			
p	y_p $\bar{y}$ s_y			b_{ip} s_{ip}				s_p	R^2	F-ratio
1	a	9.735	9.606	+.066*	−.086*	−.118	+.092	+.126			
		.060	.230	.110	.132	.014	.014	.012	.0083	.990	102.10
2	b	8.929	8.348	+.294	−.033*	−.108	+.160	+.095			
		.050	.154	.073	.089	.010	.009	.008	.0056	.994	158.07
3	c	5.246	5.350	−.071*	+.007*	−.019	+.052	+.058			
		.022	.258	.123	.148	.016	.016	.014	.0094	.909	10.09
4	a′	9.627	8.171	+.710	+.115*	−.213	+.081	+.368			
		.174	1.245	.594	.716	.078	.075	.067	.0451	.966	28.76
5	β	4394.	4420.	− 12.*	− 4.*	−100.	− 43.	+149.			
		85.	389.	186.	224.	24.	24.	21.	14.	.986	70.93
6	β'	4532.	6443.	−926.	−282.*	+13.*	− 42.*	−165.			
		73.	1264	603.	726.	79.	76.	68.	46.	.804	4.11

TABLE 3a.

Regression constants for unit cells of 10 ordinary clinopyroxenes.
(Compare with table 3 to see effect of deleting Analysis No. 326.)

		i	0	1	2	3	4	5			
		$\bar{x}$ s_x	1 0	1.942 .050	0.049 .034	0.787 .320	0.278 .303	0.582 .384	(5 variables, 4 degrees of freedom)		
p	y_p	$\bar{y}$ s_y	b_{ip} s_{ip}						s_p	R^2	F-ratio
1	a	9.735 .065	9.687 .262	+.026* .125	−.184 .182	−.125 .017	+.097 .016	+.126 .013	.0088	.991	91.09
2	b	8.932 .052	8.427 .167	+.257 .079	−.128 .116	−.115 .011	+.165 .010	+.095 .008	.0056	.995	152.67
3	c	5.246 .023	5.264 .288	−.031* .137	+.108* .199	−.012* .019	+.046 .018	+.058 .014	.0097	.922	9.52
4	a′	9.620 .182	8.964 1.054	+.342* .501	−.827 .730	−.280 .070	+.131 .064	+.369 .053	.0355	.983	46.44
5	β	4391′ 88′	4579′ 420.	− 86.* 200.	−192. 291.	−113. 28.	− 33. 26.	+149. 21.	14′	.989	69.06

compute the translation a′[101] and the angle $\beta' = c:a'$ for comparisons. By using the homogeneous set abca′ we hoped that more useful comparisons would be possible than with the conventional set abcβ. This hope was not justified by the results. The length of a′[101] is nearly equal to that of the usual axis a, and in working with x-ray powder data the two can be confused. It is therefore expedient to quote the data for a′[101] even though their accuracy is of a lower order. The spacing d(100) = a sin β probably would have been more useful.

Table 3 contains two sections which illustrate the smallness of changes produced by an increase of 10 percent in the amount of data—one section based upon the first 11 ("ordinary") clinopyroxenes, and the other (computed before analysis 326 was available) based upon only the first 10. The differences between corresponding coefficients in these tables are well within the estimated standard deviations in all cases, and we conclude that the addition of analysis 326 produced only a small improvement in our confidence in the results obtained, without significantly changing any of the results.

The johannsenite analysis, no. 294, seems to be less reliable than the others, both from its author's discussion, and from a regression study using it. The impurities reported by the author make it impossible to recast this analysis on the same basis as the others without very dubious assumptions. The basis actually tried ($Si_c = 2000$) gives results inconsistent with those of the other 12 analyses, and the johannsenite was reluctantly discarded. Proper use of it requires an additional variable, x_6, to represent Mn, and may therefore be undesirable in a study using so few data.

Tables 4 and 5 contain data based on the 12 analyses in tables 1 and 2, excluding only the johannsenite, no. 294. In table 4 the b_{ip}, describing the effects of $Si)_c$, seem to have rather too large standard errors s_{ip}. We therefore eliminated $Si)_c$ as a significant independent variable for estimating a, c, and β (note starred entries in table 4), to determine whether improved relations can be obtained with one less x. The s_p, R_p^2, and F-ratios thus obtained do not indicate much improvement, but at the same time, most of the individual regression constants b_{ip} have somewhat smaller standard errors s_{ip}, and consequently larger (better) t-ratios. It seems therefore probable that such elimination is desirable, and the constants in table 5 are presented as probably the best all-inclusive set now available for estimating lattice constants of clinopyroxenes containing significant amounts of the jadeite component. These data are not to be used for acmitic pyroxenes. Table 3, on the other hand, is probably slightly better for "ordinary" non-sodic clinopyroxenes. Certainly much greater confidence would be possible if a greater number, and a greater range, of analyses could be incorporated into the data.

Table 6 contains the residuals [y(obs.) − y(calc.)], or differences between observed and estimated values of the cell constants for the relevant analyses. Generally good predictions are possible for all cell constants except a′ and β', and the suspicion is inescapable that these exceptional ones must have greater errors in table 2 than the other cell constants abcβ. The same suspicion is of course evident from an inspection of the estimated standard deviations s_p in tables 3, 4, and 5.

TABLE 4

Regression constants for unit cells of 12 clinopyroxenes listed in tables 1-2 (excluding johannsenite, no. 294; see text)

	i	0	1	2	3	4	5			
	$\bar{x}$	1.000	1.943	0.129	0.734	0.242	0.557	(5 variables, 6 degrees of freedom)		
	s_x	.000	.049	.263	.363	.288	.387			
	y_p	$\bar{y}_p$	b_{ip}					s_p	R^2	F-ratio
		s_y	s_{ip}							
1	a	9.716	9.805	−.030*	−.258	−.126	+.096	+.128	.0097	.994	184.84
		.089	.201	.095	.021	.015	.016	.014			
2	b	8.903	8.716	+.117	−.353	−.123	+.168	+.100	.0098	.995	244.20
		.104	.204	.097	.021	.015	.016	.014			
3	c	5.245	5.323	−.058*	+.031	−.018	+.051	+.058	.0085	.911	12.25
		.021	.177	.084	.018	.013	.014	.013			
5	β	4391.	4471.	− 37.*	− 49.	−102.	− 42.	+149.	13.	.986	85.78
		81.	270.	128.	28.	20.	21.	19.			

TABLE 5

Best overall regression constants for clinopyroxenes (including jadeite), that contain Na. Certain regression constants of table 4; others after removal of $x_1 = Si)_c$ from the independent variables.

		i	0	1	2	3	4	5			
		$\bar{x}$ s_x	1.000 .000		0.129 .263	0.734 .363	0.242 .288	0.557 .387	(4 variables, 7 degrees of freedom)		
	y_p	$\bar{y}_p$ s_y	b_{ip} s_{ip}						s_p	R^2	F-ratio
1	a	9.716 .089	9.742 .013	(0)	−.255 .015	−.124 .010	+.099 .011	+.131 .009	.0085	.994	297.05
2	b	8.093 .104	8.716 .204	+.117 .097	−.353 .021	−.123 .015	+.168 .016	+.100 .014	.0093	.995	(244.20)*
3	c	5.245 .021	5.201 .013	(0)	+.038 .015	−.012 .010	+.056 .011	+.063 .009	.0083	.902	16.09
5	β	4391. 81.	4393. 18.	(0)	− 44. 21.	− 98. 15.	− 38. 16.	+153. 13.	12.	.986	124.64

* 12 observations; 5 variables, 6 degrees of freedom.

TABLE 6

Differences between observed and estimated unit-cell dimensions.
D = y(obs.) — y(calc.).

y	186	265	242	250	247	244	283	245	181	292	326	293	s_D (*)
	(Using regression constants from table 3)												
a	.007	-.011	-.004	.000	-.004	.008	.000	-.006	.005	-.002	.005		.0083
b	.005	-.007	-.002	-.002	.007	-.005	.003	-.003	-.001	.000	.005		.0056
c	-.001	.000	.007	.004	-.009	.007	.000	-.010	.010	-.003	-.005		.0094
a'	.033	-.041	-.055	-.018	.015	.021	-.013	.024	-.016	.001	.049		.0451
β	13.	-18.	- 9.	- 2.	6.	- 7.	4.	10.	-11.	3.	10.		14.
β'	-19.	20.	62.	24.	-21.	-26.	24.	-29.	17.	- 1.	-50.		46.
	(Using regression constants from table 4)												
a	.005	-.009	-.004	.006	-.006	.006	-.001	-.010	.001	-.001	.011	-.001	.0097
b	.003	-.004	-.002	.009	.003	-.008	.002	-.011	-.008	.002	.016	-.001	.0098
c	-.001	.000	.007	.003	-.009	.008	.000	-.010	.010	-.003	-.006	.000	.0085
a'	.030	-.037	-.056	-.006	.011	.017	-.015	.015	-.024	.004	.062	-.002	.0422
β	13.	-18.	- 9.	0.	5.	- 7.	4.	9.	-12.	3.	11.	0.	13.
β'	-18.	17.	63.	17.	-18.	-24.	25.	-24.	21.	- 3.	-57.	1.	42.
	(Using regression constants from table 5)												
a	.007	-.009	-.002	.006	-.006	.006	-.003	-.009	.001	.000	.012	-.001	.0085
b	.003	-.004	-.002	.009	.003	-.008	.002	-.011	-.008	.002	.016	-.001	.0098
c	.000	-.001	.011	.002	-.008	.008	-.004	-.010	.010	-.002	-.005	.000	.0083
β	13.	-18.	- 6.	- 1.	5.	- 7.	2.	9.	-12.	3.	12.	0.	12.

(*) Estimated standard deviations taken from tables 3, 4, and 5.

DISCUSSION

The regression coefficients b_{ip} in tables 3, 4, and 5 represent the amount of increase in the physical properties y_p for unit increase in the corresponding chemical components x_i. Thus for example we may calculate from b_{32} in table 5 the increase to be expected in axis b that would correspond to an increase of 10 percent (= 0.10) in the amount of octahedrally coordinated Mg as follows: (Increase in y_2) = $b_{32}\cdot$(Increase in Mg_B) = $(-0.123\cdot(0.100)$. In other words, increasing the $Mg)_B$ would *de*crease the axis b by 0.0123.

If interested in the effect of $Fe'')_B$, we must first express this component in terms of the independent variables x_i—in this case $Fe)_B = 1 - x_2 - x_3$. But the $Fe'')_B$ could not replace metals designated by x_2 without corresponding valence adjustments elsewhere, and as these are excluded by our question about the effect of increasing [only] $Fe'')_B$, we can take $Fe'')_B = 1-x_3$, so that a change in $Fe'')_B$ corresponds to an equal change of the opposite sign in $Mg)_B = x_3$, and its effect is computed accordingly.

The regression equations are all symbolized at the top of table 3 by the general formulas $y_p = \Sigma b_{ip}x_i \pm s_p$
which may be partially expanded as follows:

$$y_p = b_0 + b_{1p}x_1 + b_{2p}x_2 + \ldots . \pm s_p$$

where y_p represents in turn each of the lattice constants a, b, c, a′, β, and β' as defined in table 2, the b_{ip} are constants from tables 3, 4, or 5, and the x_i represent the relative numbers of certain metal atoms per six (not 6000) oxygen as defined in table 1. In every case the most probable value is $y_p = \Sigma b_{ip}x_i$, and s_p can be used with certain other data to set limits on y, as $Y_1 \leqslant y \leqslant Y_2$.

Example 1.—Estimate the c-axis of a hypothetical clinopyroxene $Ca(Mg_{.75}Fe''_{.25})Si_2O_6$. We use regression constants from table 3 because there is no Na present. The appropriate y_p is $y_3 = c$; we use the coefficients b_{i3} to write out the expanded equation for y_3 as follows:

$$c = y_3 = 5.350 - 0.071x_1 + 0.007x_2 - 0.019x_3 + 0.052x_4 + 0.058x_5.$$

The composition-variables are $x_1 = Si)_c = 2.000$, $x_2 = (Al,Fe''',Ti)_b = 0.000$, $x_3 = Mg)_b = 0.750$, $x_4 = (Fe'',Mn)_a = 0.000$ [not 0.75], $x_5 = Ca)_a = 1.000$. Substitution in the above equation yields the result, $c = 5.251$.

Example 2.—Present graphically the value of b so as to show the influence of the substitution of Al + Al for (Mg,Fe″) + Si in the diopside-hedenbergite series, $Ca(Mg,Fe'')Si_2O_6$. For convenience we may let u = amount of substitution of Al for (Mg,Fe″) and for Si, and v = the ratio of Fe″ to (Fe″+Mg). The lack of any terms in the second degree in the x's in our regression equations indicates that the lines should be straight, but we calculate a third point on one of the lines to help check the arithmetic. In this case we are concerned with $y_2 = b$, and we obtain from table 3 the coefficients of the x's for the regression equation,

$$b = 8.348 + 0.294x_1 - 0.033x_2 - 0.108x_3 + 0.160x_4 + 0.095x_5$$

We tabulate the x's for strategic values of u and v, and substitute in the regression equation to obtain the corresponding values of b.

		x_1	x_2	x_3	x_4	x_5	calc. b
v = 0, u = 0		.2	0	1	0	1	8.923
.5	0	.2	0	.5	0	1	8.977
1	0	.2	0	0	0	1	9.031
0	.1	1.9	.1	.9	0	1	8.901
1	.1	1.9	.1	0	0	1	8.998
0	.2	1.8	.2	.8	0	1	8.879
1	.2	1.8	.2	0	0	1	8.966

The first three rows of this table yield the points along the top line (u = 0) of figure 1; the next two determine the second line (u = .1); and the last two determine the lowest line (u = .2) of the figure. Similar diagrams can be plotted for other combinations of the independent variables, but no two-dimensional diagram can effectively show the variations of the several y's in terms of all five independent variables (x's).

Standard deviations of the several variables are estimated and recorded opposite the symbols s: s_{ip} is the standard deviation of b_{ip}; s_p is that of the regression as a whole. The s_x and s_y are the root-mean-square deviations of the several x's and y's from their respective means, $\bar{x}$ and $\bar{y}$. The ratio of any quantity q to its own estimated standard deviation, s_q is called Student's ratio and designated t. Statistical treatises (e.g., Fisher, 1958; Acton, 1959) generally contain descriptions of the use of Student's ratio to estimate whether a quantity is significantly different from zero. The meaning of "significantly" in this statement can be given precisely, but may be taken in terms of probability that the quantity b_{ip} in our problem should not (or should) be set equal to zero. For our problems, standard tables of t show that we will be right at least two-thirds of the time if we accept as significantly different from zero those quantities q for which $q/s_q > 1$—specifically, we accept b_{ip}, if $b_{ip}/s_{ip} > 1$. A commonly used, more conservative level (where, however, we would risk rather too frequent rejection of significant b_{ip}) would be $b_{ip}/s_{ip} > 2$, which for the 5 to 7 degrees of freedom in our problem would require significance in the b_{ip} about 90 percent out of all the times we might try the experiment.

Using the t-test at the level requiring $t > 1$, we reject the starred b_{ip} in table 4 and recompute the affected regressions only, obtaining the simpler, and at the same time slightly improved versions shown in table 5, where $x_3 = Si)_C$ is disregarded as having no effect on a, c, and β (p = 1, 3, and 5). The improvement is noted either in terms of increased t-ratios or in decreased s_p; it is also apparent (though small) in terms of the decreased residuals shown in table 6 for the corresponding regressions.

USE OF THE REGRESSIONS

We have already indicated in general terms the specific uses of the regressions here developed. Hey (1956) discussed this matter in reference to orthoamphiboles, and there is actually little to be added. We summarize the uses of our regressions as follows:

1. Estimating the unit-cell constants of clinopyroxenes
   a. "Ordinary" clinopyroxenes, without large amounts of jadeite, acmite, or johannsenite components, will best use the regression constants in table 3.
   b. Clinopyroxenes containing substantial amounts of jadeite-

component should be studied using the regression constants of table 5.

c. Long extrapolations into the fields representing high-acmite, or high-johannsenite varieties are not to be relied upon.

2. Estimating compositions that could produce a given set of lattice constants.

This is best performed by preliminary reference to table 2, to pick a composition that gives reasonably good agreement, followed by a study of changes that would change the lattice constants from those of this composition toward those of the unknown material under study. The regression coefficients are good estimators of the rate of change of lattice constant with change of composition in such a study.

3. Estimating lattice constants for compositions outside the ranges covered in table 1.

Extrapolation is generally not to be recommended except for

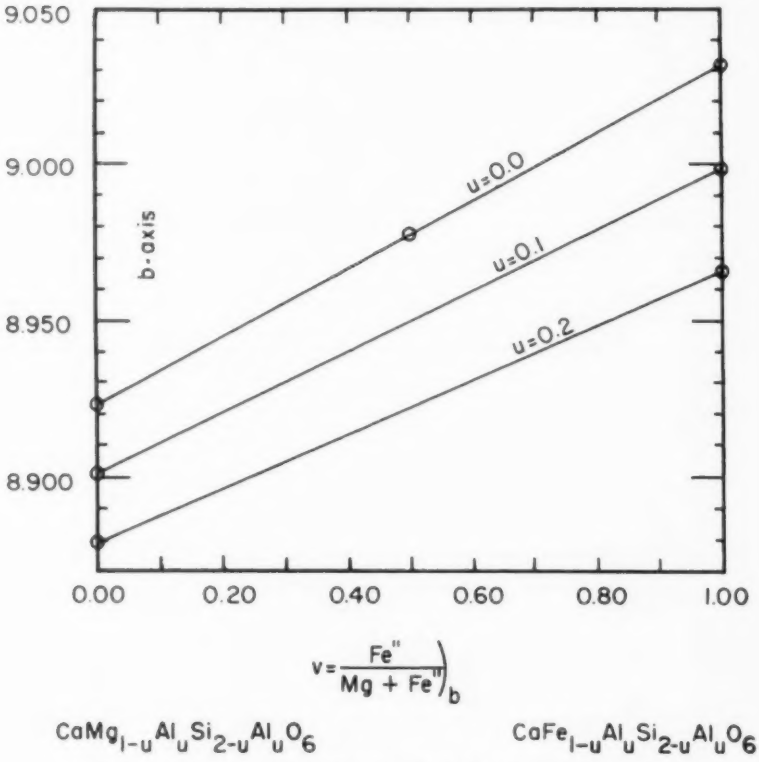

Fig. 1. Lattice constant b in a portion of the clinopyroxene system.

TABLE 7

Estimated values of y for interesting compositions not available in natural materials

Name	Composition: $(Si)_C = x_1$	$(Al\ Fe'''\ Ti)_B = x_2$	$(Mg)_B = x_3$	$(Mn, Fe)_A = x_4$	$(Ca)_A = x_5$	y—Calculated by regression*: a	b	c	β	y—Observed on synthetic material: a	b	c	β	References
Diopside	2	0	1	0	1	9.746	8.923	5.266	74°08′	9.743	8.923	5.251	74°04′	Sakata (1957)
Hedenbergite	2	0	0	0	1	9.864	9.031	5.074	75°46′	(near specimen 186, tables 1,2)				
Clinoenstatite	2	0	1	0	0	9.620	8.828	5.016	71°35′	9.618	8.828	5.186	71°38′	Kuno and Hess (1953)
Clinohypersthene	2	0	1	1	0	9.712	8.988	5.068	70°57′	9.69	8.95	5.25	< 71°27′	Kuno and Hess (1953)***
Clinoferrosilite	2	0	0	1	0	9.830	9.096	5.260	72°35′	9.7	9.1	?	71°±	Kuno and Hess (1953)***
Jadeite / Acmite****	2	1	0	0	0	9.486	8.596	5.238	73°09′					
Synthetic	1.8	0.2	0.8	0	1	9.739	8.879	5.128	74°27′	9.712	8.867	5.266	73°51′	Sakata (1957)
Synthetic**	1.6	0.4	0.6	0	1	9.732	8.835	5.182	74°45′	9.678	8.807	5.280	73°48′	Sakata (1957)

* Regression constants from table 3, except those for jadeite from table 5.

** Composition estimated by Sakata "up to about 40% [of $CaAlSiAlO_6$ component]."

*** Values of a b c β from fig. 6 of Kuno and Hess (1953).

**** Regression constants (from table 5) are based on only one specimen of jadeite and none of acmite; the regression equation formally groups these two as noted under the heading "Data and results." It is not valid to assume that jadeite and acmite therefore necessarily have equal lattice constants: the present data simply do not distinguish between them.

TABLE 8

Chemical parameters and physical properties of Brown's (1960) Skaergaard pyroxenes.

Identification											
Specimen No.	366	367	369	370	371	372	373	374	375	376	377
Brown's No. (1960)	1	2	4	5	6	7	8	9	3	10	11
Our chemical parameters, x_1, calculated from Brown's analyses, x 1000											
x_1	1882	1904	1932	1937	1925	1923	1924	1931	1908	1941	1928
x_2	103	104	90	86	87	76	65	62	95	57	88
x_3	897	833	751	724	716	684	639	543	803	211	37
x_4	143	221	273	279	306	288	292	254	241	166	146
x_5	809	759	695	685	668	675	685	739	729	816	832
Brown's observed lattice constants											
a	9.746	9.751	9.754	9.751	9.753	9.757	9.758	9.763	9.753	9.802 ca.	?
b	8.910	8.926	8.940	8.945	8.944	8.948	8.954	8.965	8.928	9.004	9.024 ca.
c	5.268	5.260	5.270	5.267	5.267	5.251	5.255	5.272	5.259	5.252 ca.	?
β	73°53′	73°57′	73°59′	74°02′	74°03′	74°06′	74°07′	74°13′	73°56′	74°45′ ca.	?
Lattice constants estimated by regressions for "ordinary" clinopyroxenes (Table 3)											
a′	9.731	9.740	9.750	9.753	9.753	9.757	9.765	9.780	9.743	9.822	9.840
b′	8.901	8.922	8.942	8.946	8.946	8.947	8.954	8.966	8.927	8.998	9.010
c′	5.254	5.255	5.254	5.254	5.255	5.255	5.257	5.259	5.256	5.265	5.269
β'	73°42′	73°37′	73°33′	73°34′	73°31′	73°36′	73°42′	74°01′	73°35′	74°50′	75°11′
Residual, D = y(obs.) − y(est.)											
a - a′	.015	.011	.004	−.002	0	0	−.007	−.017	.010	−.020	?
b - b′	.009	.004	−.002	−.001	−.002	.001	0	−.001	.001	.006	(.014)
c - c′	.014	.005	.016	.013	.012	−.004	−.002	.013	.003	−.013	?
$\beta - \beta'$	11′	20′	26′	28′	32′	30′	25′	12′	21′	−05′	?

Standard deviations (root-mean-square residuals)

$s_{(a-a')} = 0.0099$; $s_{(b-b')} = 0.0038$; $s_{(c-c')} = 0.0108$; $s_{(\beta-\beta')} = 23'$.

$s_{(b-b')} = 0.0056$ if the doubtful observation on No. 377(11) is included.

rather special cases. In the present study, it is certainly reasonable to estimate the lattice constants for $CaMgSi_2O_6$ which is fairly close to the mean composition, and close to several observations used in the regressions. It is perhaps a little less reasonable to estimate the other constants shown in table 7.

4. Constructing partial chemical variation diagrams showing lattice constants of clinopyroxene (fig. 1).

The warning is emphasized that such diagrams must not be used uncritically for inverse solutions (i.e., composition from measured lattice constants), especially if the data thus obtained differ substantially from the mean values ($\bar{x}_i$) shown in tables 3 and 5, and from all of the specimens described in tables 1 and 2.

COMPARISON WITH OTHER DATA, EXTRAPOLATED VALUES

Sakata (1959) published the lattice constants for three synthetic clinopyroxenes, one of which is close to the limit of the composition field covered by our regressions, and two of which are significantly outside that field. In table 7 we compare the axes a, b, c, and angles β reported by Sakata and by Kuno and Hess, with corresponding values calculated by our regressions. In the same table we also list certain other compositions of special interest, with their respective unit cells as calculated by our regressions. These values represent for the most part compositions outside the ranges for which we have data; therefore the reader will be well advised to use them with appropriate caution.

Brown (1960) published lattice constants for ten additional analyzed specimens of "ordinary" clinopyrozenes separated from the rocks of the Skaergaard Intrusion in East Greenland. If these had been available to us only six months sooner we could have used them in our regressions; the result would have been more satisfactory, because more independent variables of chemical composition could have been used, especially separating the rather awkward combination of Al with Fe''' and Ti, and perhaps also separating Mn from Fe''. Be that as it may, it is interesting to note how well Brown's data fit with the predictions based on our regressions (table 8). Brown reported only tentative values for a, c and β of specimen 376(10), and for b of specimen 377(11). Inasmuch as the residual differences between observed and estimated values of these constants for these two specimens are rather large (2.5 times the standard deviation in the worst case, b of specimen 377-11), it may be stated with considerable confidence that other factors than random (statistical) variation contributed to the large residual. The standard deviations at the foot of table 8 and the corresponding standard errors of the regressions (sp, table 3) show that the data of Brown do agree essentially with those on which our regressions are based.

CONCLUSION

The regressions whose constants are given in tables 3 and 5 are satisfactory predictors for the lattice constants of clinopyroxenes whose compositions are within, or not far without, the range of compositions covered in table

1. This fact tends to emphasize the essential unity of the clinopyroxene system, *sensu vasto*.

References

Acton, F. S., 1959, Analysis of straight-line data: New York, John Wiley and Sons, Inc.

Brown, G. M., 1956, The layered ultrabasic rocks of Rhum, Inner Hebrides: Roy. Soc. London Phil. Trans., ser. B, v. 240, p. 1-53.

———, 1960, Effect of ion substitution on cell dimensions of clinopyroxenes: Am. Mineralogist, v. 45, p. 15-38.

Donnay, G., et. al., 1959, Nepheline solid solutions: Mineralog. Mag., v. 32, p. 93-109.

Fisher, R. A., 1951, The design of experiments, 6th ed.: New York, Hafner Publishing Corp.

———, 1958, Statistical methods for research workers, 13th ed., New York, Hafner Publishing Corp.

Ford, W. E., 1915, A study of the relations existing between the chemical, optical, and other physical properties of the members of the garnet group: Am. Jour. Sci., ser. 4, v. 40, p. 33-49.

Henriques, A., 1958a, The influence of cations on the optical properties of clinopyroxenes, Part I.: Arkiv Mineralogi Geologi, v. 2, p. 341-348.

———, 1958b, ———, Part II.: Arkiv Mineralogi Geologi, v. 2, p. 381-384.

———, 1958c, The influence of cations on the optical properties of orthopyroxenes: Arkiv Mineralogi Geologi, v. 2, p. 385-390.

Hess, H. H., 1949, Chemical composition and optical properties of common clinopyroxenes: Part I.: Am. Mineralogist, v. 34, p. 621-666.

Hey, M. H., 1956, On the correlation of physical properties with chemical composition in multivariate systems: Mineralog. Mag., v. 31, p. 69-95.

Hori, F., 1954, Effects of constituent cations on the optical properties of clinopyroxenes: Sci. Papers, College of Gen. Educ., Univ. Tokyo, v. 4, p. 71-83.

———, 1956, Effects of constituent cations on the refractive indices of orthopyroxenes: Mineralog. Jour. (Japan), v. 1, p. 359-371.

Kuno, H., 1955, Ion substitution in the diopside-ferropigeonite series of clinopyroxenes: Am. Mineralogist, v. 40, p. 70-93.

Kuno, H., and Hess, H. H., 1953, Unit cell dimensions of clinoenstatite and pigeonite in in equilibrium in magma: Am. Mineralogist, v. 37, p. 1000-1006.

Kuno, H., and Nagashima, K., 1952, Chemical compositions of hypersthene and pigeonite relation to other common clinopyroxenes: Am. Jour. Sci., v. 251, p. 741-752.

Mertie, J. B., Jr., 1949, Charting five and six variables on the bounding tetrahedra of hypertetrahedra: Am. Mineralogist, v. 34, p. 706-716.

Sakata, Y., 1957, Unit cell dimensions of synthetic aluminian diopside: Japanese Jour. Geology Geography, v. 28, p. 161-168 [through Mineralog. Abst., v. 14, p. 178].

Schiavinato, G., 1953, Sulla johannsenite dei giacimenti a silicati manganesiferi del Monte Civillina presso Recoaro (Vicenza): Rend. Soc. Mineralog. Italiana, v. 9, p. 210-218 [through Mineralog. Abst., v. 12, p. 259).

Troeger, W. E., 1956, Optische Bestimmung der gesteinsbildende Minerale, Teil I, Bestimmungstabellen, 2nd ed.: Stuttgart, E. Schweitzerbart'sche Verlagsbuchhandlung.

Winchell, A. N., 1945 Variations in composition and properties of the calciferous amphiboles: Am. Mineralogist, v. 30, p. 27-50.

Winchell, A. N., and Winchell, H., 1951, Elements of optical mineralogy, Part II. Descriptions of minerals, 4th ed.: New York, John Wiley and Sons, Inc.

Winchell, H., 1958, The composition and physical properties of garnet: Am. Mineralogist, v. 43, p. 595-600.

Wolfe, C. W., 1955, Crystallography of jadeite crystals from near Cloverdale, California: Am. Mineralogist, v. 40, p. 248-260.

[American Journal of Science, Vol. 258, October 1960, P. 548-554]

Si - Al RELATION IN CLINOPYROXENES FROM IGNEOUS ROCKS

IKUO KUSHIRO

Geological Institute, University of Tokyo, Tokyo, Japan

ABSTRACT. By a statistical study of chemical compositions of clinopyroxenes from igneous rocks, it is found that those crystallizing from tholeiitic magma which is oversaturated with SiO_2 have higher proportions of Si and lower proportions of Al in the tetrahedral position of the pyroxene structure, whereas those from undersaturated alkali-basalt magma have lower Si and higher Al proportions. It is also noticed that the proportion of Si increases and that of Al in the tetrahedral position decreases during fractionation of the Skaergaard, Stillwater, Black Jack and Iz.-Hakone magmas. These proportions appear to depend on the molecular concentration of SiO_2 in the magma at the time of clinopyroxene crystallization. If the magma is deficient in SiO_2, a lower proportion of Si is available to the tetrahedral position and the rest of this position is filled with Al. The excess of the negative charge caused by the Si-Al substitution is compensated by the entrance of Ti, Al and Fe^{3+} in the octahedral position. This would account for the common occurrence of Ti-rich augite in the undersaturated alkalic rocks. Higher temperature of the magma would favor the higher proportion of Al in the tetrahedral position and consequently would result in the lower Si proportion. But this effect appears to be subordinate to the composition effect.

INTRODUCTION

A statistical study was carried out on the composition of clinopyroxene from igneous rocks in order to determine the physicochemical conditions controlling Si-Al substitution in the clinopyroxene structure. It is well known that clinopyroxene crystallizes from magmas of varying chemical compositions and through a wide temperature range. In this paper, the relation between the magma type and the proportions of Si, Al and Ti in the clinopyroxene and the variation of these cation proportions during fractionation are discussed.

The structure of diopside was first determined by Warren and Bragg (1928) and it has been assumed by several investigators (Warren and Biscoe, 1931; Yoder, 1950) that most other clinopyroxenes have the same type of structure. The general formula for the pyroxene was given by Warren and Biscoe (1931), Berman (1937) and Hess (1949). These investigators showed that Si in the terahedral position is partly replaced by Al. Kuno (1955) also suggested a possibility of substitution of Fe^{3+} and Ti for Si. However, the conditions controlling the Si-Al substitution have been little studied.

PROPORTIONS OF Si, Al AND Ti IN CLINOPYROXENES IN RELATION TO MAGMA TYPES

Clinopyroxenes from various igneous rocks have a wide range of atomic proportions of Si, Al and Ti. The difference of the proportions may depend upon the physical and chemical conditions of the magmas from which the clinopyroxenes crystallize.

Mafic magmas are classified into two types: tholeiitic magma including its derivatives which is generally oversaturated with SiO_2 and alkali-basalt magma including its derivatives most of which is undersaturated. The former is represented chiefly by tholeiitic basalt, dolerite, gabbro and andesite whereas the latter is represented by alkali-basalt, alkali-dolerite, trachyandesite, trachyte and syenite. As the latter magma type covers a wide compositional

range, it may be further classified into two types: one yielding feldspathoid-free rocks and the other feldspathoid-bearing rocks. Calc-alkali rocks are provisionally included in the tholeiitic magma because they are generally oversaturated with SiO_2.

The relationship between the atomic proportions of Si and Al of the clinopyroxenes in relation to their parent rocks derived from the three magma types is shown in figure 1. One hundred and forty clinpyroxenes are plotted

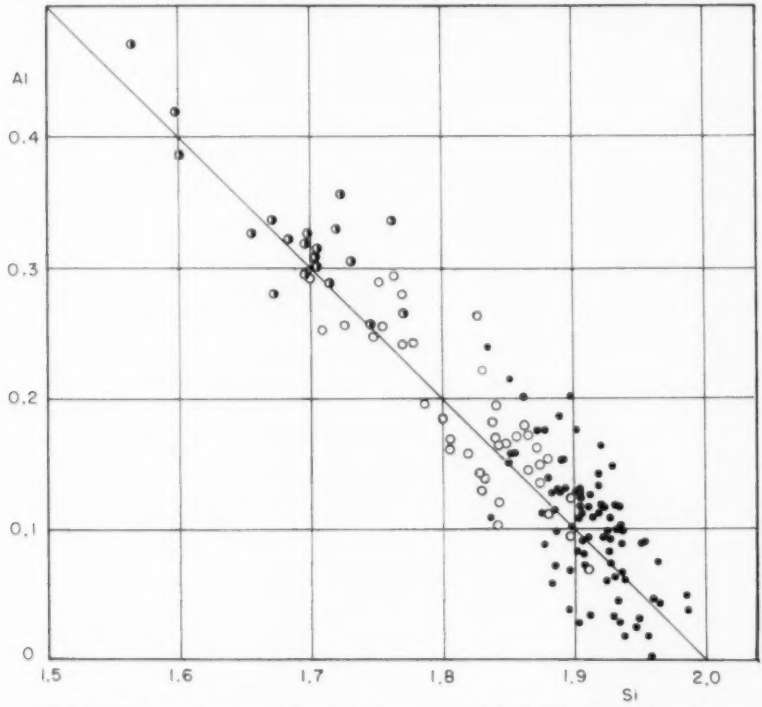

Fig. 1. Relation between the atomic proportions of Si and Al in the clinopyroxenes from the three different rock groups. Solid circles: clinopyroxenes from tholeiitic rocks. Open circles: clinopyroxenes from feldspathoid-free alkalic rocks. Half solid circles: clinopyroxenes from feldspathoid-bearing alkalic rocks. (Atomic proportions are calculated on the basis of six oxygen atoms.)

with respect to the proportions of Si and total Al calculated on the basis of six oxygen atoms. Clinopyroxenes of uncertain sources and also aegirine-augite are omitted.

It is evident from the figure that the clinopyroxenes from the tholeiitic rocks have larger proportions of Si and smaller proportions of Al, whereas those from the feldspathoid-bearing rocks have smaller proportions of Si and larger proportions of Al, and those from the feldspathoid-free alkalic rocks have intermediate Si and Al proportions. In the figure, a line which connects

the points representing saturation of the tetrahedral position, namely the points corresponding to Si + Al = 2, is drawn. That most of the points for the actual clinopyroxenes are close to the saturation line despite plotting total

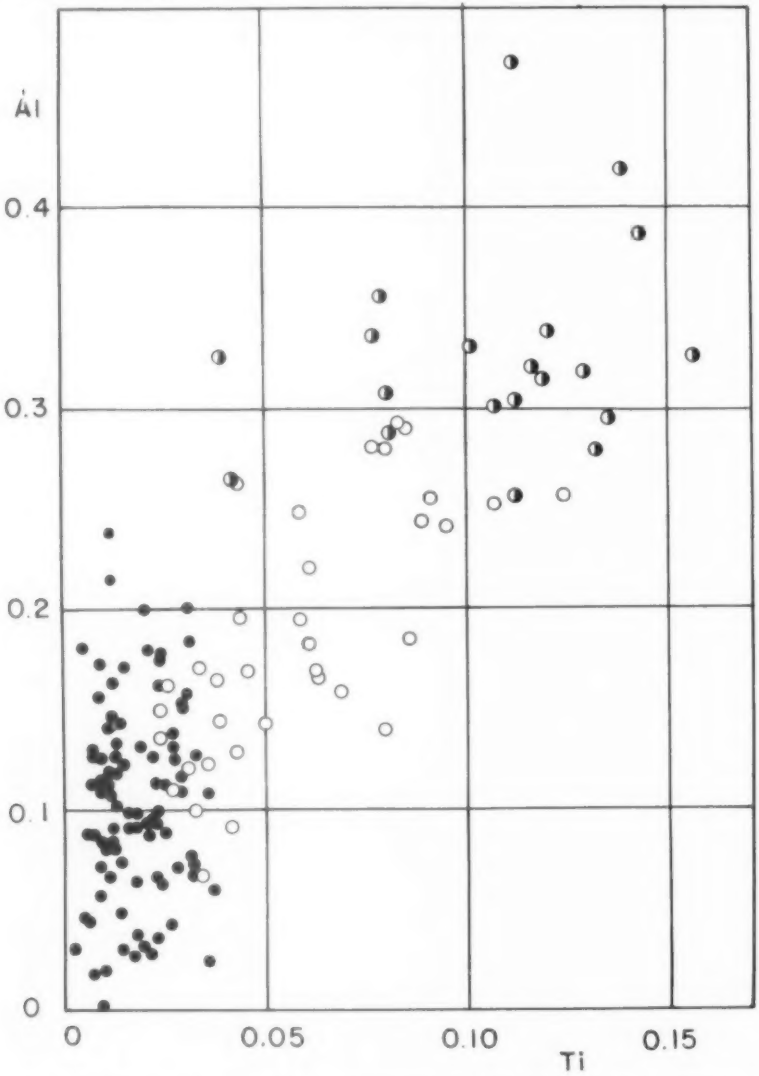

Fig. 2. Relation between the atomic proportions of Al and Ti in the clinopyroxenes from the three different rock groups. Marks are same as those in fig. 1.

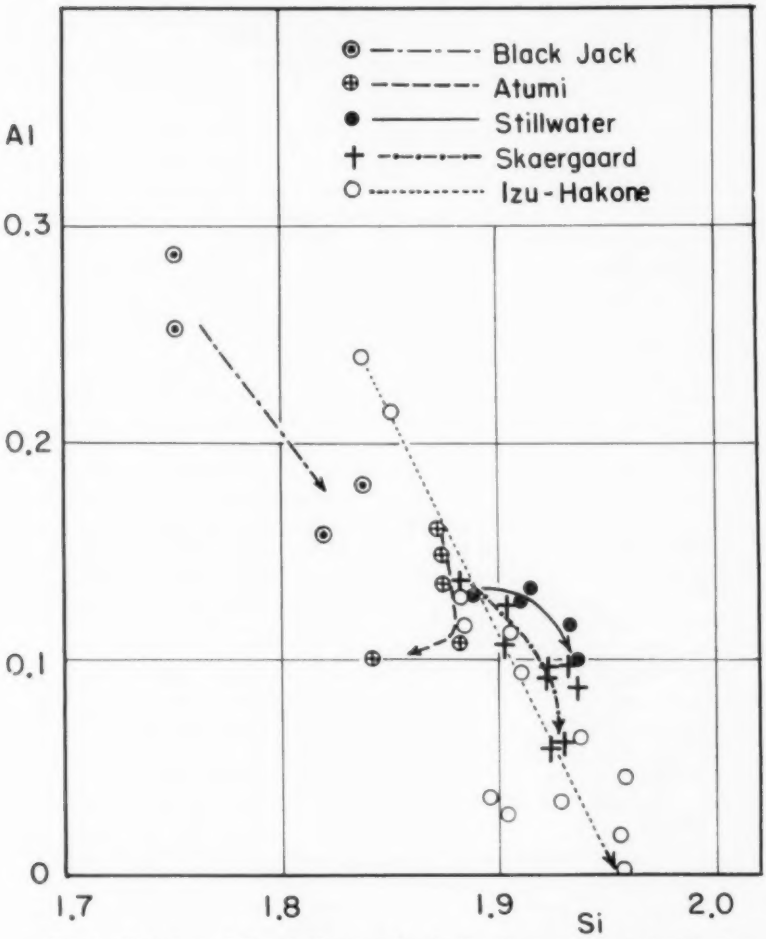

Fig. 3. Variations of Si and Al proportions in the clinopyroxenes during fractionation of the five different magmas.

Al indicates that Al in these clinopyroxenes is mainly in the tetrahedral position. The Al ions in the tetrahedral position are electrically compensated by the entrance of Ti, Al and Fe^{3+} ions into the octahedral position. The clinopyroxenes falling above the saturation line contain excess Al which enters into the octahedral position, whereas those falling below the line may have Fe^{3+} and Ti in the tetrahedral position as suggested by Kuno (1955). In figure 2, the relation between the atomic proportions of Al and Ti of the clinopyroxenes in the three different groups of rocks is shown. The clinopyroxenes from the

tholeiitic rocks are low in Ti content and also comparatively low in Al content. On the contrary, those from the feldspathoid-bearing rocks are rich in Ti and Al and those from the feldspathoid-free alkalic rocks have intermediate contents of these elements.

VARIATION OF Si AND Al PROPORTIONS DURING FRACTIONATION

Change in chemical composition of clinopyroxenes during fractionation of magmas can be studied best in some differentiated intrusive bodies. Clinopyroxenes of four such bodies, namely, the Skaergaard intrusion (Brown and others, 1957), Stillwater complex (Hess, 1949), Black Jack sill (Wilkinson, 1957) and Atumi sill (Kushiro, 1959), are examined to find the general trend of variation in the atomic proportions of Si and Al. The first two intrusions are derived from tholeiitic magma and the rest from alkali-olivine-basalt magma. Although the Skaergaard magma is undersaturated with SiO_2 and recently considered to be high-alumina basalt by Yoder and Tilley (1957) and Kuno (1960), the pyroxene relations are similar to those of tholeiitic rocks. The clinopyroxenes from tholeiitic volcanic rocks in the Izu-Hakone district (Kuno, 1955) are also examined for comparison.

In the clinopyroxenes of these rock suites, Si increases while total Al decreases generally as the fractionation proceeds (fig. 3). The trend from salite to ferropigeonite of the Izu-Hakone rocks covers the almost whole range of the tholeiitic clinopyroxenes as regard to the Si and total Al proportions. As the structure of pigeonite is slightly different from that of augite (Morimoto, 1956), pigeonite may be omitted from consideration. However, the trend from salite to Ca-poor augite of the Izu-Hakone rocks also covers the whole range of the tholeiitic clinopyroxenes.

The calculated amounts of Al in the tetrahedral and octahedral positions differ somewhat according to whether the calculation is made according to Hess' method (1949) or on the basis of the common assumption that the tetrahedral position is always completely filled with Si, Al, Fe^{3+} and Ti in the order of preference just named. However, the calculation by either method revealed that Al in the tetrahedral position also decreases during the fractionation of these intrusions and of the Izu-Hakone rocks. Brown (1957) also noticed a regular decrease of Al both in the tetrahedral and octahedral positions for the Skaergaard pyroxenes.

Trend of variation of Ti with fractionation differs in different cases. The proportion of Ti decreases in the Black Jack clinopyroxenes whereas it changes little in the Skaergaard, Stillwater, Atumi and Izu-Hakone clinopyroxenes.

FACTORS CONTROLLING Si-Al SUBSTITUTION

Si, Al and Ti proportions in the clinopyroxenes would be controlled by chemical composition, temperature and pressure of the magma from which they crystallize. The effect of pressure may be negligible.

The compositions of the magmas vary widely in the different magma types and in different fractionation stages. Although the temperature relation of the three magma types is not yet known, the temperature of the individual magma should decrease during the fractionation. Such composition and

temperature differences of the magmas may result in the varying proportions of Si, Al and Ti in different coordinations in the pyroxene structure.

It is most likely that molecular concentration of SiO_2 in the magma determines the amount of Si in the tetrahedral position of the clinopyroxene crystallizing therefrom. If the amount of Si available to the clinopyroxene is not sufficient to fill up the tetrahedral position, the rest of the position is occupied by Al (and Fe^{3+} and Ti). Thus, in the oversaturated tholeiitic magma, much Si would be available to the clinopyroxene and consequently it has a higher proportion of Si and a lower proportion of Al than the clinopyroxene in the undersaturated magma which gives rise to the feldspathoid-free alkalic rocks, and the clinopyroxene in the more undersaturated magma giving rise to the feldspathoid-bearing rocks has the lowest Si and highest Al proportions (largely in the tetrahedral position).

This hypothesis is supported by the fact that the proportion of Si in the clinopyroxenes crystallizing from the magmas of Skaergaard, Stillwater, Black Jack and Izu-Hakone increases as the fractionation proceeds during which molecular concentration of SiO_2 in the magmas increases. An exception is the clinopyroxene from the later fractionation stage of the Atumi magma, although the SiO_2 concentration in the later stage also increases during the fractionation.

The Al ions in the tetrahedral position must be accompanied by Ti, Al and Fe^{3+} ions in the octahedral position in order to maintain electric neutrality. In the clinopyroxenes crystallizing from alkalic magmas which are usually rich in TiO_2, Al ions in the tetrahedral position are largely compensated by Ti ions (fig. 2). Therefore, the clinopyroxenes from alkalic rocks are generally rich in Ti and are usually called titanaugite. It is also conceivable, however, that the high TiO_2 concentration in the alkalic magma results in the high Ti content and consequently high Al content in the clinopyroxenes. This implies that the molecular concentration of TiO_2 in the magma determines the amounts of Ti and Al in the clinopyroxenes. But this is not likely because of the following facts: during the early and middle stages of fractionation of the Skaergaard intrusion, TiO_2 molecular concentration of the magma increases (Wager and Deer, 1939) whereas Ti content of the clinopyroxene is almost constant despite the marked decrease of Al; in the Black Jack sill, TiO_2 of the magma (rock) also increases (Wilkinson, 1958) while Ti of the clinoproxene decreases; in the Atumi sill, some clinopyroxenes crystallizing from TiO_2-poor magma have a higher Ti content than those from TiO_2-rich magma. In these discussions, however, the crystallization of iron ores is not taken into consideration and therefore the possibility of the TiO_2 concentration effect cannot entirely be discarded.

Another possibility is that the temperatures of the magmas control the amount of Al in the tetrahedral position; the clinopyroxenes crystallizing at higher temperatures can contain more Al ions in the tetrahedral position than those crystallizing at lower temperatures. This hypothesis is also in accord with the decrease of the Al proportion in the tetrahedral position during the fractionation of the magmas already referred to. In silicate structures, Al tends to enter into the tetrahedral position at higher temperatures

as suggested by Thompson (1947) and Buerger (1948). However, the temperature effect alone does not appear to account for the marked difference of the Al proportion between the clinopyroxenes of the oversaturated magmas and those of the undersaturated ones.

ACKNOWLEDGMENTS

The writer is much indebted to Prof. H. Kuno and Asst. Prof. A. Miyashiro for criticism of the results and for reading the manuscript. Thanks are also expressed to Dr. F. Shido and Mr. S. Banno of the Geological Institute, University of Tokyo, for their helpful discussions.

REFERENCES

Berman, H., 1937, Constitution and classification of natural silicates: Am. Mineralogist, v. 22, p. 333-415.

Brown, G. M., Vincent, E. A. and Brown, P. E., 1957, Pyroxenes from the early and middle stages of fractionation of the Skaergaard intrusion, East Greenland: Mineralog. Mag., v. 31, p. 511-543.

Buerger, M. J., 1948, The role of temperature in mineralogy: Am. Mineralogist, v. 33, p. 101-121.

Hess, H. H., 1949, Chemical composition and optical properties of common clinopyroxenes: Am. Mineralogist, v. 34, p. 621-666.

Kuno, H., 1955, Ion substitution in the diopside-ferropigeonite series of clinopyroxenes: Am. Mineralogist, v. 40, p. 70-93.

———— in press, High-alumina basalt.

Kushiro, I., 1959, Preliminary note on alkali-dolerite of Atumi district, northern Japan: Japanese Jour. Geology Geography, v. 30, p. 259-272.

Morimoto, N., 1956, The existence of monoclinic pyroxenes with the space group C_{2h}^5 – $P2_1/c$: Japanese Acad. Proc., v. 32, p. 750-752.

Thompson, J. B., 1947, Role of aluminum in rock forming silicates: Geol. Soc. America Bull., v. 58, p. 1232.

Wager, L. R. and Deer, W. A., 1939, Geological investigation in East Greenland. Pt. III. The petrology of the Skaergaard intrusion, Kangerdlugssuaq, East Greenland: Medd. Om. Grønland, v. 105, no. 4, p. 1-352.

Warren, B. E. and Bragg, W. L., 1928, The structure of diopside $CaMg(SiO_3)_2$: Zeitschr. Kristallographie, v. 69, p. 168-193.

Warren, B. E. and Biscoe, J., 1931, The crystal structure of the monoclinic pyroxenes: Zeitschr. Kristallographie, v. 80, p. 391-401.

Wilkinson, J. F. G., 1957, The clinopyroxenes of a differentiated teschenite sill, near Gunnedah, New South Wales: Geol. Mag. 94, p. 123-134.

———— 1958, The petrology of a differentiated teschenite sill, near Gunnedah, New South Wales: Am. Jour. Sci., v. 256, p. 1-39.

Yoder, H. S., 1950, The jadeite problem. Part I: Am. Jour. Sci., v. 248, p. 226-248.

Yoder, H. S. and Tilley, C. E., 1957, Basaltic magmas: Geophys. Lab. Ann. Rept. 1956-1957, p. 156-161.

[American Journal of Science, Vol. 258, October 1960, P. 555-573]

JADEITE-ROCKS AND GLAUCOPHANE-SCHISTS FROM ANGEL ISLAND, SAN FRANCISCO BAY, CALIFORNIA

T. W. BLOXAM

Department of Geology, University College, Swansea, Wales

ABSTRACT. The rocks of Angel Island comprise a series of Franciscan (Jurassic) arkosic graywackes with subordinate amounts of conglomerate and radiolarian chert. Almost all the graywackes have been metamorphosed to jadeite-bearing metagraywackes independently of proximity with basic or ultrabasic intrusions. A diabase sill, originally intrusive into the sedimentary series, has also been metamorphosed and its feldspar converted to chlorite, lawsonite, and jadeite. Glaucophane occurs in the altered diabase and is particularly abundant at its margins. Towards the diabase the jadeite-bearing metagraywackes become richer in glaucophane and pass into jadeite-free schistose glaucophane-rocks. Chemical analyses show that the change is accompanied by some desilication and an addition of Fe, Mg, Ca, Ti, and possibly Na. This metasomatism, which may have preceded, or coincided with, the metamorphism, was probably hydrothermal in nature and localized along igneous contacts and shear-planes. Similar, but more extensive developments of glaucophane-schist, also derived from graywacke, occur in association with a dike of serpentinized pyroxenite. Hydrothermal processes directly related to the serpentinization may have played a significant part in the chemical alteration of the graywacke. Movements along serpentinite contacts complicates the relationships and many large masses of glaucophane-schist and jadeite-bearing metagraywacke occur as tectonic inclusions within the serpentinite. Plagioclase is absent from, and considered unstable in, all the metamorphic assemblages. While jadeite appears to be stable in the arkosic metagraywackes deficient in Fe, Mg and Ca; its place is taken by acmitic-jadeite and eventually glaucophane in the glaucophane-schists.

INTRODUCTION

Angel Island is one of the largest of a number of islands in San Francisco Bay, and lies about half a mile from the tip of Tiburon Peninsula from which it is separated by Raccoon Strait (fig. 1). The area of the island is about one square mile and its geology was first described by Ransome in 1894 (see also Bloxam, 1955). It is of particular interest since some of the earliest conclusions about the occurrence and possible origin of the California glaucophane-schists were based on relationships observed on this island. With one or two exceptions the shore around the island is accessible at low tide, but high grass or tree-covered slopes behind the beach generally make it impossible to follow outcrops continuously inland.

The island is composed essentially of six major rock-groups (fig. 2):

(1) Franciscan (Jurassic) graywackes, conglomerates and radiolarian cherts.
(2) Jadeite-bearing metagraywackes derived from the Franciscan graywackes. This is the dominant rock-type on the island.
(3) Glaucophane-schists derived from graywackes, cherts, and basic igneous rocks.
(4) A large and apparently concordant sheet of altered diabase ("fourchite" of Ransome) intrusive into the Franciscan sediments. The diabase is extensively glaucophanized, particularly at its margins.
(5) Pillow-lavas at Point Blunt.
(6) A vertical dike-like body of serpentinite and pyroxenite near the western end of the island.

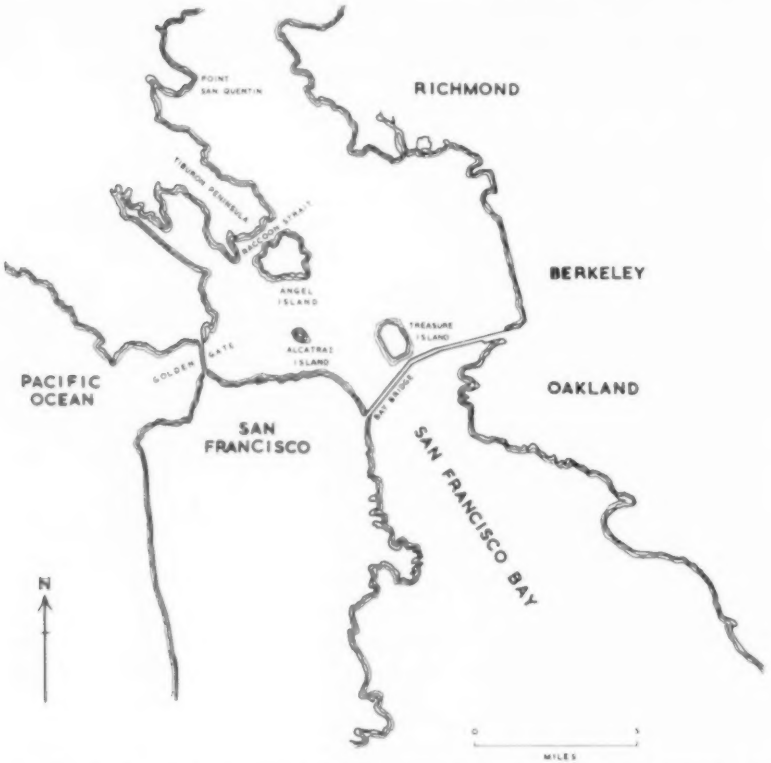

Fig. 1. Geographical position of Angel Island in relation to the San Francisco Bay area.

Ransome (1894) estimates that the total thickness of the Franciscan rocks on the island is at least 2,000 feet.

The major structure of the island is relatively simple and consists of a synclinal trough with its axis plunging to the north-east. This feature is particularly emphasized by the arcuate outcrops of the altered diabase sheet. However, as Ransome has shown (1894, p. 193), there are associated minor folds which may locally add considerable complication to the structure. In addition the present writer has mapped numerous NNW faults which do not appear on Ransome's map and complicate relationships along the shore, particularly in the region between Point Knox and Point Blunt (fig. 3).

The serpentinite dike appears to represent a boundary between structures to the east which are relatively simple and have low dips, and structures to the west which are more complex, considerably faulted, and generally have vertical dips.

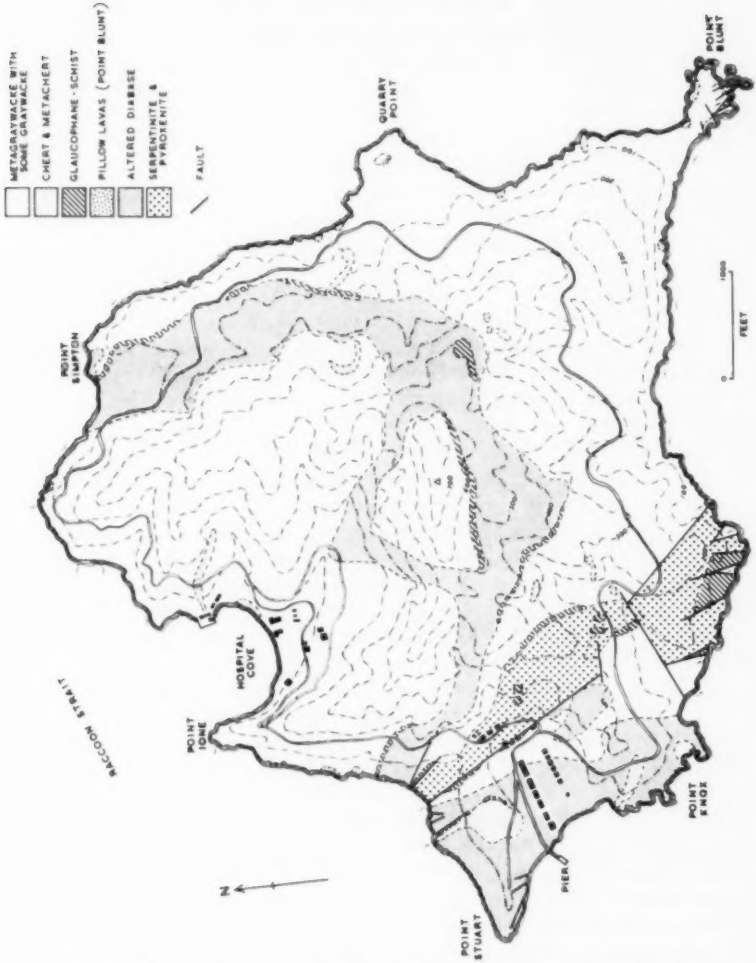

Fig. 2. Geological map of Angel Island. Modified after F. L. Ransome, 1894.

FRANCISCAN SEDIMENTS AND JADEITIC METASEDIMENTS

General statement.—The Franciscan graywackes which make up the bulk of the island have, with minor exceptions, been metamorphosed, the characteristic rock-type being glaucophane-poor jadeite-bearing metagraywacke (Bloxam, 1956; 1959). Except in extreme cases, distinguishing graywacke from metagraywacke by eye in the field is difficult or impossible; while in thin sections it is essentially dependent upon the efficiency of the optical microscope.

However, the difference in density between the two can be recognized in the field using a suitable heavy liquid (Turner, personal communication).

Of the "graywacke" specimens collected over 90 percent were found to be metamorphosed and about 80 percent of this number jadeite-bearing. Ransome (1894) failed to observe the widespread jadeitic metamorphism of the graywackes, confining his attentions to the more obvious developments of glaucophane-schist to be described subsequently (p. 566-569).

Franciscan graywackes.—Examples of least altered graywacke occur at Quarry Point and near Point Campbell. The outcrops are well bedded with occasional conglomerate bands and thin friable shales. Almost all the graywackes are sheared along planes parallel to the bedding (Ransome, 1894, p. 198). This appears to be a characteristic feature of many Franciscan graywackes in California (Bloxam, 1959) and tends to accentuate the original bedding. Seldom, however, is the shearing sufficiently intense to destroy the original clastic textures of the graywacke which in hand specimens contain obvious fragments of bright green chert, black shale and streaky carbonaceous (?plant) material.

Thin sections of the rock display abundant fragments of angular quartz and chert. Fresh clastic twinned albite is also characteristic and in some specimens makes up 35 percent of the fragments. Splinters of shale and more rounded pieces of variolitic basalt are common, the whole being cemented by sub-parallel strings of mica, chlorite and a little calcite. The mica and chlorite define the original bedding but also exhibit evidence of secondary growth in association with the later shearing. In addition a brown micaceous mineral occurs which resembles biotite but is almost isotropic suggesting some type of vermiculite. It may have been derived from stilpnomelane (p. 559).

Ransome (1894, p. 231) only gives a silica determination from the Quarry Point graywacke (table 1, column 1), but a new analysis is given in table 1, column 2. For comparison an analysis of Franciscan graywacke by Taliaferro (1943, p. 136) is also included in table 1, column 3. It has been noted elsewhere (Taliaferro, 1942, p. 83; Bloxam, 1956; 1959) that the Franciscan graywackes tend to be rather arkosic and remarkably constant in chemical composition over wide areas in California.

Metagraywackes.—It is convenient to divide the metagraywackes into two mineralogic groups: (1) *Quartz-albite-mica-lawsonite-crossite* and, (2) *Quartz-jadeite-mica-lawsonite-crossite*. Hence the division is defined by the reaction albite = jadeite + quartz, and it is assumed that, for a given chemical composition, rocks with jadeite develop under conditions of higher total pressure than those with albite (Fyfe, Turner and Verhoogen, 1958, p. 177).

(1) *Quartz-albite-mica-lawsonite-crossite.*—The first signs of metamorphism in the graywackes occurs in the groundmass and in some of the basic igneous fragments. Using a Leitz 6L objective and X8 eyepiece (x 360) fibres of a deep-blue amphibole appear within the chloritic areas. Precise optical determinations are difficult at this magnification, but larger crystals in more advanced stages have intense pleochroism from colorless to deep violet, $2V_a$ = 0-10°, and a low birefringence characteristic of crossite.

TABLE 1

	1	2	3	4	5	6
SiO_2	70.50	70.31	71.72	69.77	70.04	69.14
TiO_2	—	0.36	0.35	0.41	0.14	0.37
Al_2O_3	—	14.03	13.23	14.82	13.88	15.08
Fe_2O_3	—	0.85	0.30	1.21	0.91	1.51
FeO	—	2.61	3.58	1.35	2.26	0.84
MnO	—	0.10	nil	0.03	0.07	0.03
MgO	—	2.07	1.81	2.38	2.11	1.08
CaO	—	1.31	1.80	1.99	1.79	2.79
Na_2O	—	4.12	2.72	3.89	4.01	5.31
K_2O	—	1.19	1.29	1.01	0.97	1.28
H_2O^+	—	2.37	2.53	2.96	3.15	1.96
H_2O^-	—	0.23	0.15	0.20	0.25	0.08
P_2O_5	—	0.05	0.09	0.08	nil	0.00
CO_2	—	0.09	0.32	0.10	0.07	0.12
		99.69	99.89	100.20	99.65	99.59
SG		2.78	—	2.89	2.91	2.91

1. Franciscan "sandstone", Quarry Point, Angel Island (Ransome, 1894, p. 231. Analyst, F. L. Ransome)
2. Franciscan graywacke, Quarry Point, Angel Island. Analyst, T. W. Bloxam.
3. Franciscan graywacke, Buckeye Gulch (Taliaferro, 1943, p. 136). Also $ZrO_2 = 0.04\%$.
4. Jadeite-bearing metagraywacke, Point Simpton, Angel Island. Analyst, T. W. Bloxam.
5. Jadeite-bearing metagraywacke, Point Blunt, Angel Island. Analyst, T. W. Bloxam.
6. Jadeite-bearing metagraywacke, Valley Ford (Bloxam, 1956, p. 98. Analyst, E. H. Oslund).

Dispersed among the fibers of mica and chlorite are idiomorphic crystals of lawsonite, often bent, but generally lying parallel to the bedding/foliation. The mineral is particularly abundant in the basic igneous fragments. Recrystallization of the groundmass begins to effect the detrital quartz, chert, and albite fragments, which lose their sharp boundaries and are invaded by needles of pale green actinolite, often fringed with crossite. The brownish vermiculite noted previously (p. 558) frequently passes into fibers of stilpnomelane while the latter may also replace some of the whispy mica. Tiny garnet aggregates are common and are probably a manganese-rich variety.

(2) *Quartz-jadeite-mica-lawsonite-crossite.*—The incoming of jadeite cannot be determined visually in hand specimens, but in thin sections the mineral replaces the detrital albite. This reaction (albite = jadeite + quartz) appears to be extremely fast and sensitive to changes in metamorphic conditions. Metagraywackes of the type previously described change, within an inch or less, into jadeite-bearing metagraywackes of almost identical texture except that jadeite has developed to the complete exclusion of detrital albite.

The jadeite usually occurs as colorless radiating groups of elongated prisms which may be grouped about an area of cloudy sub-isotropic material with speckled polarization colors; probably lawsonite (Bloxam, 1956). While the average size of the jadeite crystals is from 0.1-0.3 mm (plate 1A and B), one exceptional metagraywacke contains jadeites up to 0.8 mm (plate 1C). In addition to its crystal habit, the jadeite is readily distinguished by its extremely strong dispersion which makes accurate optical determinations difficult. In some cases the usually colorless jadeite may be faintly greenish, probably representing more acmitic varieties. This change in composition is particularly common in metagraywackes containing abundant glaucophane. Optical data

PLATE 1

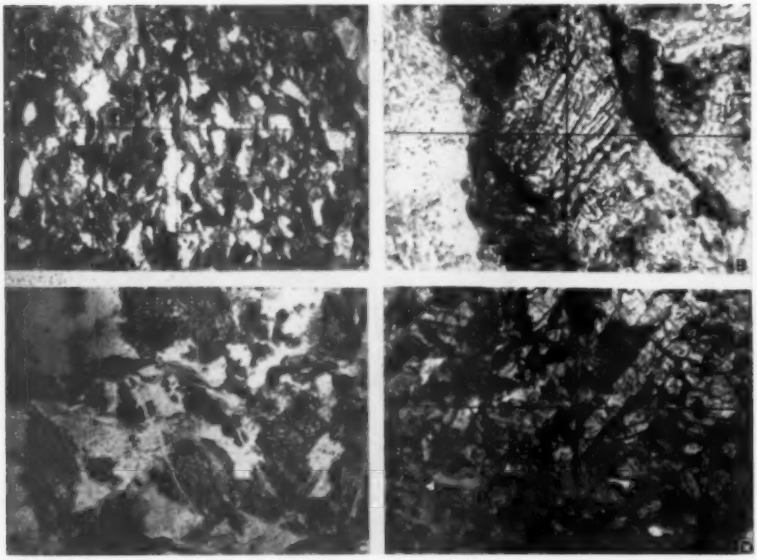

A. Jadeite-bearing metagraywacke. The specimen is slightly foliated and contains abundant clastic quartz, chert, and shale fragments. Ordinary light x 23.

B. Jadeite-bearing metagraywacke; same field as above. Sub-radiate jadeite occupies the center of the field. Ordinary light x 305.

C. Jadeite-bearing metagraywacke with large jadeite aggregates and clastic quartz. The specimen is virtually unfoliated. Ordinary light x 77.

D. Altered diabase. Sub-variolitic phase of the main sheet with outlines of original plagioclase crystals preserved (e.g. just right of center), granular pyroxene, and iron ore. The lawsonite and glaucophane are not readily distinguishable. Ordinary light x 67.

for jadeites from ten Angel Island metagraywackes cover the following range (sodium light): $\beta = 1.658 - 1.672$, $2V_\gamma = 62° - 83°$, $\gamma:c = 43° - 55°$ ($y = b$). The birefringence is low and averages 0.010. These data are in fair agreement with that for an analyzed jadeite from Valley Ford (Bloxam, 1956, p. 490). It has been observed that the faintly greenish (acmitic) jadeites give the lower values for $2V\gamma$ but have a higher birefringence ($\sim$0.015): their dispersion is also weaker (Bloxam, 1959, p. 106).

Lawsonite and crossite continue to crystallise and build larger individuals, the latter mineral often forming fringes around the pale green (acmitic) jadeite but rarely about the colorless jadeite. The development of crossite is quite selective and is most abundant in association with chlorite and shale fragments which presumably have a composition more appropriate to its development. This localization of a particular mineral's development confirms the chemical evidence that there has been very little migration of material during metamorphism.

Stilpnomelane is not common in these rocks, although the same indeterminate brown micaceous mineral noted previously (p. 558) is quite abundant.

PLATE 1

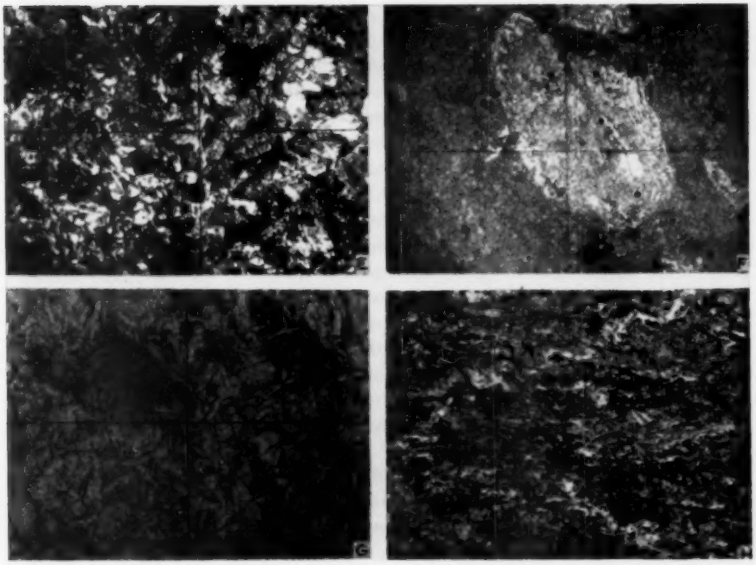

E. Altered diabase; same field as D. The speckled appearance of the plagioclase is due to replacemnt by lawsonite and chlorite. Nicols crossed x 67.

F. Altered porphyritic diabase. The subhedral crystal of plagioclase in the center of the field has been altered to lawsonite, chlorite, and a little jadeite. Ordinary light x 11.

G. Altered porphyritic diabase; same field as above showing details of plagioclase replacement. Abundant idiomorphic lawsonite is present with a "brush-like" aggregate of jadeite just above and left of center. Ordinary light x 110.

H. Glaucophane-rich schist derived from graywacke marginal to the altered diabase. Ordinary light x 36.

Ransome (1894, p. 216), describing a "Franciscan sandstone" makes frequent reference to the presence of "zoisite". It is probable that the mineral is in fact jadeite since the strong dispersion and form of the jadeite are very like those of clinozoisite.

Two analyses of the jadeite-bearing metagraywackes, one from Point Simpton and the other from Point Blunt are given in table 1, columns 4 and 5. The similarity of the analyses to those of the graywackes (table 1, columns 1, 2 and 3) and to a jadeite-bearing metagraywacke from Valley Ford (table 1, column 6) is evident.

Other associated metasediments.—Conglomerates or pebbly facies of the graywackes together with radiolarian cherts are the commonest sedimentary types associated with the graywackes.

(1) *Altered conglomerates.*—In the region of Point Blunt and on the shore about 900 feet south of Point Ione, conglomerates are quite abundant. They are not sharply defined bands but merely coarser phases of the associated metagraywackes which form the matrix about the pebbles. The pebbles, like

the smaller fragments in the metagraywacke, consist of chert, variolite, quartzite, and shale. Ransome (1894, p. 197) described pebbles of a holycrystalline igneous rock of granitic affinities composed of quartz, altered feldspar, green hornblende, and blue amphibole (crossite in the present writer's specimens). Most of the crossite occurs as mantles or feathery replacements of the green hornblende. Since the crossite-bearing pebbles are contained in rocks (jadeitic-metagraywackes) which Ransome regarded as *unmetamorphosed* graywackes, he found it extremely difficult to account for their origin.

(2) *Radiolarian chert.*—Interbedded with the graywackes and metagraywackes are radiolarian cherts which are generally red in color but, when recrystallized, develop green or bluish tints. Ransome (1894, p. 199) noted the radiolarian cherts near Hospital Cove which exhibit sedimentary facies gradational with the graywackes. When associated with unaltered graywacke the radiolarian cherts generally contain abundant tests of *Radiolaria* and are deeply stained by abundant "dusty" iron oxide and some manganese. Some of those associated with the metagraywackes are recrystallized but show little further alteration. Others may contain abundant stilpnomelane and riebeckite and probably represent more impure varieties (cf. p. 560).

THE ALTERED DIABASE

The intrusive sheet of altered diabase can be conveniently divided into: (1) the main arcuate sheet east of the serpentinite dike and, (2) discontinuous outcrops west of the serpentinite dike. In addition, small isolated masses of altered diabase occur in several other places (fig. 2) and probably represent off-shoots from the main sheet (Ransome, 1894, p. 202).

Ransome (1894, p. 200) described the altered diabase as "fourchite" (Williams, 1890), but admitted that this was only for want of a better term. His difficulty in naming the rock was due to the fact that he did not fully recognize its metamorphic character, although he did observe that blue-amphibole was a common constituent (1894, p. 206). Furthermore, lawsonite, which is always abundant, had yet to be described (Ransome, 1895), although he gives the optical properties of an "unknown mineral" in the rock which is clearly lawsonite.

For the most part the altered diabase preserves undisturbed igneous textures of three main types: (a) granular and slightly ophitic, (b) fine-grained porphyritic and, (c) variolitic. Textural types (a) and (b) are developed in all exposures and are representative of the coarser interior and chilled marginal phases respectively. Type (c) is more restricted in its development and confined to certain phases of the western exposures of diabase, particularly near Point Knox.

(1) *The main sheet*: (*a*) *granular and sub-ophitic phases.*—Samples of the altered diabase near Point Simpton serve as typical examples of the main sheet which is very uniform in composition over its whole outcrop.

In general the rock is finer-grained than the average diabase and the pyroxene, which is the only original constituent preserved, tends to be granular but also slightly sub-ophitic towards the altered plagioclase (plate 1D and E). The pyroxene is colorless and has the following optical properties: $\alpha =$

1.681, $\beta = 1.687$, $\gamma = 1.711$, $2V_\gamma = 53°$, $\gamma : c = 43°$; the corresponding composition being close to Ca_{40} Mg_{45} Fe_{15} (Hess, 1949, p. 649). Frequently the pyroxene shows marginal alteration to chlorite, glaucophane, and green acmitic-jadeite. In some cases a little jadeite occurs as independent fibrous aggregates which have developed from the material of the groundmass, probably feldspar.

Although the outlines of the original plagioclase crystals are frequently preserved, they are completely altered to dense aggregates of colorless chlorite which is isotropic and has n = 1.630. Associated with the chlorite are abundant idiomorphic prisms of lawsonite and occasional feathery aggregates of jadeite (e.g. plate 1G).

The original constituents of the fine-grained groundmass cannot be recognized but, judging by the amount of lawsonite present, it must have been very feldspathic.

Interwoven between the pyroxene crystals and forming a further constituent of the groundmass is crossite in extremely small fibers tightly matted together forming an apparently uniform deep-blue background.

The most significant feature of the altered diabase is the complete elimination of feldspar and its replacement by chlorite, lawsonite, and jadeite. This chloritization of the feldspar bears some resemblance to that described by Vuagnat and Jaffé (1954) from Alpine variolites and pillow-lavas associated with serpentinites, although their rocks do not contain glaucophane-schist type minerals.

An analysis of this phase of the altered diabase is given in table 2, column 2, together with Ransome's original analysis of what is probably the same rock-type (table 2, column 1).

(b) *Fine-grained porphyritic phases.*—Except where it reaches the shore near Point Simpton and between Point Knox and Point Stuart, the junction between altered diabase and adjacent metagraywackes is seldom exposed. When contact phases are exposed they are fine-grained and usually strongly porphyritic.

The constituents of the rock are the same as those in the courser phases but the primary pyroxene occurs as sub-radiate laths or fine brush-like groupings, representing a transitional texture between the sub-ophitic and variolitic types described below.

The altered feldspar phenocrysts are of particular interest since they illustrate the development of chlorite, lawsonite, and jadeite within the former crystal boundaries of the phenocrysts (plate 1F and G).

(2) *Altered diabase west of the serpentinite dike*: (c) *variolite.*—The largest mass of altered diabase in this part of the island forms the cliffs at Point Stuart and crops out at various places along the shore to the S S E. While the altered diabase exhibits facies identical to those already described, in the immediate neighbourhood of the lighthouse south of the old Military Post, much of it consists either of intrusive breccia or develops a type of spheroidal structure (Ransome, 1894, p. 201). This latter feature is not pillow-structure and each bulbous projection is little more than 2 to 4 inches in size. The effect is to give the outcrops a rubbly appearance and is a type of auto-

TABLE 2

	1	2	3	4	5	6	7
SiO_2	46.98	46.52	52.89	52.86	48.26	50.31	42.06
TiO_2	—	0.92	1.12	1.49	2.51	0.10	—
Al_2O_3	17.07	13.76	13.20	11.17	12.81	1.15	2.72
Fe_2O_3	1.85	2.23	4.93	2.94	4.10	2.02	
FeO	7.02	6.84	3.22	8.93	9.15	3.18	2.88
MnO	—	0.07	0.12	0.03	0.16	0.11	—
MgO	8.29	9.30	5.67	7.70	6.71	22.68	39.53
CaO	12.15	12.16	10.95	4.77	8.76	17.32	nil
Na_2O	2.54	1.91	2.56	5.30	2.93	0.12	—
K_2O	0.53	0.23	0.13	0.02	0.10	0.01	—
H_2O^+	4.86*	5.15	2.09	3.21	3.47	2.82	12.04*
H_2O^-		0.39	0.25	0.25	0.32	0.08	
P_2O_5	0.09	0.10	0.18	0.15	0.36	0.03	nil
CO_2	—	0.21	2.45	0.27	0.01	0.31	—
	101.38	99.79	99.76	99.09	99.65	100.24	99.23
SG	3.20	3.22	3.02	3.11	3.21	3.09	2.61

* loss on ignition

1. "Fourchite" (altered diabase) from main sill, Angel Island. Coarse main phase (Ransome, 1894, p. 231. Analyst, F. L. Ransome).
2. Altered diabase from main sill, Angel Island. Coarse main phase. Analyst, T. W. Bloxam.
3. Variolitic diabase from marginal phase of sill, Point Knox, Angel Island. Analyst, T. W. Bloxam.
4. Glaucophanized marginal phase of the diabase, Point Stuart, Angel Island. Analyst, T. W. Bloxam.
5. Glaucophanized marginal phase of the diabase, Point Simpton, Angel Island. Analyst, T. W. Bloxam.
6. Partially serpentinized pyroxenite, 900 feet N. E. of Point Stuart, Angel Island. Analyst, T. W. Bloxam.
7. Serpentinite, hard nodule in crushed matrix, Angel Island (Ransome, 1894, p. 231. Analyst, F. L. Ransome).

breccia. Ransome (1894, p. 209) considers it probable that these phases of the intrusive were emplaced in a brecciated condition at very shallow depth.

Texturally they are fine-grained rocks with a flinty fracture and contain altered feldspars mainly in the form of spherulites and larger sub-radiate fibrous bundles, all of which have been altered to chlorite. Much of the rock consists of brown glass, some of which represents pyroxene, a few aborescent fibres of which can occasionally be seen. Except where they are sheared the variolitic rocks contain no glaucophane.

An analysis of the variolitic diabase is given in table 2, column 3.

(3) *Marginal glaucophanization of the altered diabase.*—With the exception of the variolites, all varieties of altered diabase contain lawsonite and glaucophane (± jadeite). However, where they have been sheared, glaucophane becomes extremely abundant and schistose glaucophane rocks are produced from the diabase. A good example of this is to be seen on the shore between the old pier and Point Stuart where massive spheroidally weathering altered diabase is traversed almost at beach-level by numerous sub-horizontal shear-planes. The rock becomes increasingly cataclastic and detached blocks and fragments lie in a sinuous web of pale blue glaucophane; the rock-changing in color from dark green to blue. Small vertical shear planes and faults

which cut the diabase are often completely filled with massive clumps of glaucophane.

Two analyses of strongly sheared and glaucophanized diabase are given in table 2, columns 4 and 5.

PILLOW LAVA

The only exposure of pillow-lava on the island occurs on the sea-cliff at Point Blunt, just below a small lighthouse (Ransome, 1894, p. 202). The pillow-lava is in fault contact with conglomeratic metagraywackes to the west and east and lies beneath metagraywacke forming the cliff-slope above.

The pillows are ellipsoidal in shape and vary in size from about one to three feet. The tops are convex and the bottoms concave, fitting around, or sending downward protuberances into spaces between lower pillows. Wilson's (1940) criteria indicate that the lavas are the right way up, but the adjacent metagraywackes dip at high angles.

In thin sections the pillow-lavas have a variolitic texture and are almost identical to the variolitic phases of the altered diabase, with fine brush-like and spherulitic groupings of feldspar set in a matrix of brown glass. Like that in the altered diabase, the feldspar has been largely replaced by chlorite.

The matrix between the pillows consists mainly of calcite in which are scattered globular aggregates of brown glass similar to that forming the pillows. Associated with the glass and occupying branching veins are irregular patches of pumpellyite (cf. Bloxam, 1958; 1959, p. 102).

SERPENTINITE AND PYROXENITE

Traversing the western part of the island is a prominent almost vertical dike-like sheet of serpentinite which trends approximately N N W and attains a maximum width of about 500 feet. The major boundaries of the serpentinite are usually faults and the term "dike" is used more in a descriptive sense since the marginal metasediments are generally vertical, suggesting that the serpentinite may well have been a concordant sheet or sill.

The serpentinite is always strongly sheared, particularly at its contacts, and consists of greenish slickensided masses within which are nodules of less sheared serpentinite (table 2, column 7). Both types are almost completely serpentinized and consist of a dense aggregate of colorless twinned clinochlore which have $\beta = 1.591$, $\gamma - \alpha = 0.008$, $2V_\gamma \sim 10°$, and X parallel to the elongation. With one or two exceptions, pseudomorphs are rare and, when present, are always after pyroxene, no olivine, or evidence of its former presence, having been detected (Ransome, 1894, p. 222). The few opaque minerals consist mainly of parallel streaky clusters of iron-ore and occasional deep brown crystals of chrome-spinel (picotite).

Partially serpentinized specimens of pyroxenite have been obtained from the dike. The analyzed rock (table 2, column 6) consists of diallagic pyroxene up to 5 mm in length, partially replaced by serpentine which also appears to invade the rock along a network of branching veinlets. The optical properties of this pyroxene are identical with that in the altered diabase (p. 562-563).

GLAUCOPHANE-SCHISTS ASSOCIATED WITH THE INTRUSIVE IGNEOUS ROCKS

General statement.—In addition to the extensive developments of jadeite-bearing metagraywacke which carry variable, but generally small amounts of blue-amphibole, there are a group of schistose glaucophane-rich rocks which owe their origin in part to processes controlled largely by proximity to both the altered diabase and the serpentinite. While the relationship of the glaucophane-schists to the diabase and serpentinite is very similar, much more glaucophane-schist is associated with the serpentinite than with the diabase (fig. 2).

Ransome (1894) noted that "sandstones and cherts" in contact with the altered diabase and serpentinite had been converted to glaucophane-schists. He states that "In no single instance has any schist been found upon the island that does not bear the above relation either to the fourchite (altered diabase) or the serpentinite" (1894, p. 211). It will be recalled, however (p. 558), that Ransome had overlooked the rather less obvious metamorphic character of graywackes over nearly the whole of the island.

(1) *Glaucophane-schists associated with the altered diabase.*—Glaucophane-schist forms an apparently continuous zone adjacent to the lower and upper surfaces of the altered diabase (Ransome, 1894, p. 195). However, many of the exposures described by Ransome are no longer available due to subsequent building on the island.

Actual contacts have not been found inland, but the presence of glaucophane-schist between jadeitic-metagraywacke country rock and the altered diabase can be reasonably inferred by sporadic exposures of schist along the approximate line of junction (Ransome, 1894, p. 211). At its widest the glaucophane-schist zone is seldom greater than about 6 feet, but may swell to some 12 feet.

Contacts between the altered diabase and metasediments are exposed on the shore near Point Simpton, and also to the west where the sheet reaches the shore again between Point Ione and Point Stuart. At Point Simpton the bottom of the sheet becomes progressively glaucophanized and sheared towards the metagraywackes beneath, and contains numerous inclusions of glaucophanized graywacke (table 3, column 4). The contact itself is largely a mélange comprising sheared and glaucophanized diabase and metagraywacke, riddled with veins and pods of glaucophane, quartz, and calcite. The graywacke below has been converted to tough blue glaucophane-schist consisting of abundant fibrous glaucophane, lawsonite, and subordinate actinolite which define the schistosity, together with mica and streaky clusters of brown sphene (plate 1H). Quartz is present, some of which probably represents recrystallized chert fragments. No jadeite occurs (table 3, column 3).

About 12 inches further down, the rock becomes paler in color and less schistose; glaucophane decreases in amount and aggregates of "dusty" green and partially glaucophanized acmitic-jadeite appear. Quartz is more abundant in the form of recrystallized chert fragments, and the rock is referred to as "transitional glaucophane-schist" in table 3, column 2. About 3 feet below the contact the transitional glaucophane-schist merges into normal buff-colored jadeite-bearing metagraywacke with a little crossite (table 3, column 1).

TABLE 3

	1	2	3	4
SiO_2	69.77	60.63	57.18	48.26
TiO_2	0.41	1.21	1.06	2.51
Al_2O_3	14.82	15.98	13.77	12.81
Fe_2O_3	1.21	1.11	0.89	4.10
FeO	1.35	3.62	6.01	9.15
MnO	0.03	0.11	0.18	0.16
MgO	2.38	4.07	6.56	6.71
CaO	1.99	4.34	5.11	8.76
Na_2O	3.89	3.59	4.41	2.93
K_2O	1.01	1.00	0.87	0.10
H_2O^+	2.96	3.36	3.23	3.47
H_2O^-	0.20	0.31	0.26	0.32
P_2O_5	0.08	0.01	0.08	0.36
CO_2	0.10	0.42	0.61	0.01
	100.20	99.76	100.22	100.06
SG	2.89	2.96	3.15	3.21

1. Jadeite-bearing metagraywacke, 3 feet below altered diabase, Point Simpton (see table 1, column 4).
2. Quartz-glaucophane-schist (from graywacke), transitional glaucophane-schist, 1 foot below altered diabase, Point Simpton. Analyst, T. W. Bloxam.
3. Glaucophane-schist (from graywacke), contact phase with altered diabase, Point Simpton. Analyst, T. W. Bloxam.
4. Glaucophanized marginal phase of the diabase, Point Simpton (see table 2, column 5).

It is probable that the above assemblages (quartz-glaucophane-lawsonite; quartz-jadeite/acmite-glaucophane-lawsonite and quartz-jadeite-lawsonite-crossite) may owe their development to differences in bulk chemical composition rather than large changes in pressure. Hence in rocks with progressively more Fe and Mg the place of jadeite is taken by jadeite-acmite and eventually glaucophane (cf. Brothers, 1954, p. 620; Bloxam, 1956, p. 496; 1959, p. 102; Fyfe, Turner and Verhoogen, 1958, p. 176).

West of the serpentinite dike, and about 1,000 feet E N E from Point Stuart, the altered diabase is in contact with metacherts which form a thick band in the metagraywackes. Large wedges of disrupted metachert have been caught up by the instrusive diabase which is also full of smaller metachert fragments (Ransome, 1894, p. 217). As at Point Simpton, the marginal diabase has been extensively glaucophanized together with the associated metacherts which have been altered to flinty dark-bluish schists with regularly alternating bands of paler bluish-pink suggestive of original bedding. The metacherts are highly siliceous and consist essentially of an even-grained quartz mosaic riddled with stilpnomelane and riebeckite. The habit of the stilpnomelane is characteristic of that in many other Franciscan metacherts and consists of a number of ragged fibres arranged in small sheaf-like or "bow-tie" bundles. The mineral is frequently replaced by riebeckite which often preserves the form of the stilpnomelane aggregates. The paler bands are richer in lawsonite and contain glaucophane together with very small inter-locking granules of garnet, probably manganese-rich (Bloxam, 1959, p. 104).

(2) *Glaucophane-schists associated with the serpentinite.* (a) *General relationships.*—Serpentinite contacts on the island are less favorably exposed and when they do occur are always faults. Ransome (1894) observed that glaucophane-schists were also developed marginal to the serpentinite dike and

that many large masses of glaucophane-schist occured on the *upper* (west) side of the dike which he considered to be hading at about 35° to the south-west. The present writer was unable to confirm this hade, the dike appearing nearly vertical in the cliff sections examined. Ransome also oversimplified the structure and omitted numerous NNW trending faults which make interpretation of the relationships extremely difficult. Nevertheless, wherever glaucophane-schists appear they occur either directly in association with serpentinite or in circumstances from which this relationship can be reasonably inferred.

Inland exposures are poor but outcrops of glaucophane-schist are nearly always interposed between the metagraywackes and serpentinite along its western boundary. Cliff sections along the southern shore are extensively faulted, so that within a few feet, there may be rapid alternations of serpentinite, glaucophane-schist and metagraywacke (fig. 3). These rapid variations may not be entirely tectonic but could represent original interfingering between the intrusive serpentinite and sediments which has been further complicated by faulting along the serpentinite contacts (e.g. Wilson, 1943, p. 196.)

In addition to glaucophane-schists developed marginal to the serpentinite, numerous massive blocks of glaucophane-schist and occasionally metagraywacke occur as inclusions within the serpentinite. While some may represent rafts of sediment caught up during the emplaceemnt of the serpentinite, the majority are probably tectonic inclusions (Brothers, 1954, p. 623.)

All the major faults post-date the Franciscan sedimentary and igneous rocks and the metamorphism, and, while they cannot be definitely dated on Angel Island, are probably related to post-Jurassic to Recent diastrophism during the evolution of the California Coast Range (Reed and Hollister, 1951).

(b) *Detailed relationships.*—The best locality for examining these relationships is along the shore about 1,000 feet ESE from the lighthouse at Point

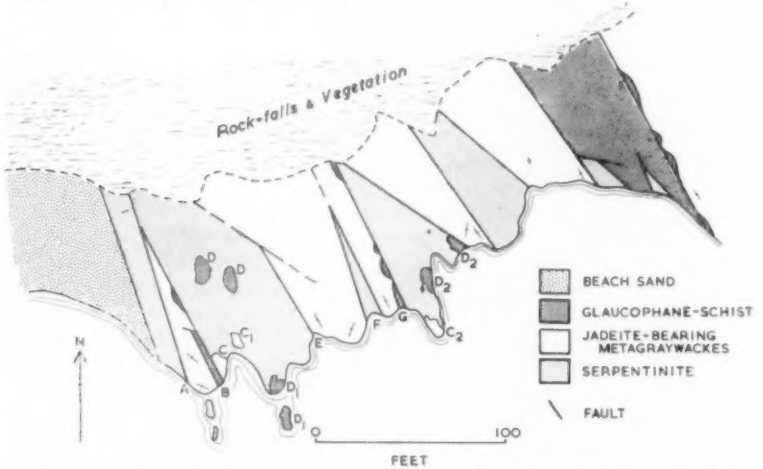

Fig. 3. Sketch-map of shore-section 1000 feet ESE from the lighthouse at Point Knox.

Knox, beginning at the eastern end of a sandy bay. A sketch map of the locality is given in figure 3.

Rising above the sand at the end of the sandy bay is a sheared wedge of serpentinite bounded on either side by faults which bring it into contact with a vertical strip of jadeite-bearing metagraywacke to the east (fig. 3A). Thinly laminated chert bands containing riebeckite and stilpnomelane also occur in the metagraywacke. Interposed between these metasediments and another faulted mass of serpentinite is a zone of fault breccia containing broken-up glaucophane-schist derived from metagraywacke (fig. 3B). A small wedge of shattered metagraywacke bounded in part by serpentinite lies on the eastern side of the fault (fig. 3C), and a similar, but larger mass (fig. $3C_1$), is completely surrounded by the serpentinite. A little further up the sea-cliff some large masses of glaucophane-schist (D) are also enclosed by the serpentinite (tectonic inclusions), while others form a small promontary near sea-level (fig. $3D_1$). The serpentinite terminates eastwards against a fault (fig. 3E), which introduces a wider belt of jadeite-bearing metagraywacke cut by a small fault-wedge of serpentinite (fig. 3F); followed by another fault introducing more serpentinite (fig. 3G). Along this fault-zone discontinuous pods of brecciated glaucophane-schist are exposed similar to those in locality B, except that they have originated from cherts and contain abundant quartz, stilpnomelane, and riebeckite. The adjacent serpentinite encloses one large mass of metagraywacke and two of glaucophane-schist (fig. 3, C_2 and D_2).

INTERPRETATION OF THE CONTACT RELATIONSHIPS

(1) *Altered diabase contacts.*—Ransome (1894) considered that the development of glaucophane-schists from sedimentary formations marginal to the diabase was the result of contact alteration associated with the *emplacement* of the basic magma. It has been demonstrated, however, that the diabase has also been metamorphosed, hence the metamorphism must post-date the diabase and is not directly associated with its emplacement.

Chemical analyses (table 3) show that the regionally prevalent jadeite-bearing metagraywackes have been modified in chemical composition near the diabase, the principle changes involving loss of Si and gains in total Fe, Mg, Ca, Ti, and possibly a little Na. Very similar chemical changes were noted by the writer at Valley Ford (Bloxam, 1959, p. 110) in association with the glaucophanization of jadeite-bearing metagraywackes.

The evidence is compatable with Turner and Verhoogen's (1951, p. 244) hypothesis that active solutions may have risen along suitable paths afforded by shear planes (e.g. igneous contacts). Their effect has been to modify the composition of the arkosic graywacke into one more appropriate to the development of glaucophane.

(2) *Serpentinite contacts.*—Faulting at the serpentinite contacts largely obscures the original relationships and no complete transition from jadeite-bearing metagraywacke into glaucophane-schist has been observed. Instead, the glaucophane-schist occurs as broken-up lenses in fault-zones between jadeite-bearing metagraywackes and serpentinite. However, by implication, it

is probable that the relationships are the same as those between the glaucophane-schists and diabase.

Ransome's analysis of the serpentinite is given in table 2, column 7. If the serpentinite has in fact been derived from pyroxenite their respective analyses (table 2, columns 6 and 7) indicate considerable changes in composition; Mg and water having been added; some Si and all the Ca removed. It is possible, therefore, that serpentinization of the pyroxenite may have played a direct part in the redistribution of certain elements in its vicinity (Turner and Verhoogen, 1951, p. 244).

It has already been noted (p. 566) that relatively more glaucophane-schist is associated with the serpentinite than with diabase. This may be due in part to the processes outlined above and also to the easier access of solutions, whatever their origin, along shear zones associated with the serpentinite (Turner and Verhoogen, 1951, p. 244).

SUMMARY AND DISCUSSION

(1) Arkosic Franciscan graywackes, which form the major rock-type on Angel Island, have been metamorphosed to glaucophane-poor jadeite-bearing metagraywackes with virtually no change in chemical composition. Jadeite has formed mainly from detrital albite (albite = jadeite + quartz).

(2) The development of the jadeite-bearing rocks may be described as regional in extent and is not related to proximity with basic or ultrabasic intrusions.

(3) A sheet of diabase intrusive into the graywackes has also been metamorphosed and its original feldspar converted to chlorite, lawsonite, and jadeite (± glaucophane). The marginal phases of the diabase are sheared and become progressively enriched in glaucophane.

(4) At contacts with the altered diabase the graywackes have been desilicated and enriched in Fe, Mg, Ca, Ti, and possibly Na; leading to the development of glaucophane-schist. Away from the contact-zone the glaucophanized metagraywackes grade into normal arkosic jadeite-bearing metagraywacke. Similar relationships also occur where the diabase comes into contact with radiolarian cherts.

(5) Serpentinite contacts with the graywackes are extensively faulted, but evidence has been presented which suggests that the relationship of glaucophane-schist to serpentinite is the same as that with the altered diabase.

(6) The chemical alteration of graywackes marginal to the diabase and serpentinite is probably due to the activity of hydrothermal solutions of uncertain origin which have been localized along contact zones and associated shear planes. They may be earlier than, or contemporaneous with, the metamorphism, and some may be directly related to serpentinization.

(7) Plagioclase is considered to be unstable in all these metamorphic assemblages, and is replaced by jadeite, lawsonite, and chlorite. Jadeite only appears to be stable in arkosic metagraywackes poor in Fe, Mg and Ca; its place being taken by acmitic-jadeite and glaucophane in rocks with higher proportions of these elements (e.g. glaucophane-schists).

The mineralogical relationships are summarized in table 4.

TABLE 8

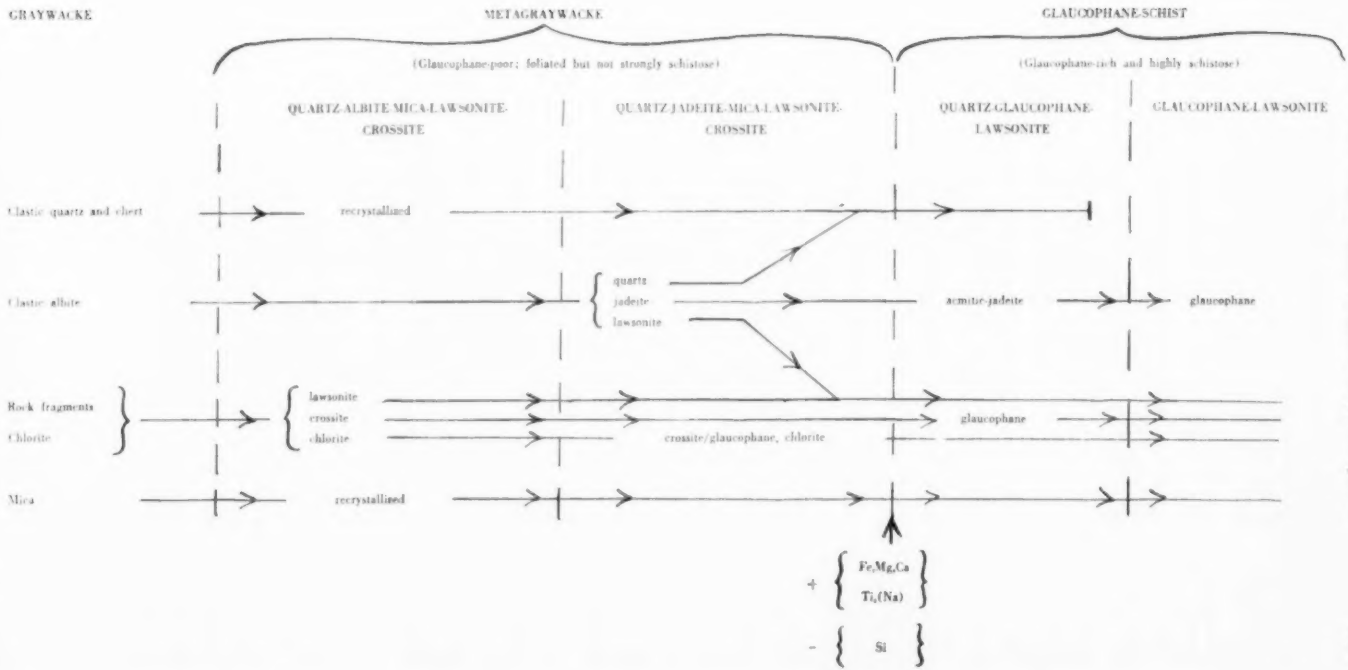
GRAYWACKE
METAGRAYWACKE
(Glaucophane-poor; foliated but not strongly schistose)
GLAUCOPHANE-SCHIST
(Glaucophane-rich and highly schistose)
QUARTZ-ALBITE-MICA-LAWSONITE-CROSSITE
QUARTZ-JADEITE-MICA-LAWSONITE-CROSSITE
QUARTZ-GLAUCOPHANE-LAWSONITE
GLAUCOPHANE-LAWSONITE
Clastic quartz and chert
recrystallized
Clastic albite
quartz
jadeite
lawsonite
acmite-jadeite
glaucophane
Rock fragments
Chlorite
lawsonite
crossite
chlorite
glaucophane
crossite/glaucophane, chlorite
Mica
recrystallized
+
Fe,Mg,Ca
Ti,(Na)
-
Si

The early investigations of Ransome (1894) and Lawson (1895) established the fact that in many parts of California glaucophane-schists of the Franciscan were intimately associated with intrusive bodies of serpentinite; they were considered to have been produced by contact metamorphism and metasomatism accompanying the emplacement of the ultrabasic magma. The glaucophane-schist-serpentinite association in California still appears to be valid on the evidence of more recent field mapping. Wilson (1943, p. 197) states that . . . "The origin of the (glaucophane) schists by pneumatolytic action accompanying the ultra-basic intrusions seems demonstrated by the proximity of the schists to these intrusive bodies, and their gradation into unaltered sediments both along and across the strike". Similar conclusions have been reached by Taliaferro (1941; 1943) who found that the elements most commonly introduced into the marginal rocks were Na, Mg, Ca, Ti and Al; the metamorphism and metasomatism being genetically connected with the ultrabasic magma (see also Crittenden, 1951, p. 25-26). Crittenden notes that . . . . "The most extensive areas of glaucophane-bearing rocks in the San Jose-Mount Hamilton area are those associated with the long narrow serpentine sill . . . . (and) occur as narrow lenses mostly along the western, presumably upper, margin of the sill, and as irregular areas interfingering with the serpentine and sediments". The similarity between these observations and those made on Angel Island is apparent.

Turner and Verhoogen (1951, p. 244) and Fyfe, Turner and Verhoogen (1958, p. 225) conclude that the development of glaucophane-schist by hydrothermal metamorphism at intrusive contacts or more remote points situated on zones of dislocation is well established (cf. Borg, 1956). In addition the effects of later movements often complicates the original relationships and numerous authors have confirmed the plastic mobility of serpentinite in fault-zones and along tight isoclinal fold axes (Wilson, 1943, p. 196-197; Taliaferro, 1943; Gealey, 1951).

As more data accumulate it is becoming clear that extensive areas of Franciscan graywacke, hitherto regarded as unmetamorphosed, have been altered to jadeite-bearing metagraywackes (Bloxam, 1956; 1959; McKee, 1958). Similar rocks have also been described from Celebes (de Roever, 1955) and Japan (Seki and Shidô, 1959). In California glaucophane-rich schists may represent a particular phase of the widespread metamorphism in areas of appropriate lithology, or in rocks suitably modified in chemical composition.

ACKNOWLEDGMENTS

The present work was undertaken in the University of California, Berkeley. The writer wishes to thank Professor F. J. Turner for his guidance and encouragement, and for reading the manuscript. Thanks are also accorded to the Commonwealth Fund of New York for a Harkness Fellowship that enabled the writer to work at Berkeley, and also for defraying the cost of some chemical analyses. Colonel Keene Saxon of the Presidio, San Francisco, kindly gave the writer permission to visit Angel Island. Grateful thanks are also accorded to Professor F. H. T. Rhodes, University College, Swansea, for his help and encouragement.

References

Bloxam, T. W., 1955, Glaucophane-schists and associated rocks at two Californian localities: Geol. Soc. America Bull. (Abst.), v. 66, p. 1644-1645.

————, 1956, Jadeite-bearing metagraywackes in California: Am. Mineralogist, v. 41, p. 488-496.

————, 1958, Pumpellyite from South Ayrshire: Mineralog. Mag., v. 31, p. 811-813.

————, 1959, Glaucophane-schists and associated rocks near Valley Ford, California: Am. Jour. Sci., v. 257, p. 95-112.

Borg, I. Y., 1956, Glaucophane schists and eclogites near Healdsburg, California: Geol. Soc. America Bull., v. 67, p. 1563-1584.

Brothers, R. N., 1954, Glaucophane schists from the North Berkeley Hills, California: Am. Jour. Sci., v. 252, p. 614-626.

Crittenden, M. D., 1951, Geology of the San Jose-Mount Hamilton area, California: Calif. Dept. Nat. Res., Div. Mines Bull. 157, p. 1-74.

de Roever, W. P., 1955, Genesis of jadeite by low-grade metamorphism: Am. Jour. Sci., v. 253, p. 283-298.

Fyfe, W. S., Turner, F. J., and Verhoogen, J., 1958, Metamorphic reactions and metamorphic facies: Geol. Soc. America Mem. 73, p. 1-259.

Gealey, W. K., 1951, Geology of the Healdsburg Quadrangle, California: Calif. Dept. Nat. Res., Div. Mines Bull. 161, p. 1-50.

Hess, H. H., 1949, Chemical composition and optical properties of common clinopyroxenes, part 1: Am. Mineralogist, v. 34, p. 621-666.

Lawson, A. C., 1895, A contribution to the geology of the Coast Ranges: Am. Geologist, v. 15, p. 342-356.

McKee, B., 1958, Jadeite alteration of sedimentary and igneous rocks: Geol. Soc. America Bull., (Abst.), v. 69, p. 1612.

Ransome, F. L., 1894, Geology of Angel Island: Univ. Calif. Pub. Dept. Geology, v. 1, p. 193-235.

————, 1895, On lawsonite, a new rock-forming mineral from the Tiburon Peninsula, Marin County, California: Univ. Calif. Pub. Dept. Geology, v. 1, p. 301-312.

Reed, R. D., and Hollister, J. S., 1951, Geology of California: Am. Assoc. Petroleum Geologists, Tulsa.

Seki, Y., and Shidō, F., 1959, Finding of jadeite from the Sanbagawa and Kamuikotan metamorphic belts, Japan: Japan Acad. Proc., v. 35, p. 137-138.

Taliaferro, N. L., 1941, Geologic history and structure of the central Coast Range of California: Calif. Dept. Nat. Res., Div. Mines Bull. 118, p. 119-163.

————, 1942, Geologic history and correlation of the Jurassic of south-western Oregon and California: Geol. Soc. America Bull., v. 53, p. 71-112.

————, 1943, The Franciscan-Knoxville problem: Am. Assoc. Petroleum Geologists Bull., v. 27, p. 109-219.

Turner, F. J., and Verhoogen, J., 1951, Igneous and metamorphic petrology: New York, McGraw-Hill.

Vuagnat, M., and Jaffé, F., 1954, Sur les ophisphérites de la région des Gets (Haute-Savoie): Archives des Sci. Soc. de physique et de Histoire Nat. de Genève, v. 7, p. 5-14.

Williams, J. F., 1891, The igneous rocks of Arkansas: Ann. Rpt. Geol. Survey Arkansas for 1890, v. 2.

Wilson, I. F., 1943, Geology of the San Benito Quadrangle, California: Calif. Jour. Mines and Geology, v. 39, p. 183-270.

Wilson, M. E., 1941, Noranda district, Quebec: Geol. Survey Canada Mem. 229, p. 1-162.

[American Journal of Science, Vol. 258, October 1960, P. 574-582]

SYSTEMS S-Na_2O-H_2O AND S-H_2O: APPLICATION TO THE MODE OF ORIGIN OF NATURAL ALKALINE POLYSULFIDE AND THIOSULFATE SOLUTIONS*

R. H. ARNTSON[1], F. W. DICKSON[2], and GEORGE TUNELL[3]

ABSTRACT. Sulfur reacts with aqueous NaOH to form sodium sulfide and sodium thiosulfate; in the presence of excess sulfur the polysulfide complex ion $S_x^=$ forms, where "x" is approximately five. The saturation concentrations of sulfur in aqueous NaOH solutions allowed to react with excess of orthorhombic sulfur have been determined at 25°C and one atmosphere pressure. Inasmuch as alkaline aqueous solutions are known to exist in nature, the reaction of sulfur with NaOH solutions suggests a possible mode of origin of natural sodium polysulfide and thiosulfate solutions. Alkaline aqueous solutions encountering elemental sulfur would react to produce sodium polysulfide and sodium thiosulfate, substances which are capable of forming soluble complex ions with ore-forming substances.

INTRODUCTION

Geologists speculating on the processes involved in the formation of ore deposits have been hampered by the scarcity of pertinent physical chemical data. There is general agreement that one fundamental source of ore-forming substances is magmas, which, in the course of crystallization, give off fluids capable of transporting ore metals. Agreement is less wide as to possible mechanisms by which the ore-forming elements along with other constituents separate from the parent magma, or the physical and chemical character of the transporting media, or the factors controlling deposition of the ore minerals under either deep-seated or shallow conditions. The purpose of this paper is to present our experimental studies on the system S–Na_2O–H_2O, to discuss other work on the system S–H_2O, and to consider the possible modes of formation of alkaline polysulfide and thiosulfate solutions which may be capable of transporting certain ore-forming components under conditions which prevail at shallow depths in the Earth's crust.

EXPERIMENTAL WORK

The saturation curves of orthorhombic sulfur in aqueous Na_2S solutions (system S–Na_2S–H_2O) at 25°C and 50°C determined by Arntson, Dickson, and Tunell (1958) show behavior explainable by the assumption that various reactions which compete for sulfur shift differentially with changing temperature and Na_2S concentrations. NaOH is present in the solutions as a consequence of the hydrolysis of Na_2S to NaHS. Therefore, since sulfur is known to react with NaOH solutions (Mellor, 1930, p. 516) the solubility of orthorhombic sulfur in aqueous NaOH solutions (system S–Na_2O–H_2O) was studied at 25°C and one atmosphere pressure. The experimental data are presented in tables 1 and 2 and figure 1.

Experimental mixtures were prepared by diluting carbonate-free saturated NaOH solutions with boiled distilled water and mixing with orthorhombic

* Institute of Geophysics Paper Number 135, University of California, Los Angeles, California.

[1] Shell Development Company, P. O. Box 481, Houston 1, Texas.
[2] Division of Physical Sciences, University of California, Riverside, California.
[3] Department of Geology, University of California, Los Angeles, California.

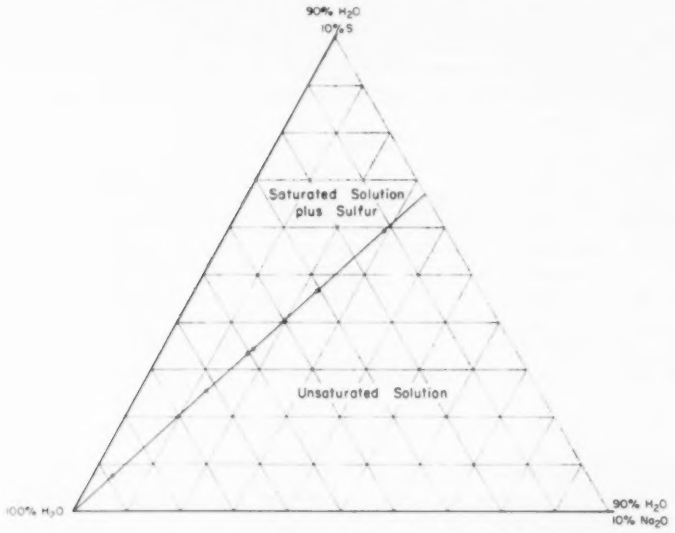

Fig. 1. Saturation curve of orthorhombic sulfur in the system S-Na_2O-H_2O at 25°C and 1 atmosphere pressure, in the concentration range from 90 percent to 100 percent water.

sulfur in tetrafluorethane bottles in an oxygen-free nitrogen atmosphere. Sufficient solid sulfur was added to ensure complete reaction and to maintain at all times the presence of excess solid phase. The bottles were rotated at constant temperature (25°C ± 0.02°C) for times ranging from five days to several weeks. The sulfur concentration of mixtures allowed to react for five days agreed well (within ± 0.01 percent) with the sulfur concentration of mixtures of the same initial NaOH concentration allowed to react for several weeks, indicating that equilibrium was probably attained in five days.

The saturated solutions were analyzed by a modification of a procedure of Dickson and Tunell (1958) which involved the use of H_2O_2 to oxidize sulfide ion to sulfate ion. In preparation for analysis the saturated solutions were filtered through a fritted glass filter to remove suspended solid sulfur and placed in a weight buret which was then allowed to come to room temperature. The filtered sample was divided into two portions, one to be analyzed for sodium in the form of Na_2SO_4, and the other to be analyzed for total sulfur in the form of $BaSO_4$. To the samples was first added concentrated NH_4OH followed by the addition of five percent H_2O_2 to oxidize all dissolved sulfur to sulfate. The role of the NH_4OH was to prevent immediate precipitation of sulfur when the H_2O_2 was first added. The sodium was determined by weighing as Na_2SO_4, and the Na_2O and NaOH percentages in weight per cent were calculated from the weight of the Na_2SO_4. The total sulfur was determined by weighing as $BaSO_4$, and the S concentration in weight percent was calculated from the weight of $BaSO_4$. Water percentages were determined by difference.

TABLE 1

Compositions (in weight percent) of solutions saturated with orthorhombic sulfur in the system S–Na_2O–H_2O at 25.00°C ± 0.02°C and 1 atmosphere pressure, calculated as Na_2O, S, and H_2O

Percentage by Weight		
Na_2O	S	H_2O (by difference)
0.38	0.75	98.87
1.26	2.53	96.21
1.63	3.33	95.04
1.70	3.42	94.88
2.30	4.64	93.06
2.93	5.92	91.15

TABLE 2

Compositions of solutions (in weight percent) saturated with orthorhombic sulfur in the system S–Na_2O–H_2O calculated as NaOH, S, and H_2O

Percentage by Weight		
NaOH	S	H_2O (by difference)
0.49	0.75	98.76
1.63	2.53	95.84
2.11	3.33	94.56
2.20	3.42	94.38
2.97	4.64	92.39
3.78	5.92	90.30

CHEMICAL DISCUSSION

According to Mellor (1930, p. 516) solid sulfur reacts with sodium hydroxide solutions to form sodium polysulfide and sodium thiosulfate by a reaction such as:

$$(2n + 4)S + 6\,NaOH \rightarrow 2Na_2S_{(n+1)} + Na_2S_2O_3 \qquad (1)$$

where "n" is the number of sulfur atoms linked to sulfide ion. If the equation is correct, the mole ratio of $Na_2S_{(n+1)}$ to $Na_2S_2O_3$ in saturated solutions should be 2 to 1. The ratio can be calculated from the experimental data on the basis of the following assumptions: (1) that no other species of chemical substance is present in significant quantities in the saturated solution; and (2) that the average value of "n" (3.77 ± 0.03) determined by Arntson, Dickson, and Tunell (1958, p. 718) for solutions of Na_2S saturated with orthorhombic sulfur at 25°C holds for solutions in the system S–Na_2O–H_2O. The following equations can then be written:

$$2\,[Na_2S_2O_3] + (n+1)\,[Na_2S_{(n+1)}] = [S]:$$
$$[Na_2S_2O_3] + [Na_2S_{(n+1)}] = [Na_2O],$$

where: enclosure by brackets indicates concentration in moles per kilogram in the saturated solution, [S] and [Na_2O] are known by analysis.

For convenience let [$Na_2S_2O_3$] be designated A, and [$Na_2S_{(n+1)}$] be designated B. Then, $2A + (n+1)B = [S]$ and $A + B = [Na_2O]$; by solving the two equations simultaneously for B, and by substituting for "n" the value 3.77, the following expression is obtained: $B = [S] - 2\,[Na_2O] / 2.77$. Table 3 presents the equilibrium data converted to moles per kilogram together with the calculated concentrations and mole ratios. The calculated ratio of B to A ($NaS_{(n+1)}/Na_2S_2O_3$) ranges from 1.9 to 2.4 and averages somewhat less than 2.2. Considering errors inherent in the calculation and uncertainties involved in the assumptions, 2.2 is in reasonable agreement with the theoretical value, 2.0; hence, the calculations provide strong supporting evidence that the reaction is as postulated.

The saturation curve of figure 1 approximates a straight line on the scale of the figure. When plotted on a larger scale a slight concavity toward the unsaturated solution field is noticeable, indicating that diluting a saturated solution with water produces a slightly undersaturated solution, and conversely, removal of water by evaporation causes sulfur in small quantities to precipitate.

Our experiments involved using rather highly concentrated NaOH solutions. It would be of considerable interest to know the nature of the reaction which takes place in only slightly alkaline or neutral solutions. Studies by Cherbuliez and Weibel (1936) indicate that in near neutral solutions at temperatures up to 100°C the following reaction takes place:

$$4\,S + 3H_2O \rightarrow 2H_2S + S_2O_3^{--} + 2H^+ \qquad (2)$$

In pure water, as the reaction proceeds, the solution very rapidly becomes acidic; dissolving as much as 0.6 mg sulfur in a liter of water increases the acidity sufficiently to cause the reaction to cease.

In slightly buffered solutions, such as in ordinary tap water, reaction with sulfur proceeds to a considerable extent (Cherbuliez and Weibel, 1936, p. 798). In presence of excess sulfur, polysulfides form by the following reaction:

$$H_2S + x\,S \rightleftarrows H_2S_x. \qquad (3)$$

Our experiments were carried out with sufficient sulfur present to more than saturate the solutions. The nature of the reaction products which form when the reaction is carried out with a deficiency of sulfur remains an open question. Reactions are possible which produce a combination of sulfide ion and thiosulfate ion, according to the following equation:

$$6OH^- + 4\,S \rightarrow 2S^{--} + S_2O_3^{--} + 3H_2O \quad . \qquad (4)$$

The possibility that mixtures of sulfide and polysulfide ions along with thiosulfate ions will be formed cannot be excluded. The evidence available in the literature which bear on this point allow no definite conclusions.

GEOLOGIC IMPLICATIONS

Interest has long been centered on the minerals deposited in and near hot spring outlets in the hope that the nature of the solutions capable of transport-

TABLE 3

Data of table 1 converted to moles per kilogram of saturated solution; and calculated concentrations of $Na_2S_2O_3$ and $Na_2S_{(n+1)}$ and their mole ratios

Moles per Kilogram				
Na_2O	S	$Na_2S_{(n+1)}$	$Na_2S_2O_3$	$\frac{Na_2S_{(n+1)}}{Na_2S_2O_3}$
0.061	0.234	0.040	0.0212	1.9
0.203	0.789	0.138	0.065	2.1
0.263	1.039	0.185	0.078	2.4
0.274	1.067	0.187	0.087	2.2
0.371	1.447	0.254	0.117	2.2
0.473	1.846	0.325	0.148	2.2

ing components of the ore minerals could be deduced. The reaction of sulfur with water and alkaline solutions provides a mechanism for the production in nature of sulfide and thiosulfate ions, substances which are capable of forming complexes with the metallic components of ore minerals.

Cherbuliez and Herzenstein (1936) discussed the geochemical significance of the reaction of sulfur with water. They pointed out that the sulfur content of natural thermal waters may in part result from the reaction of native sulfur with hot ground water, and with this in mind they examined the composition of waters from several hot springs (table 4). The amount of thiosulfate ion was less than the amount predicted by equation (2). The discrepancy was interpreted by Cherbuliez and Herzenstein to mean: (1) that much of the H_2S was formed by decomposition of sulfide minerals; or (2) that a portion of the $S_2O_3^{--}$ initially formed by the reaction of sulfur with water has decomposed. Reaction of thiosulfate with oxygen was rejected as unlikely, first, because of the persistence of H_2S in the solutions, which would not happen if oxygen were present; and secondly, the absence of the polythionates, in view of the known fact that polythionates result from partial oxidation of $S_2O_3^{--}$ ion. The hydrolysis of $S_2O_3^{--}$ ion to H_2S and SO_4^{--} ion by the following reaction was considered:

$$S_2O_3^{--} + H_2O \rightleftarrows H_2S + SO_4^{--} \quad . \qquad (5)$$

In acid solutions this reaction is known to take place, but has not been observed to take place in neutral or alkaline solutions, except in the presence of catalytic agents such as Cd^{++}. Cherbuliez and Herzenstein therefore postulate that much of the H_2S and $S_2O_3^{--}$ found in the waters they examined was formed by the reaction of sulfur and water, with the comparatively low amount of $S_2O_3^{--}$ explained by the hydrolysis of $S_2O_3^{--}$ to H_2S and SO_4^{--} (eq. 5) catalyzed by metal ions such as Cd^{++}.

Thiosulfate ion has been detected in hot spring waters in the United States (Clarke, 1924, p. 196) and a related substance, tetrathionate ion ($S_4O_6^{--}$), was detected in water of volcanic origin from Mt. Lassen (Day and Allen, 1925, and Allen and Day, 1927). The possible ore-carrying role of thiosulfate ion has not been carefully considered, in spite of the known tendency

TABLE 4

Analysis of hot springs waters for H_2S, $S_2O_3^{--}$ and polythionic sulfur according to Cherbuliez and Herzenstein (1936)

Source	H_2S gm/liter	$S_2O_3^{--}$ gm/liter	Polythionic sulfur gm/liter
Piestany Tchécoslovaquie	0.0109	<0.0002	0
Alvaneu Grisons	0.0054	0.0017	0.0007 (?)
Rietbad St. Gall	0.0170	0.0017	
Schinznach Argovie	0.1734	0.0017	
Gurnigel Berne	0.0891	0.0022	
Balmquelle Lenk, Berne	0.1377	0.0036	0.0004
Ileana Bains d'Hercule Roumanie	0.0153	0.0038	0.0004
Heustrich Berne	0.0350	0.0058	0
Regina Maria Bains d'Hercule Roumanie	0.1146	0.0190	0

for many metallic ions to form soluble complex ions with thiosulfate. Some metals capable of forming complex ions with thiosulfate are copper, cadmium, zinc, cobalt, nickel, platinum, and silver. Very little is known, however, of the stability of such complexes at elevated temperatures and pressures, or of the composition of solid phases which may separate from metallic thiosulfate solutions subjected to changing conditions.

That alkaline solutions exist at shallow depths in the earth's crust seems probable. Studies of the water from hot springs associated with ore minerals indicate that, although the waters are generally near seven in pH, some waters have pH's as high as nine. For example, at Steamboat Springs, Nevada, Brannock, Fix, Gianella, and White (1948) found that the pH of the hottest springs (presumably those least modified by mixing with ground water) is near nine. The pH of superheated water at Amedee Hot Springs, from which mercury sulfide appears to be precipitating at the present time, is slightly greater than nine (Dickson, Tunell, Lawrence and Horton, 1957). If, as is commonly believed, the alkaline water now flowing out at the surface represents diluted and chemically modified hypogene solutions it is reasonable to suppose that at depth at somewhat higher temperatures and pressure the solutions were also alkaline. Near neutral and alkaline waters encountering elemental sulfur would react to form solutions of sulfide ion and thiosulfate ion, or perhaps polysulfide ion and thiosulfate ion.

That sulfide ion is capable of forming complexes with certain ore-forming substances such as HgS, Sb_2S_3, As_2S_3, and Au_2S_3 has been amply demonstrated

in the laboratory. Systematic studies of systems containing sodium sulfide, water, and metallic sulfides are few in number, but those which are available allow some inferences to be drawn as to the processes effective in the transport and deposition of ore minerals.

The structure and mineralogy of epithermal mercury and antimony sulfide deposits have led some ore geologists to conclude that HgS and Sb_2S_3 are transported in and deposited from aqueous solutions at slight depths below the surface where pressures probably do not exceed 100 atmospheres and where temperatures are in the range from 50°C to 200°C (Lindgren, 1933). Stibnite and cinnabar deposits are commonly found where there are evidences of past or present hot springs activity, and this leads to the conclusion that some stibnite and cinnabar deposits were formed by the action of similar ascending solutions. Some geologists hold that the last remnants of the ore solutions, greatly modified by dilution with ground waters and perhaps by oxidation and acidification, have issued, and in some places still continue to issue, as hot springs.

When reasoning is based on the chemical character of waters flowing out at the surface, a distinction must be maintained between solutions actively transporting metal sulfides, and those which are in the process of depositing or which have deposited metal sulfides. Where deposits of cinnabar, stibnite or sulfur have formed or are forming by deposition from hot spring solutions, it is obvious that the conditions which have prevailed or prevail are those conducive to deposition. When the solutions issue at the surface they are apt to have already been super-saturated by physico-chemical changes which have taken place below the Earth's surface. The effect of dilution by ground waters less alkaline than the ore-carrying solution would be to diminish the sulfide ion concentration and the overall alkalinity. Reaction with downward percolating acids formed at the surface would convert part of the Na_2S to H_2S, resulting in a more nearly neutral or acid solution; oxidation by dissolved oxygen could precipitate sulfur. Therefore, one would expect that modification of alkaline hypogene waters rising from depth would tend to produce more nearly neutral solutions.

Evidences as to the chemical character of the solutions which are capable of transporting the constituents of stibnite and cinnabar can be obtained from the study of the sequence of deposition of ore and gangue minerals in rock specimens. Textures indicating simultaneous deposition of several minerals can be explained only by deposition from a solution capable of transporting the appropriate chemical components simultaneously; thus, textural studies allow severe restrictions to be placed on the possible types of solutions. Petrographic studies by Dickson and Tunell (1955) indicate an intimate spatial and time association of cinnabar with the silica minerals. Arntson (1958) noted that stibnite shows a similar close relation to the silica minerals. Such associations suggest that the ore-forming solution must be able to dissolve HgS, Sb_2S_3, and SiO_2. Aqueous Na_2S solutions long have been known to be capable of dissolving and transporting these substances (Christy, 1879; Knox, 1906; Dryer, 1940; Krauskopf, 1951); recent studies by Dickson and Tunell (1955) and Arntson (1958) add support to the hypothesis that aqueous Na_2S solutions

are likely carrier solutions of mercury and antimony sulfides. Therefore, mineralogic, petrographic, and laboratory studies support the concept that alkaline sulfide solutions are involved in the transport of the components of some of the metal sulfides and silica minerals found in epithermal and hot spring deposits. Such alkaline sulfide solutions may form by reaction of elemental sulfur with slightly alkaline water.

CONCLUSIONS

The reaction of sulfur with NaOH solutions provides a possible mechanism for the production of alkaline Na_2S and $Na_2S_2O_3$ solutions in nature under shallow earth conditions, by the reaction of alkaline solutions with elemental sulfur. Conclusions from hot spring water studies are consistent with the hypothesis that some hypogene solutions are alkaline. The ore-forming components of metallic sulfides such as HgS and Sb_2S_3 could be dissolved and transported in solution as soluble complex ions. Deposition of the metal sulfides from solutions would take place in response to variations in temperature or pressure, or by reaction with ground waters or host rocks.

ACKNOWLEDGMENTS

This work was supported by a grant of the National Science Foundation. Our gratitude is expressed to Dr. K. J. Hsu, Shell Development Company, Houston, Texas, and to Dr. Thane H. McCulloh, Division of Physical Sciences, University of California, Riverside, California, for their careful review of the manuscript.

REFERENCES

Allen, E. T. and Day, A. L., 1927, Steam wells and other thermal activity at the Geysers, California: Carnegie Inst. Washington, pub. no. 378, p. 33.

Arntson, R. H., 1958, Solubility of metallic sulfides in certain aqueous ore-forming solutions: M. A. Thesis, Univ. California, Los Angeles.

Arntson, R. H., Dickson, F. W. and Tunell, G., 1958, Saturation curves of orthorhombic sulfur in the system S-Na_2S-H_2O at 25°C and 50°C: Science, v. 128, p. 716-718.

Brannock, W. W., Fix, Philip F., Gianella, Vincent P., and White, Donald E., 1948, Preliminary geochemical results at Steamboat Springs, Nevada: Am. Geophys. Union Trans., v. 29, p. 211-218.

Cherbuliez, E. and Herzenstein, Anna, 1935, Sur la portée géochimique de l'hydrolyse du soufre par l'eau: Helv. Chim. Acta, v. 19, p. 801-806.

Cherbuliez, E. and Weibel, R., 1936, Sur l'hydrolyse du soufre par l'eau au-dessous de 100°: Helv. Chim. Acta, v. 19, p. 796-801.

Christy, S. B., 1879, Genesis of cinnabar deposits: Am. Jour. Sci., v. 117, p. 453-463.

Clarke, F. W., 1924, The data of geochemistry: U. S. Geol. Survey Bull. 770.

Day, A. L. and Allen, E. T., 1925, The volcanic activity and hot springs of Lassen Peak: Carnegie Inst. Washington, pub. no. 360, p. 115-117.

Dickson, F. W., and Tunell, George, 1955, Geochemical and petrographic aspects of mercury ore deposits: Final report, Office of Naval Research, Contract Nonr 233 (12), Project NR 081-174.

———— 1958, Equilibria of red HgS (cinnabar) and black HgS (metacinnabar) and their saturated solutions in the systems HgS-Na_2S-H_2O and HgS-Na_2S-Na_2O-H_2O from 25°C to 75°C at 1 atmosphere pressure: Am. Jour. Sci., v. 256, p. 654-679.

Dickson, F. W., Tunell, G., Lawrence, E. F., and Horton, R., 1957, Deposition of mercuric sulfide at Amedee Hot Springs, California (Abstract): Geol. Soc. America Bull., v. 68, p. 1822.

Dryer, R. M., 1940, Geochemistry of quicksilver mineralization: Econ. Geology, v. 35, p. 17-48 and 140-157.

Knox, J., 1906, Zur Kenntis der Ionenbildung des Schwefels und der Komplexionen des Quecksilbers: Zeitschr. für Electrochemie, v. 12, p. 477-481.

Krauskopf, Konrad B., 1951, Physical chemistry of quicksilver transportation in vein fluids: Econ. Geology, v. 46, p. 498-523.

Lindgren, Waldemar, 1933, Mineral deposits, 4th ed.: New York, McGraw-Hill Book Co.

Mellor, J. W., 1930, A comprehensive treatise on inorganic and theoretical chemistry, v. 10, S. Se: New York, Longmans, Green and Co.

[American Journal of Science, Vol. 258, October 1960, P. 583-604]

ARGON DIFFUSION IN GLAUCONITE, MICROCLINE, SANIDINE, LEUCITE AND PHLOGOPITE*

J. F. EVERNDEN, G. H. CURTIS, R. W. KISTLER, and J. OBRADOVICH

Department of Geology, University of California, Berkeley

ABSTRACT. Data on the diffusion of argon in sanidine, microline, phlogopite, glauconite, and leucite are presented. We conclude from these data that:

(1) Dynamic lattice changes markedly influence argon loss at the time of the changes:
(2) If argon diffusion takes place under conditions of no lattice changes, all argon will be lost at a single activation energy;
(3) Glauconite and phlogopite have essentially identical diffusion characteristics;
(4) The parameters of the diffusion equations for both feldspar and mica are only explainable on an hypothesis of extreme ordering of the diffusing argon atoms;
(5) Glauconites (and illites), due to their fine grain-size, are susceptible to high argon loss at a temperature of 100° C if that temperature is maintained for a few million years. Thus, knowledge of the burial history of a sample is absolutely essential for each glauconite dated;
(6) Feldspar diffusion appears to be a complex of lattice and grain-boundary diffusion, with the lattice unit having dimensions of 10-30 microns;
(7) Heating a mica of 1 millimeter thickness to 300° C for a few million years should remove all pre-existing argon, thus rendering impossible the dating of events prior to the last heating.

INTRODUCTION

Few data have been published on the diffusion of rare gases through mineral lattices. Work up to 1951 (principally on helium in glass) is discussed in Barrer (1951). Gentner and his associates (1954a, 1954b, 1953) investigated the diffusion of argon and helium in sylvite (reviewed by Curtis and Reynolds, 1958), and in 1957 Reynolds made a comparative study of argon content and argon diffusion in mica and feldspar.

The data obtained in the present study are discussed in three parts:

1. The form of the diffusion curves, log D vs 1000/T, as related to grain characteristics and to changes in lattice structure.
2. A quantitative interpretation of the straight-line portions of the diffusion curves in terms of the theory of absolute reaction rates as applied to diffusion problems.
3. Implications of the log D vs 1000/T curves with respect to the K/A dating of particular minerals.

ACKNOWLEDGMENTS

The authors are grateful to their colleagues J. Verhoogen, J. H. Reynolds, A. Pabst, C. M. Gilbert, and C. Meyer for help and suggestions. Particularly we acknowledge the help of Charles Meyer in conducting the experiments with glauconite under high water vapor pressure and for making D.T.A. runs of glauconite and phlogopite.

SAMPLES AND METHODS

Samples of glauconite from the Domengine formation of California (~45 m.y.), of leucite from a flow at "Cava di Lava dell' Acquacetosa, Italy (~0.8

* Work supported by the U. S. Atomic Energy Commission and the Adolph C. and Mary Sprague Miller Institute for Basic Research in Science.

m.y.), of microcline from a pegmatite at Bedford, Ontario (~1,000 m.y.), sanidine from the Bishop Tuff in Owens Valley, California (~1.0 m.y.), and of phlogopite from a pegmatite at Renfrew, Ontario (~1,000 m.y.), were used for the experiments. The glauconite, taken from a well-core at 4,600 feet, was given to us by the Standard Oil Company of California. The leucite was collected by Evernden with the aid of A. C. Blanc. The microcline and phlogopite were taken from the collection of the Department of Geology at the University of California. The sanidine-bearing samples were collected by us and by members of the U. S. Geological Survey.

Except for the microcline and phlogopite specimens, which were parts of single crystals, the samples were concentrated using bromoform and a Frantz magnetic separator and were sized with Tyler screens. The microcline was prepared by crushing 100 grams of a single crystal to pass a 200 mesh Tyler screen. This crushed sample was then sized in a Haultain infrasizer and 5 grams of the 35 micron fraction were used for the run. The mean diameter of this fraction was determined by measuring a number of grains under a microscope. The two phlogopite samples were prepared by splitting a large book of mica into sheets approximately 5 x 10 cm x 16.5 microns. The thickness was determined by weighing the sheets and measuring the density. These sheets were then cut into two size-fractions, one of 5 grams containing approximately 500 squares 15,000 microns on a side and one of 5 grams containing approximately 25,000 squares 2,000 microns on a side.

The experimental procedure was essentially the same for all but one of the specimens. Each was outgassed for 12-24 hours at 150° C in an evacuated system, following which it was heated in increments of 75° C - 150° C to the fusion point near 1200° C. (See tables for details of heating schedules.) A spike of A^{38} was added at the beginning of each temperature increase which, together with the radiogenic argon released, was collected at the end of the specified period. Contaminating gases were removed with CuO and Ca furnaces in series with N_2 cold traps. Whenever possible, runs were conducted on a continuous basis, with the sample being allowed to cool only during clean-up of the gas on the CuO furnace (20 mins. at 650° C) and transfer of the sample through a valve to the Ca furnace (20 mins.). When the experiments were interrupted, however, and the system allowed to cool, the valve to the sample was closed so that argon released during the shut-down period and succeeding warm-up would be collected with the next increment. The error thus introduced to any increment is very small and is offset by the advantage of collecting the total sample for comparison later with a duplicate sample collected during a single fusion run.

The above procedure was altered for some glauconite. One sample of glauconite was run in the foregoing manner. Another was held at constant temperature in vacuo while cuts were collected at intervals. Four additional samples each weighing approximately one gram were wrapped individually in silver foil and placed in stainless steel bombs. Two of them were subjected to pressures of 1,000 p.s.i. of water vapor and heated at 300° C and 500° C respectively for 24 hours. The two others were placed under pressure of 10,000 p.s.i. H_2O and heated at 400° C and 600° C respectively for 8¼ hours.

The remaining argon was then extracted and purified from each of the samples and the amount lost during heating under pressure was computed by subtraction from the known total amount of radiogenic argon per gram of sample. The specific data obtained from the runs appear in tables.

Owing to variations in grain-shape and assumed direction of argon diffusion, it was necessary to use several mathematical models in the computation of diffusion coefficients. In all cases, it was assumed that argon distribution was uniform throughout the crystal grains at the beginning of heating and that the external argon pressure was maintained at zero. As the gas was being released into a volume very large relative to grain dimensions and was being continuously adsorbed on activated charcoal. this latter assumption is valid.

The models become standard diffusion problems with particularly simple initial and boundary conditions. In the cases of leucite and feldspar, we assumed radial diffusion in spherical grains, the diameter being the mean of that of the size-range used. For biotite, we entertained two possible diffusion models. Where diffusion was assumed to be parallel to cleavage, the mathematical model used was radial diffusion in a very long cylinder. Where diffusion was assumed to be perpendicular to cleavage, the mathematical model used was diffusion in a plane sheet. The formulas appropriate to the solution of all of these problems are given in detail by Crank (1900). The formulas and graphs there given are expressed in terms of fraction of total diffusing material lost as a function of diffusion coefficient (D) and time (t). D and t appear only as their product, so fraction lost (f) is really expressed as a function of the single variable (Dt). As an example of the computation procedure, consider the formula (6.22) (Crank, 1900, p. 87) for small losses from spherical grains, and consider that n increments of argon are obtained within the range of argon loss for which this formula is valid. If subscripts indicate the time sequence of obtained increments,

$f_1 = 6\pi^{-\frac{1}{2}}a^{-1}(D_1t_1)^{\frac{1}{2}}$ (retaining only the first term for illustrative purposes)
Solve for D_1 with f_1 and t_1 known.

$f_1 + f_2 = 6\pi^{-\frac{1}{2}}a^{-1}(D_1t_1 + D_2t_2)^{\frac{1}{2}}$
Solve for D_2 with f_1, f_2, D_1, t_1, and t_2 known.

$\sum_1^n f_i = 6\pi^{-\frac{1}{2}}a^{-1}(\sum_1^n D_it_i)^{\frac{1}{2}}$ Solve for D_n with $\sum_1^n f_i$, $\sum_1^{n-1} D_it_i$, and t_n known.

When the losses become such that this particular formula is no longer valid, the same approach can be used when using graphs such as figure 6.4, page 90. The fraction of argon lost at a given value of (Dt) is only determined after total release of argon from the sample.

DISCUSSION

The form of the log D vs 1000/T°K curves as related to grain characteristics and changes in lattice structure.—One of the principal conclusions of this study is that the exact form of curved parts of the plots of $\log_{10}$ D vs 1000/T°K is a function of the changes in the crystal lattice induced by the varying physical conditions during heating. The rates of lattice changes are, in part,

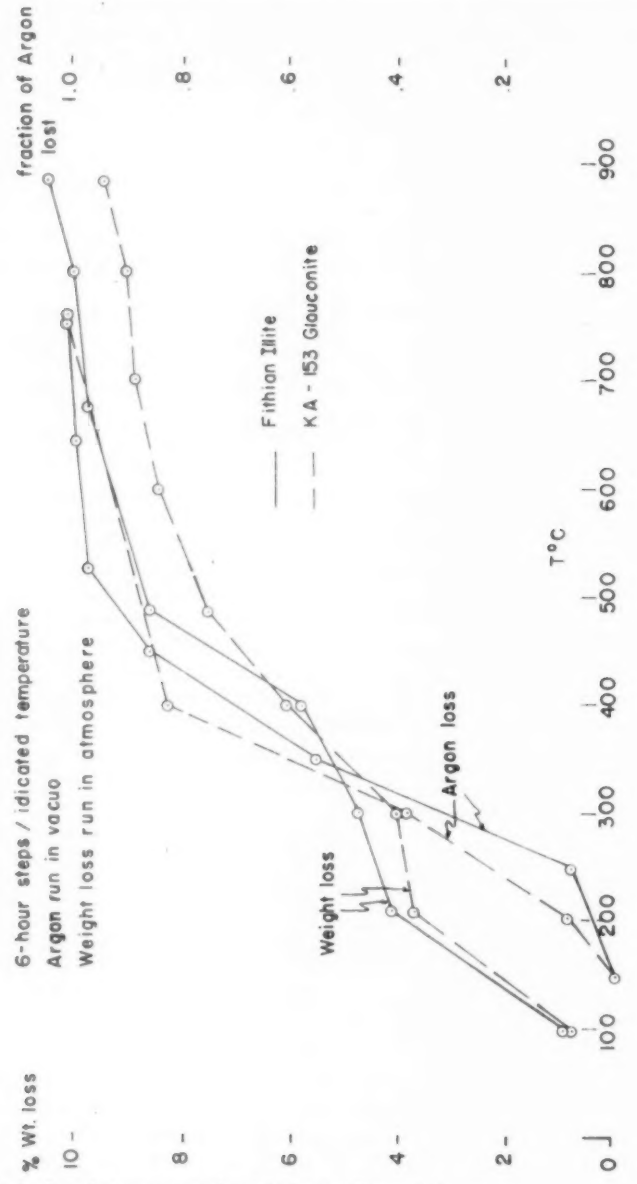

Fig. 1. Cumulative argon and weight loss in illite and glauconite.

functions of rate of heating; therefore, the heating schedule itself controls the form of the diffusion curve within the range of temperatures encompassing the lattice change. Straight-line portions of the curves, however, imply no lattice changes, and different heating schedules probably have little or no effect upon these portions of the curves. Because loss of hydroxyl water from certain minerals such as the clays and micas constitutes a major lattice change, changes in H_2O pressure can also effect the shape of diffusion curves obtained for particular heating schedules. Hydroxyl loss, once initiated, is itself a temperature-dependent diffusion process.

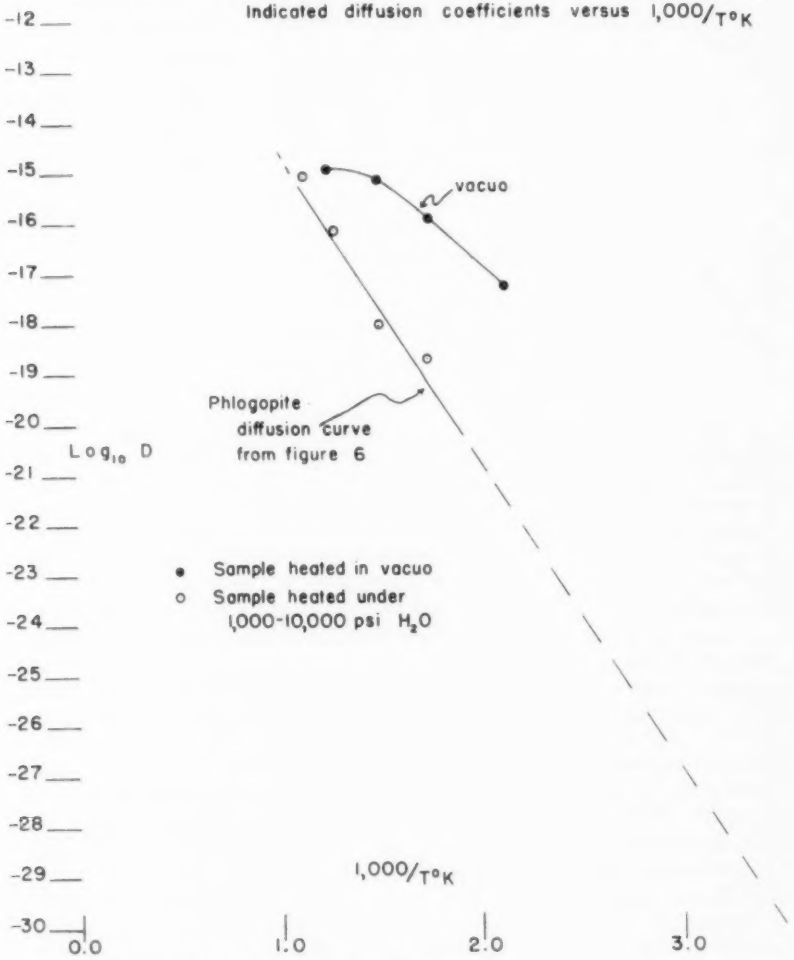

Fig. 2. Argon diffusion in glauconite (K A-153).

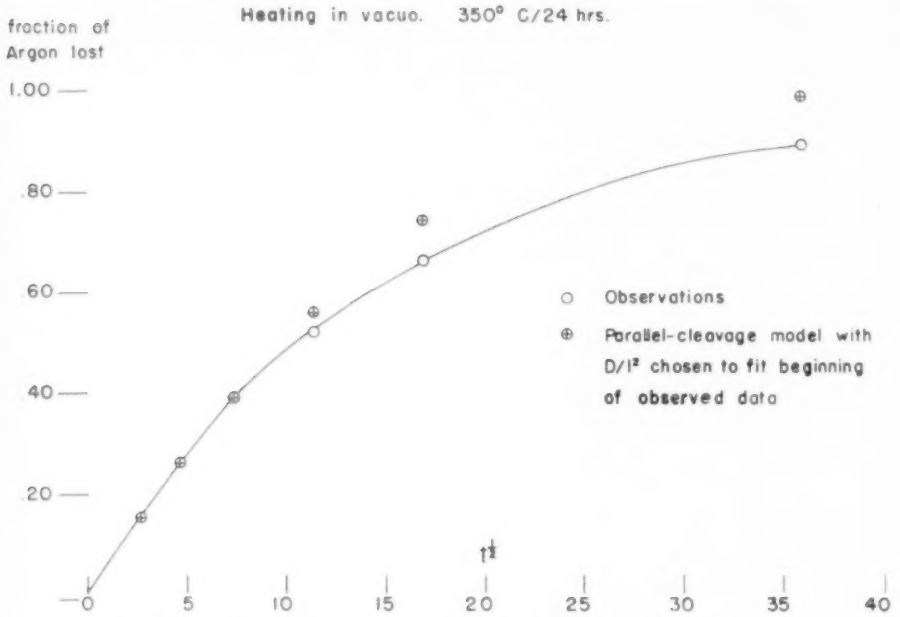

Fig. 3. Argon less as a function of time in glauconite (K A 153-4).

Consider first the experiments on glauconite (table 3). Figure 1 shows that there is a close correlation between hydroxyl water-loss and argon-loss, with water-loss being initiated at about 200° C under the conditions of this experiment. The temperature during these experiments was increased approximately 100° C every 6 hours. A DTA curve of this same material, in which the specimen was heated to 1,000° C in the space of 90 minutes, showed the hydroxyl loss to occur between 550° C and 600° C. Plots of log D vs 1000/T for argon diffusion for these two heating schedules would be very different.

Comparing the glauconite heated in progressive stages with the glauconite kept at constant temperature (see figs. 2 and 3), there is in the former an apparent decrease in the rate of change of the diffusion coefficient above 350° C, whereas in the latter the diffusion coefficient appears to decrease as a function of time. In both cases the decreases in the diffusion coefficients is probably related to the establishment of stable lattice configurations after elimination of most of the hydroxyl water. Owing to the different heating schedules, the hydroxyl water was eliminated at different temperatures.

Argon losses of 3 percent to 97 percent were obtained from the glauconite samples heated under high water vapor pressure. The data plot on a straight line (fig. 2) having the same slope as the phlogopite diffusion curve in the same temperature range, indicating that total argon loss for glauconite can be achieved at a single activation energy. The rate of argon loss and thus

the diffusion coefficients are significantly less than those obtained for the glauconite heated in vacuo. Thus, it is clear that when glauconite is heated under conditions barring hydroxyl loss, the diffusion coefficients follow closely an exp(−a/T) law, implying stability of lattice and a necessarily greater energizing of argon atoms by heating for a given diffusion rate. It will be noted also that there is no tendency for the slope of the log D vs 1000/T curve to decrease at high temperatures or at high argon loss, again illustrating that the abnormal behaviour of the diffusion curve obtained in vacuo is a function of lattice changes independent of argon diffusion.

Although the samples of glauconite are in the form of pellets, a thin-section of the pellets mounted in canada balsam shows that they are not single crystals but aggregates of very small crystals. It was not possible to measure directly the size of the crystals in these aggregates, but an estimate of their size was obtained by comparing their water-loss and argon-loss curves with those of Fithian illite, of which Grim (1953) has measured the size with an electron microscope. The two sets of curves are so similar, and the crystal lattices are so similar, there can be little doubt that the true sizes of the individual crystals are approximately the same and that the diffusion unit is the crystal grain, not the pellet of glauconite. Comparison of the glauconite and phlogopite data brings out the significant point that the activation energy for argon diffusion in glauconite under conditions of no water-loss is identical to that for phlogopite under similar conditions. The D_0 value is probably similar but as the exact dimensions of the glauconite grains are not known, this cannot be confirmed. The dimensions used for glauconite, 1 micron wide and 0.1 micron thick, are probably within an order of magnitude of the correct value.

Further evidence of the relation between crystal change and accelerated argon loss is afforded by data from leucite (table 4). Almost complete elimination of radiogenic argon was achieved at 550° C in one to two days, a remarkably short time. The data indicate that $D_{490} = 7.47 \times 10^{-11}$ while $D_{550} = 6.30 \times 10^{-10}$. Interpretations of these data on the basis of the formula $D = D_0 \exp(-E/RT)$ yields an $E = 44{,}200$ cal/mole and $D_0 = 330$ cm^2/sec which indicates a $D_{0°C}$ of 10^{-33} cm^2/sec. All of our other results suggest that these values are meaningless in terms of argon diffusion in a static leucite lattice. As is well known, however, the temperature range in which these data were obtained is the range in which leucite undergoes a second-order λ transition from a pseudoisometric structure to a true isometric habit. Figure 4 shows the character of this transformation with the change taking place over the temperature range 300° C — 603° C. Figure 4 indicates that electrical conductance behaves similarly to argon diffusion, indicating an increased ease of mass transport through the lattice during the period of recrystallization.

The form of the diffusion curve obtained for microcline from Bedford, Ontario, is now readily explained (see table 1 and fig. 5). This is pegmatitic feldspar containing 11.0 percent potassium and 1.6 percent sodium. We can reasonably expect it to be an intergrowth of two alkali feldspars and to have low-temperature triclinic crystal habit. The transformation from a two-feldspar intergrowth to a single homogeneous feldspar is a function of sodium content,

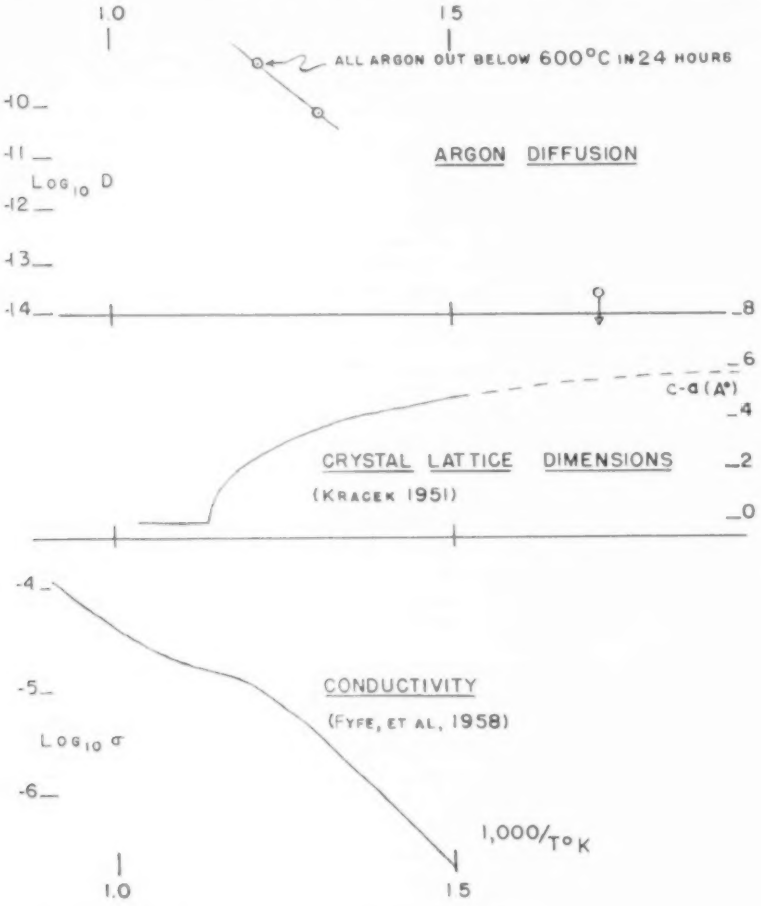

Fig. 4. Leucite characteristics as a function of temperature.

and in a highly potassic feldspar the equilibrium temperature is 400 – 500° C (Smith and Mackenzie, 1958). This is a sluggish reaction, however, and in order for it to go to completion in a short time, the temperature must be taken well above the equilibrium temperature. A second transformation, triclinic-to-monoclinic, is initiated above 1,000° C. The Bishop Tuff sanidine, used for the other feldspar diffusion runs, is a high-temperature feldspar of monoclinic crystal habit and homogeneous one-feldspar characteristics. Thus, if the argon diffusion curves are influenced by lattice changes, we should expect the microcline curve to show anomalous features that can be correlated with the two possible lattice adjustments, and we should expect the sanidine

diffusion curve to show no such features. The data confirm this expectation (fig. 5). The microcline curve shows an abnormal rate of rise above 450° C, flattens, and indicates decreased values of D in the range 690° – 850° C. It then rises on a slope about equal to the low-temperature portion of the curve

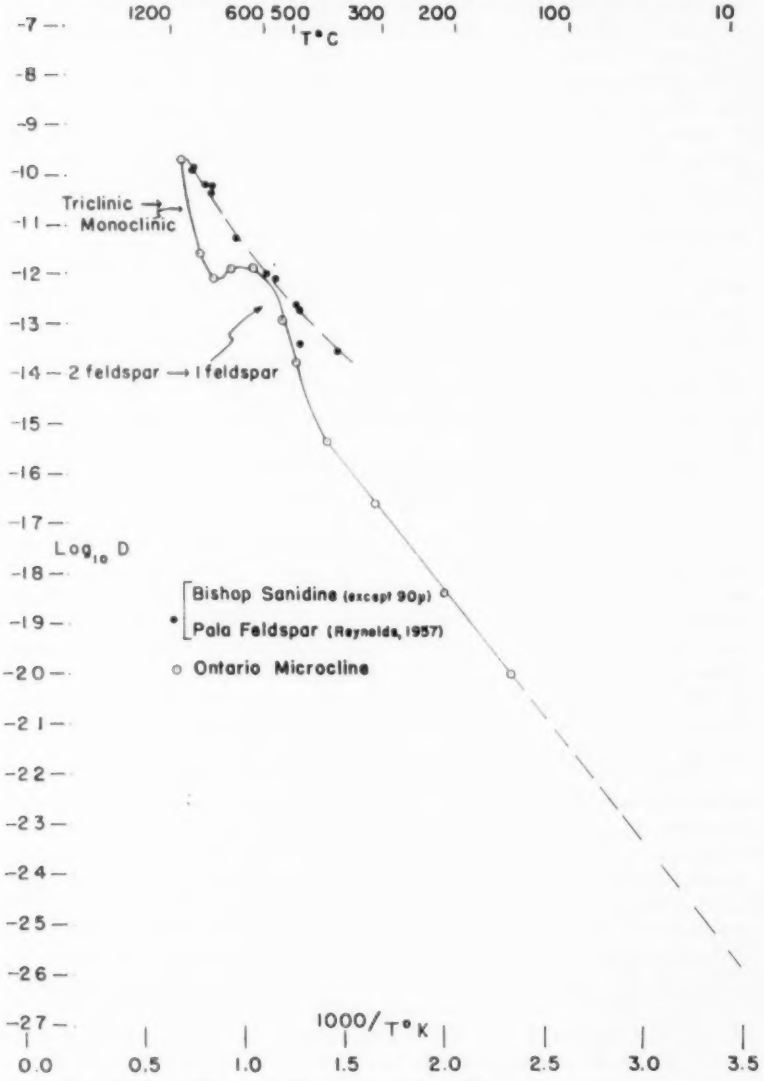

Fig. 5. Feldspar diffusion coefficient versus 1000/T°K.

and, in the neighborhood of 1,000° C, rises sharply again. The sanidine data show neither of these upward excursions of the diffusion curve, yielding simply a slightly convex line throughout the temperature range 500° – 1,050° C. The irregularities of argon diffusion rates in microcline are initiated at temperatures that coincide roughly with those at which lattice changes occur and are probably produced by the lattice adjustments. During the transformation from two feldspars to one homogeneous feldspar beginning at about 450° C argon diffusion rates increase. After the transformation has been completed, the diffusion coefficients return to a value virtually that expected on the basis of extrapolating the low-temperature straight-line portion of the curve, implying that the diffusion characteristics of the homogeneous feldspar are similar to those of the two-phase feldspar. The sharp rise in diffusion rate above 1,000° C is correlated with the initiation of the triclinic-monoclinic transformation.

The data obtained by Reynolds (1957) on a perthitic microcline were, unfortunately, not selected so as to bring out the relationships considered here. The high-temperature triclinic-monoclinic transformation was not observed because Reynolds used grain sizes and a heating schedule such that all argon was removed from his samples at 930° C and he made no run at a higher temperature. His temperature steps from 600° C to 930° C in both runs were such as would probably prevent observation of the phase transformation from two to one feldspar.

Our conclusion is that the irregularities of the feldspar curve are due to lattice changes and that the exact form of the log D vs 1,000/T plot is a function of the heating schedule.

Finally, we consider the phlogopite data with respect to lattice changes and argon diffusion (table 2). These data were obtained from two different size-fractions of the same phlogopite. The two samples, as described above, consisted of particles of the same thickness but of different diameter-to-thickness ratio, approximately 1,000/1 and 100/1. Our intention was to compute diffusion coefficients for the two runs using two different diffusion models, one parallel to cleavage, the other perpendicular to cleavage. The proper model should yield similar diffusion coefficients for both biotite samples, while the improper model should yield markedly different diffusion coefficients.

Figures 6 and 7 show the plots based upon both diffusion models. These results suggest that we observed diffusion perpendicular to cleavage at low temperatures, diffusion probably parallel to cleavage at intermediate temperatures, and diffusion perpendicular to cleavage at high temperatures. The point of initiation of diffusion parallel to cleavage is correlated with the sharp break in the diffusion curves at 600° – 670° C. Our interpretation is that, having exceeded the equilibrium temperature for phlogopite at low pressure, lattice destruction was initiated with expulsion of water, probably with separation of layers and consequent rise in the diffusion rate parallel to cleavage. At high temperatures, after removal of most of the water, the remaining material established a new lattice with consequent return to diffusion loss dominantly parallel to the short dimension of the particles, i.e., normal to cleavage, and to an activation energy comparable to that of the low-temperature portion of

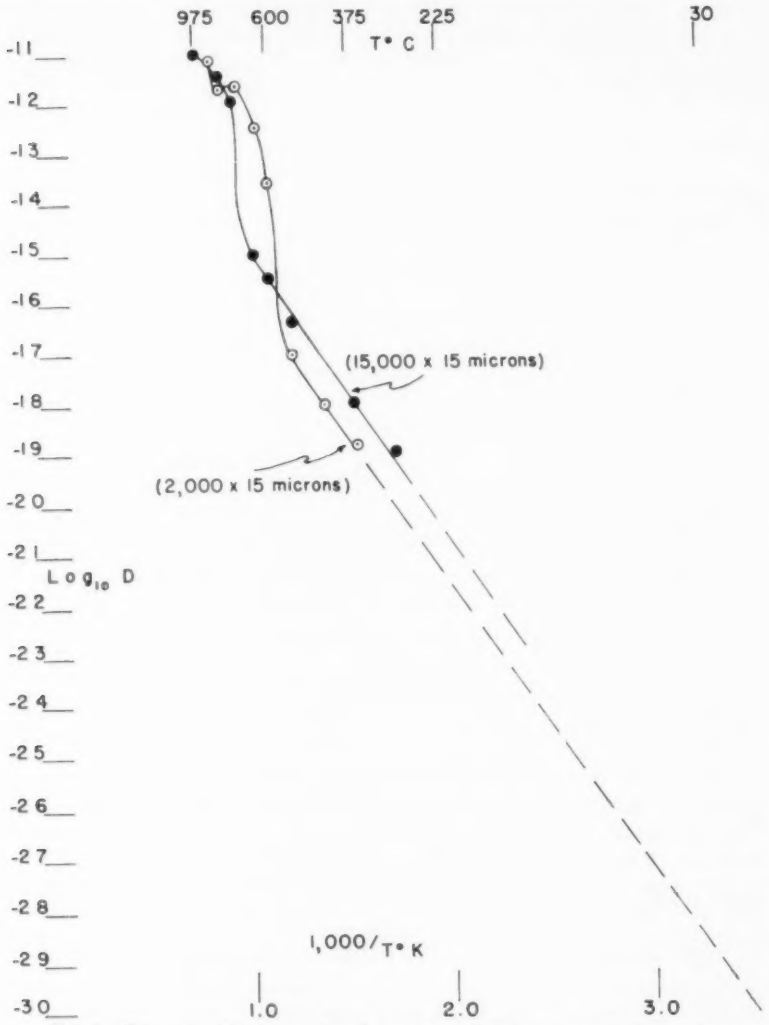

Fig. 6. Phlogopite diffusion curves. Assumption: diffusion perpendicular to cleavage.

the curve. It should be noted that if our interpretation is correct, slight changes in the heating schedule will alter the shape of the diffusion curve radically in the range of active water-loss; therefore, little significance should be given to the actual slope of the diffusion curve in this range.

The comparative behavior of phlogopite and glauconite should be noted, for both are mica-type lattices. Glauconite, probably because of its small

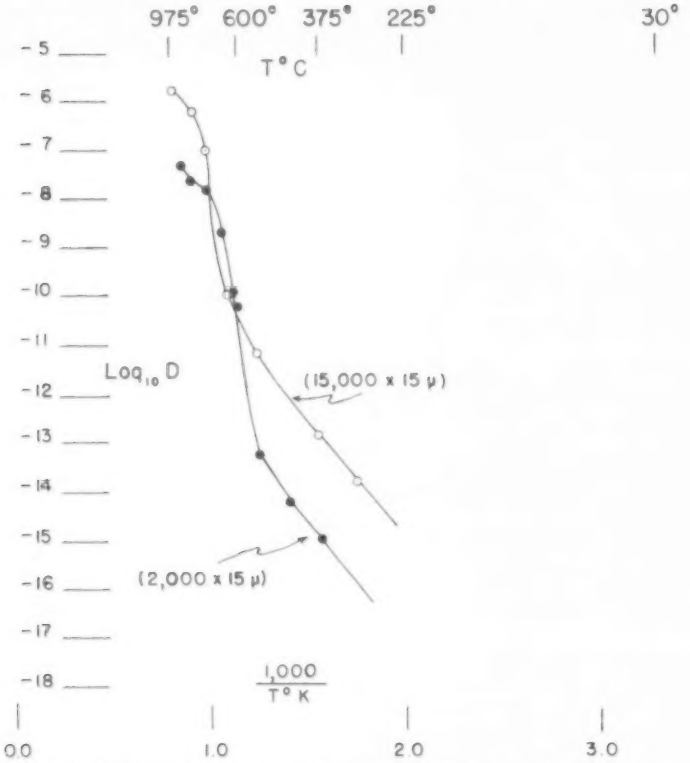

Fig. 7. Phlogopite diffusion curves. Assumption: diffusion parallel to cleavage.

grain-size, lost all of its argon in the low-temperature portion of the curve. That the biotite lost only one percent of its argon in this portion of the curve need not be interpreted as a measure of the amount of argon available in a certain lattice position but simply as the result of large grain-size and short time of heating. The glauconite results prove that all argon can be lost from a mica-type lattice at a single activation energy.

We conclude for phlogopite as for the other minerals tested that the irregularities of the diffusion curve are manifestations of dynamic lattice change. They are not to be considered as indications of argon atoms in several lattice positions of different activation energies.

Quantitative interpretation of the straight-line portions of the diffusion curves in terms of the theory of absolute reaction rates as applied to diffusion problems.—The two different plots of the Renfrew phlogopite data show that the low-temperature portion of the curve must be interpreted in terms of diffusion perpendicular to cleavage. Thus, we must assume movement of argon atoms from a position of low potential energy in a potassium site across a high

potential energy barrier (movement through the octahedral layer) to another position of low potential energy in another potassium-type site. The pertinent diffusion equation is then $D = D_0 \exp(-E/RT)$ where $D_0 = 10^{-8}$ cm²/sec and $E = 28{,}000$ cal/mole. The diffusion coefficient will be of the general form $D = \lambda^2 k\sigma$ where

λ = distance between positions of low potential energy = 10 A° in mica
k = specific reaction rate (see below)
σ = probability that there will be two lattice holes in series (octahedral and potassium layers). A consideration of this problem suggests a value between 1/10 and 1/100. We shall use 1/30.

We shall consider Eyring's transmission coefficient as equal to 1. The specific reaction rate may be written as

$$k = \frac{F\ddagger'}{F}\left(\frac{KT}{2\pi m^*}\right)^{1/2}\frac{1}{\delta}\, e^{-E_0/RT} \qquad \text{(Eyring, et al., 1941, p. 188)} \qquad (A)$$

where $F\ddagger'$ = the complete partition function for the activated state
F = the complete partition function for the inactivated state
K = Boltzman's constant = 1.38×10^{-16} erg/deg
T = temperature in degrees Kelvin
m^* = effective mass of an argon atom in the direction of diffusion = $40 \times 1.66 \times 10^{-24}$ gram
δ = width of the top of the potential energy surface, assumed here to to be of the order of 1 A° or 10^{-8} cm.
E_0 = difference between the zero-level energy per mole of the activated atoms and the inactivated atoms.
R = the gas constant = 1.986 cal_{15}/deg/mole

$$\text{or} \quad k = \left(\frac{KT}{2\pi m^*}\right)^{1/2}\frac{K_c}{\delta} \qquad (B)$$

where $K_c = \frac{F\ddagger'}{F}\, e^{-E_0/RT} = \exp(-\Delta F\ddagger/RT)$ (op. cit., p. 195)

$= \exp 1 - E_{exp}/RT)\ \exp(\Delta S\ddagger/R)$ (op. cit., p. 199)
= equilibrium constant for diffusion system

where $\Delta F\ddagger$ = standard free energy change of activation, the quantity determining the rate of diffusion
E_{exp} = "experimental activation energy", i.e., the value obtained from the slope of the log D vs 1000/T plot
$E_{exp} = E_0 - Nh/2\nu = E_0$ for an argon atom
$\Delta S\ddagger$ = entropy of activation

Consider D in the form

$$D = \lambda^2\sigma\frac{F\ddagger'}{F}\left(\frac{KT}{2\pi m^*}\right)^{1/2}\frac{1}{\delta}\, e^{-E_0/RT}$$

In Eyring's standard development, it is considered that $\frac{(2\pi m^* KT)^{1/2}}{h}\delta = 1$

so that $D = \lambda^2\sigma\frac{F\ddagger'}{F}\left(\frac{KT}{h}\right)e^{-E_0/RT}$

It must be noted that the significance of the equality used above is concerned with the expression for translational degrees of freedom. From Eyring (op. cit.),

$$f\ddagger_{tr(1)} = \frac{(2\pi m^* KT)^{1/2}}{h}\delta \qquad \text{(p. 189)} \qquad \text{(C)}$$

if $F\ddagger'$ is written as $F\ddagger f\ddagger_{tr(1)}$

$$D = \frac{KT}{h}\frac{F\ddagger}{F}e^{-E_0/RT} \qquad \text{(D)}$$

and if $\frac{(2\pi m^* KT)^{1/2}\delta}{h} = 1$, $F\ddagger = F\ddagger'$ in value, and K_c is, in value, equal to

$$\frac{F\ddagger}{F}e^{-E_0/RT}$$

Eyring argues (op. cit., p. 189) that since the combination of equations (A, C) leads to an expression independent of δ, there is no restriction on its magnitude. In equation (D) this is true, but an inspection of equation (B) shows that the value of chosen does have an effect on the values of $\Delta S\ddagger$ and $\Delta F\ddagger$. Eyring argues that δ is approximately 10^{-8} for $f\ddagger'_{tr(1)} = 1$. This depends upon the values of m^* and T. If $m^* = 40 \times 1.66 \times 10^{-24}$ and $T = 900°$ K, $\delta = 10^{-9}$ cm for $f\ddagger'_{tr(1)} = 1$, a value probably too low. If δ is chosen as approximately 10^{-8}, $f\ddagger_{tr(1)} = 10$ and $F\ddagger' = 10\ F\ddagger$, and we must then write

$$\left(\frac{KT}{2\pi m^*}\right)^{1/2}\frac{1}{\delta} = \left(\frac{KT}{h}\right)10^{-1}, \text{ etc.}$$

and $K_c \neq K\ddagger$ but must be used in the form $\frac{F\ddagger'}{F}e^{-E_0/RT}$.

The pertinent thermodynamic equation for D is then

$$D = \lambda^2\sigma\left(\frac{KT}{h}\right)10^{-1}e^{-\Delta F\ddagger/RT}$$

Now, in using these equations, we attempt to explain the observed quantitative aspects of the diffusion curve in terms of reasonable assumptions applied to reaction rate theory. The immediate problem is the value of $D_0 = 10^{-8}$.

This is an abnormally small value and an attempt must be made to understand its significance. To this end, we consider the following postulates as being valid descriptions of an argon atom in the inactivated and activated states:

(i) in the inactivated state, $F = \frac{(2\pi m^* KT)^{3/2}}{h^3}v$

i.e., the partition function of this state is described by terms for three degrees of translational freedom where v = volume available to an isolated argon atom in the inactive state, this volume being estimated as 40×10^{-24} cm^3.

(ii) in the activated state, $F_{\ddagger}' = \dfrac{(2\pi m^* KT)^{1/2}}{h} \delta$

i.e., the partition function of this state is described by a term for one degree of translational freedom. Thus, we are hypothesizing that an argon atom in the activated state is so constrained that it has freedom of movement only in the direction of diffusion.

If we set $\lambda = 10A^\circ = 10^{-7}$ cm, $\sigma = 1/30$, then $D_o =$

$$\frac{h^2 v}{(2\pi m^*)^{3/2}(KT)^{1/2}} \times \frac{10^{-15}}{3}$$

$= 6 \times 10^{-8}$cm^2/sec, a D_o value nearly equal to that actually observed. A hypothesis of such high ordering of the argon atoms in the activated state must imply a large negative entropy. Using the thermodynamic form of the diffusion equation, such a negative value is obtained.

$$6 \times 10^{-8} = \frac{10^{-14}}{30} e^{1+\Delta S_{\ddagger}/R} \left(\frac{KT}{h}\right) 10^{-1}$$

$\Delta S_{\ddagger} = -22$ cal.

$\Delta F_{\ddagger} = \Delta H_{\ddagger} - T\Delta S_{\ddagger} = 46{,}000$ cal/mole

The D_o and $E_{exp} = E_o$ values for the microcline diffusion are

$D_o = 5.3 \times 10^{-9}$ cm^2/sec

$E_o = 23{,}000$ cal/mole

If we apply the same analysis to the microcline as was applied to the phlogopite, we must use $v = 60 \times 10^{-24}$ cm^3, $\lambda^2 = 50 \times 10^{-16}$, $\sigma = 1/6$, and it is apparent that we must again assume essentially total loss of two degrees of freedom in the activated state in order to explain the observed value of D_o. Making this assumption, we obtain $\Delta S_{\ddagger} = -27$ cal, $\Delta F_{\ddagger} = 45{,}700$ cal/mole.

It is obvious that the diffusion coefficients presented for feldspar in no way explain the general observation that feldspar crystals are unsatisfactory for K/A age-dating purposes because of incomplete retention of radiogenic argon. Discussion of this important point occurs in the following section of this paper.

It is significant that the observed values of D_o for the diffusion of helium in silica glass are in the range 10^{-5} ($D = 10^{-5} \exp(-10100/RT)$). Analysis along the lines outlined above (using m^* = mass of helium atom, and $T = 900^\circ$ K) suggests either that $\sigma = 1/900$, which seems doubtful, or that the extreme ordering displayed in argon diffusion is not quite achieved in the diffusion of helium in silica glass. The implied values of $\Delta S_{\ddagger}$ and $\Delta F_{\ddagger}$ for helium diffusion in glass are

$$10^{-5} = \frac{10^{-14}}{30} e^{1+\Delta S_{\ddagger}/R} \left(\frac{KT}{h}\right) \quad (3) \qquad \text{so } \Delta S_{\ddagger} = -20 \text{ cal}$$

$\Delta F_{\ddagger} = 26{,}000$ cal/mole.

Implications of the log D vs 1000/T curves with respect to the K/A dating of particular minerals.—The processes of diffusion discussed have an important bearing both on the application of the K/A method to geologic problems and on the technique itself.

First, what is the probable form of the log D vs 1000/T curves at temperatures below those reached by our experiments and above 0° C? In the case of the glauconite-phlogopite curve, it seems certain that straight-line extrapolation of the low-temperature portion of the curve of figure 6 yields nearly the correct values of D for these materials. The independence of the experimentally determined values of D of grain size and the dependence of D upon water-loss suggest that there is no causative phenomenon which would lead to argon loss at rates greater than those obtained by the extrapolation

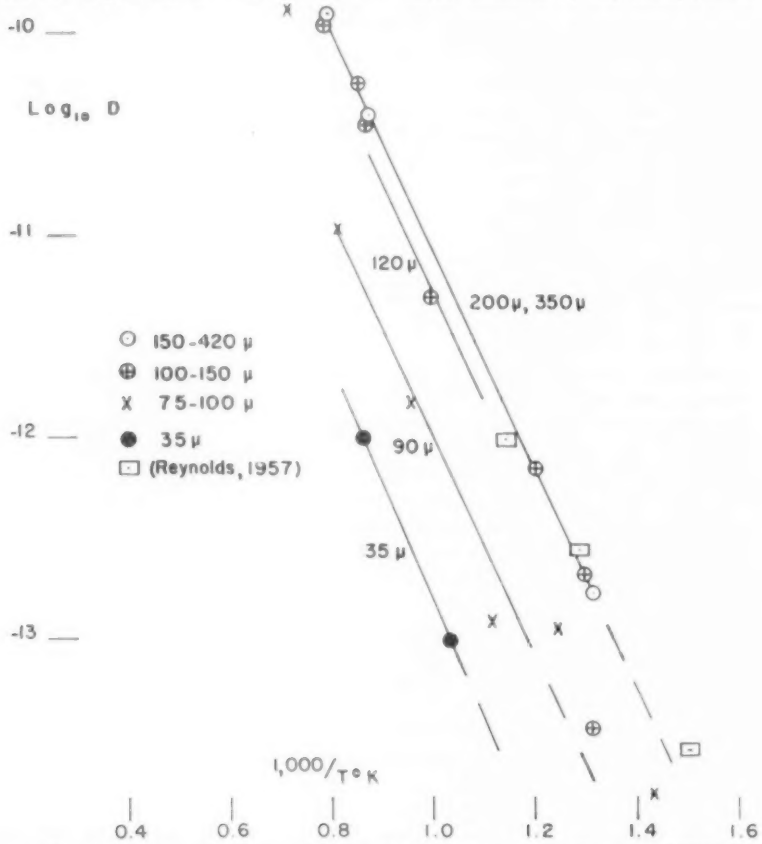

Fig. 8. Feldspar diffusion coefficients. Value of D as a function of 1000/T°K and grain size.

Run procedure: successive cuts on sample heated in vacuo.

shown on figure 6. Further, data obtained from glauconite suggest that values of D as low as those indicated by the straight-line extrapolation are required to explain the observed retentivity of glauconite. For example, a determined age of 490 m.y. for a shallowly buried lower Middle Cambrian glauconite suggests an argon retentivity of at least 90 per cent for the glauconite. Such retentivity requires that $D = 10^{-29}$ cm^2/sec. If the retentivity were greater, even smaller values of D would be required.

In the case of potassium feldspar, the situation is grossly different. There seems to be an obvious correlation between grain size of sample and determined value of D. Figure 8 is a composite plot of all available log D vs 1000/T data against respective grain diameters. (We note here that in Reynolds' paper (1957), the lowest point on the feldspar curve, fig. 2, p. 182, was misplotted.) A detailed evaluation of these data is not possible as we do not have sufficient correlative data on size distribution in each of the samples; however, we interpret the apparent decrease of diffusion coefficient with decreasing grain size to mean that the significant dimension for lattice diffusion in feldspar is at least as small as the finest material used and is probably in the range of 10-30 microns. The high per cent losses observed in coarse-grained material are thus due to grain-boundary diffusion taking place in a matrix of sub-units of these dimensions composing the coarser grains. The D value of this grain-boundary diffusion is uncertain, but the spacing of the lines on figure 8 suggest that it is high. For coarse grains, then, a plot of log D vs 1000/T should show a definite knee in the curve at some temperature below that reached in our experiments.

To illustrate the above hypothesis let us assume the significant diffusion diameter of feldspar sub-units to be 35 microns, the diffusion value to be 10^{-24} cm^2/sec (sample at 55°-60° C or equivalent to 2500-3000 feet depth and using straight-line extrapolation of data for 35 micron diameter microcline), and the grain boundary diffusion coefficient to be essentially infinite. Such material will lose one-third of its argon in 10^9 years.

Extrapolated low-temperature values of D of figure 2 show that the conditions for argon retentivity in glauconite are limited. This is due to the extremely fine size of the individual grains composing glauconite pellets. Computations based upon the curve of figure 2 indicate that for glauconite grains 0.1 micron thick, the fraction of argon lost in 10 m.y. will be 0.004 at 20° C, 0.04 at 50° C, and 0.4 at 100° C. Such temperatures occur at depths of several thousand feet, and the implication is strong that deeply buried glauconite will be useless for K/A age-determinations. Support for this conclusion is provided by a set of samples taken from the same stratigraphic horizon, but from different depths, in the San Joaquin Valley, California. The sample localities are listed in table 5. The depths listed are the present depths of the bed at the sample localities. As the San Joaquin Valley has been subsiding since sometime in the Cretaceous, it is reasonably sure that the present order of depth of these samples is also the order of maximum depth reached by these samples. The period of time that each sample remained at a particular depth is uncertain, and no attempt has been made to reconstruct the burial history of each sample. The correlation of core-depth and indicated

age confirms nicely the general prediction of the diffusion data. It is thus clear that the burial history of glauconite samples must be evaluated accurately to obtain meaningful K/A dates.

For phlogopite, we again inspect the predictions of the extrapolated diffusion curve. Assuming the mica grains to be one millimeter thick, the relation between fraction lost (f) and temperature maintained for 100,000 years is as follows: $T = 20°$ C, $f = 4 \times 10^{-6}$; $T = 50°$ C, $f = 4 \times 10^{-5}$; $T = 95°$ C, $f = 4 \times 10^{-4}$; $T = 150°$ C, $f = 4 \times 10^{-3}$; $T = 225°$ C, $f = 4 \times 10^{-2}$; $T = 320°$ C, $f = 0.4$. The fraction lost is directly proportional to the square root of the time and of the diffusion coefficient and inversely proportional to the significant diffusion dimension.

It is apparent that the conditions imposed upon phlogopite (mica in general?) in order that its retentivity be greater than 95 per cent for 10^8 years are severe. For example, it would seem that regional metamorphism of comparatively low grade (350° C) should destroy the possibility of dating events prior to metamorphism. The tabulation above does suggest that important data on temperatures of magmatic intrusions might be obtained by detailed sampling of mica-bearing country rock, where the mica pre-dates the intrusion. The calculations of Jaeger (1957) suggest that such sampling will have to be done within hundreds and even tens of feet of such contacts, since the maximum temperatures in the country rocks are maintained for such short times.

Regarding the implications of these diffusion data for experimental procedure, there are two points of significance. First, definite limitations are put upon the bake-out temperature for glauconite. The senior author stated in an address published in the Proceedings of the Geological Society of London (Evernden, 1959) that our results indicated no loss of radiogenic argon from glauconite heated in vacuo at 200° C for 12 hours. This statement is in error owing to a miscalculation. There was marked loss at 200° C, but none was detected at 150° C. We now limit our bake-out temperature to 100° C and accept the strong increase in atmospheric argon contamination.

Secondly, the diffusion work on sanidine was initially stimulated by a desire to learn the relationship between loss of radiogenic argon and of atmospheric argon, and to determine the isotopic composition of the "atmospheric argon". Data to be published show that the 40/36 ratio in the low-temperature cuts is identical to that of atmospheric argon and that the atmospheric argon is, in large part, more easily eliminated from a sample than is radiogenic argon. These and other data indicate that "atmospheric argon" is atmospheric argon, i.e., it is argon from the atmosphere adsorbed on and diffusing into the crystal grains in the near-surface environment of the Earth. The environment before collection of the sample determines the degree of elimination of atmospheric argon that can be achieved by heating without serious loss of the radiogenic argon. In a sample of sanidine obtained from a fresh unweathered glass matrix we were able to reduce the atmospheric argon content to 0.4×10^{-11} moles per gram without affecting the radiogenic argon by more than 3-5 percent.

TABLE 1

Argon diffusion in feldspar

Run procedure: successive cuts on sample heated in vacuo

	Cut No.	A_R^{40} moles	A_{At}^{40} moles	$\Sigma(A_R^{40}\%)$	Temp.	Time	D(cm^2/sec)
Bishop Sanidine							
250-420 microns	320 B	0	17.65×10^{-11}	0	430° C		
	320 C	0.51×10^{-11}	4.38	2.35%	490	20 hr	1.7×10^{-13}
	320 D	6.46	6.20	32.1	870	20	4.0×10^{-11}
	320 E	5.72	3.74	58.4	990	19	1.3×10^{-10}
	320 F	9.04	9.21	100	1150	3	1.2×10^{-9}
150-250 microns	321 B	0.36	7.14	1.6	490	20	3.8×10^{-14}
	321 C	1.13	2.68	6.5	560	17	7.8×10^{-13}
	321 D	9.86	6.84	49.6	900	17	6.0×10^{-11}
	321 E	5.20	9.55	72.3	1000	18	1.1×10^{-10}
	321 F	6.35	4.40	100	1170	3	
105-150 microns	328 B	0.2		1.0	450		
	328 C	1.22	4.23	6.9	500	20	2.3×10^{-13}
	328 D	5.08	19.7	31.5	725	20	5.1×10^{-12}
	328 E	8.38	10.4	72.1	880	20	3.6×10^{-11}
	328 F	5.76	18.6	100	1125	2	
75-105 microns	320½ A	0.32		2.6	425	19½	1.7×10^{-14}
	320½ B	0.60		7.5	530	21¼	1.2×10^{-13}
	320½ C	0.37		10.5	625	22	1.2×10^{-13}
	320½ D	2.06		27.4	770	21	1.5×10^{-12}
	320½ E	4.19		61.7	945	24	1.1×10^{-11}
	320½ F	4.69		100	1120	18½	$> 1.3\times10^{-10}$
Microline							
35 micron	402 A	0.95	36.6	.0076	155	44	9.6×10^{-21}
	402 B	6.52	57.8	.059	220	67	3.8×10^{-19}
	402 C	42.1	105.7	.393	325	48	2.3×10^{-17}
	402 D	90.2	22.9	1.11	430	20	4.0×10^{-16}
	402 E	655	17.5	6.30	500	20	1.4×10^{-14}
	402 F	1586	23.8	18.9	550	21	1.1×10^{-13}
	402 G	3573	32.6	48.2	650	19	1.2×10^{-12}
	402 H	1957	26.4	63.7	750	21½	1.1×10^{-12}
	402 I	1575	16.8	75.2	850	20	7.8×10^{-13}
	402 J	1652	12.6	88.3	950	22	2.5×10^{-12}
	402 K	1479	26.9	100	1120	5½	$> 2.0\times10^{-10}$

TABLE 2

Argon diffusion in phlogopite

Run procedure: successive cuts on sample heated in vacuo

Cut No.	A_R^{40} moles	A_{At}^{40} moles	$\Sigma(A_R^{40}\%)$	Temp.	Time	D(cm²/sec) [PERP]α	D(cm²/sec) [PARA]β
			15 x 15,000 microns				
349 A	6.38×10^{-11}	224×10^{-11}	*	150° C	48 hr		
349 B	0	26	0 %	225	48	1.5×10^{-20}	2.5×10^{-15}
349 C	1.60	14	.017	300	24	1.7×10^{-19}	2.8×10^{-14}
349 D	1.85	12	.025	375	12	1.2×10^{-18}	2.0×10^{-13}
349 E	12.7	16	0.12	450	6	6.5×10^{-17}	1.1×10^{-11}
349 F	5.60	49	0.16	525	6	5.6×10^{-17}	9.3×10^{-12}
349 G	27.0	18	0.36	600	6	5.0×10^{-16}	8.4×10^{-11}
349 H	28.3	16	0.56	680	6	9.3×10^{-16}	1.6×10^{-10}
349 I	1622	142	12.4	750	6	7.6×10^{-13}	1.3×10^{-7}
349 J	3191	22	35.6	825	6	5.5×10^{-12}	8.2×10^{-7}
349 K	4154	18	65.9	900	6	1×10^{-11}	4.3×10^{-6}
349 L	2843	17	86.6	975	6	2×10^{-11}	6.8×10^{-6}
349 M	1840	20	100	1250 melt	2		
			15 x 2,000 microns				
349½ A	2.5	28	*	155	48		
349½ B	0	39	0	225	48		
349½ C	0.12	68	.0009	300	47	2.6×10^{-22}	
349½ D	3.04	21	.025	375	47	1.8×10^{-19}	1.1×10^{-13}
349½ E	3.27	18	.050	450	24	1.1×10^{-18}	7.0×10^{-13}
349½ F	11.6	27	.141	525	21	1.2×10^{-17}	7.3×10^{-12}
349½ G	666	45	5.33	600	12	3.3×10^{-16}	1.7×10^{-10}
349½ H	1642	35	18.1	675	10½	4.0×10^{-15}	2.5×10^{-9}
349½ I	2391	16	36.8	750	5¼	2.7×10^{-12}	2.1×10^{-8}
349½ J	1532	19	48.7	825	6	2.4×10^{-12}	3.0×10^{-8}
349½ K	3184	26	73.5	900	6	8.0×10^{-12}	7.3×10^{-8}
349½ L	Final cut lost. Percentages obtained by comparison with run KA 349.						

* Increment of A_R^{40} obtained here considered to be a function of sample preparation and thus ignored.

α Diffusion assumed to be perpendicular to cleavage.

β Diffusion assumed to be parallel to cleavage.

TABLE 3

Argon diffusion in glauconite

Run No.	Cut No.	A_R^{40} moles	A_{At}^{40} moles	$\Sigma(A_R^{40}\%)$	Temp.	Time	D(cm^2/sec) [PERP]
153 C	Run procedure: successive cuts on sample heated in vacuo						
	153C-1	0×10^{-11}	0×10^{-11}	0 %	150° C	6 hr	
	153C-2	9.98	8.4	8.4	200	6	6.4×10^{-18}
	153C-3	36.2	14	38.8	300	6	1.3×10^{-16}
	153C-4	60.0	23	89.2	400	6	8.1×10^{-16}
	153C-5	12.1	8	99.3	525	6	1.3×10^{-15}
	153C-6	0.78	22	100	720	6	
153-5-1	Run procedure: 24 hr/500°C/1000 psi; remaining argon extracted & measured						
	13.4			41.6*	500	24	7.8×10^{-17a}
153-5-2	Run procedure; 24 hr/300°C/1000 psi; remaining argon extracted & measured						
	33.5			96.9*	300	24	2.6×10^{-19a}
153-5-3	Run procedure: 8¼ hr/400°C/10,000 psi; remaining argon extracted & measured						
	32.7			96.2*	400	8¼	9.6×10^{-16a}
153-5-4	Run procedure: 8¼ hr/600°C/10,000 psi; remaining argon extracted & measured						
	2.0			5.8*	600	8¼	$9.1\times^{-19a}$

*percentage of argon retained after treatment specified. The three KA 153 runs listed in Table 5 served as calibration for original argon content of each sample above.

[a] computed on basis of argon lost during treatment specified (i.e., for run 153-5-1, fraction lost = 1 — .416 = .584.

TABLE 4

Argon diffusion in leucite

Run procedure: successive cuts on sample heated in vacuo

	Cut No.	A_R^{40} moles	$\Sigma(A_R^{40}\%)$	Temp.	Time	D(cm^2/sec)
Leucite						
	348 A	0×10^{-11}	0 %	310° C	20 hr	$<3\times10^{-14}$
	348 B	36.1	52.2	490	20	7.5×10^{-11}
	348 C	31.2	97.3	550	20	6.3×10^{-10}
	348 D	1.9	100	675	20	
	348 E	0		1100	20	

TABLE 5

Indicated ages of basal Kreyenhagen cores

Sample No.	Location*	Depth	Indicated Age
KA 267	Sec. 19-T 23S-R 19E	12,175'	20×10^6 years
KA 160	Sec. 14-T 21S-R 14E	10,790	26
KA 265	Sec. 21-T 20S-R 16E	9,200	29
KA 154	Sec. 33-T 16S-R 17E	8,050	38
KA 285	Sec. 10-T 15S-R 17E	6,300	36
KA 153-1	Sec.18-T 20S-R 15E	4,600	44
KA 153-2	"	"	44
KA 153-3	"	"	44
KA 189	Hernandez Valley	Surface	45

*Mt. Diablo B & M

REFERENCES

Barrer, R. M., 1951, Diffusion in and through solids: Cambridge, Cambridge University Press.

Crank, J., 1900, Mathematics of diffusion: New York, Oxford University Press.

Curtis, G. H., and Reynolds, J. H., 1958, Notes on the potassium-argon dating of sedimentary rocks: Geol. Soc. America Bull., v. 69, p. 151-160.

Evernden, J. F., 1959, Dating of Tertiary and Pleistocene rocks by the potassium-argon method: Geol. Soc. London Proc., no. 1565, p. 17-19.

Eyring, H., Glasstone, S., and Laidler, K. J., 1941, The theory of rate processes: New York, McGraw-Hill Book Co.

Fyfe, W. S., Turner, F. J., and Verhoogen, J., 1958, Metamorphic reactions and metamorphic facies: Geol. Soc. America Mem. 73.

Gentner, W., and Trendelenberg, E., 1954, Experimentelle Untersuchungen über die Diffusion von Helium in Steinsalsen und Sylvinen: Geochim. et Cosmochim. Acta, v. 6, p. 261-267.

Gentner, W., Goebel, K., and Prag, R., 1954, Argonbestimmungen an Kalium-Mineralen III: Geochim. et Cosmochim. Acta, v. 5, p. 124-133.

Gentner, W., Prag, R., and Smits, F., 1953, Argonbestimmungen an Kalium-Mineralen II: Geochim. et Cosmochim. Acta, v. 4, p. 11-20.

Grim, R. E., 1953, Clay mineralogy: New York, McGraw-Hill Book Co.

Jaegar, J. C., 1957, The temperature in the neighborhood of a cooling intrusive sheet: Am. Jour. Sci., v. 255, p. 306-318.

Kracek, F. C., 1951, Phase transformations in one-component silicate systems, Contribution to phase transformations in solids: New York, John Wiley & Sons, p. 257-277.

Reynolds, J. H., 1957, Comparative study of argon content and argon diffusion in mica and feldspar: Geochim. et Cosmochim. Acta, v. 12, p. 177-184.

Smith, J. V. and MacKenzie, W. S., 1958, Alkali feldspars: IV. The cooling history of high-temperature sodium-rich feldspars: Am. Mineralogist, v. 43, p. 872-889.

[American Journal of Science, Vol. 258, October 1960, P. 605-607]

SALT- AND FRESH WATER RELATIONSHIPS IN TWO TERMINAL STREAM BARS

JAMES P. HEATH

Department of Biology, San Jose State College, San Jose, California

ABSTRACT. Salt water even more concentrated than seawater was found in the terminal bars of two California streams. There was evidence of movement of the fresh water beneath this.

INTRODUCTION

The subsurface relationships of fresh and salt waters have been considered in the past primarily from the standpoint of invasion by the salt and generally on a very large scale. For example, the recent work of Perlmutter, Geraghty and Upson (1959) deals with an area of about 200 square miles. The theory of the relationships was dealt with extensively by Hubbert (1940).

The present study was an outgrowth of biological problems involving the movement of fresh water through the terminal bars of two local streams. The results were so in contrast with expectation that the study was pursued to provide the additional geological data.

The sand bars are located at the terminal of Waddell Creek, Santa Cruz County, California (lat. 37° 6′ N, long. 122° 17′ W) and of Scott Creek about five miles southeast. These are fluctuating streams in which the summer flow is greatly reduced (Waddell) or may even cease (Scott). During times of moderate flow, a barrier of sand closes off a lagoon, and surface flow to the sea is lacking. It was in bars of this status that all samples were taken.

METHODS

Early samples were taken at the water table by simply digging a pit to the necessary depth. Samples were analyzed for specific gravity with a Westphal balance but the confusing results suggested a need for greater accuracy. These samples and all later ones were then titrated with silver nitrate and the conversion to salinity made according to the formula of Lyman and Fleming (1940). Later samples were also obtained by the use of an auger welded to the end of a pipe which had about six inches of perforated surface just above the weld. This was used to get one sample from beneath the water table (table 1) but the resistance to turning in the fine sands of Waddell bar prevented the taking of more significant samples of this type. Stations were established at various distances from the lagoon. The last station of each series was located at the upper limit of the wave wash. The low tide existing at the time of each survey was a moderate one, but was sufficient to expose the area of constant drainage from the sand; that is, the area of seepage.

The early study was made in November, 1958 when both streams were holding full lagoons but with the bars intact. The later study of Waddell Creek was done in July, 1959. This was a very dry year and a time of greatly reduced flow. In fact, Scott Creek had completely ceased all flow at this time.

RESULTS

In the interpretation of the results of these studies, two items should be considered: first, the sand of the bar at Waddell Creek is very fine while that of Scott Creek is quite coarse, and second, waves at some high tides break over the bar and carry some salt water into the lagoon of both streams.

The most striking find of 1958 was that in the mid-bar areas the salinity at the surface of the water table was greater than that of the sea. Furthermore, this salinity increased with distance from the lagoon. At Waddell Creek, 90 feet from the lagoon, salinity reached 37.98‰ while sea water was but 35.82‰. Since seepage areas on the seaward side of the bar showed outflow of reduced salinity (26.39‰ at Waddell), the layer of concentrated salt water must remain virtually uninfluenced by deeper flow. Scott Creek bar, even with the coarser sands, also provided a concentration (35.77‰) greater than sea water (35.60‰).

The second item of significance is that, in spite of the evident lack of movement of the surface water of the water table relative to the waters beneath, there is an overall movement of considerable extent. In fact, at Scott Creek it was sufficient actually to reduce the salinity of the sea itself. Waves at the bar showed a salinity of 33.07‰ while waves sampled upwind (upcurrent) showed 35.60‰ salinity.

TABLE 1

Salinities per mil at the water table in the bars of Waddell and Scott Creeks

Distance from lagoon	0′	30′	100′	116′ Seep	Sea at Seep	Sea Upwind
Salinity ‰	8.80	34.81	35.77	35.14	33.07	35.60

SCOTT CREEK, November, 1958

Distance from lagoon	0′	30′	60′	90′	112′ Seep	Sea
Salinity ‰	21.13	35.14	36.91	37.98	26.39	35.82

WADDELL CREEK, November, 1958

Distance from lagoon	0′	50′	50′*	90′	140′	150′ Seep	Sea
Salinity ‰	1.95	2.90	2.21	2.95	34.50	34.30	34.33

* Two feet below water table.

WADDELL CREEK, July, 1959

CONCLUSIONS

There appear to be two conclusions to be drawn from these cases: 1) that in small passages (sand) it is possible for the normal density relationships to be inverted and to remain in this state for some time, and 2) that movement deeper in a water table may have little influence on the movement of water at the surface of that water table.

It seems probable that the concentration of the water in the bar is an evaporative effect but the rate does not appear likely to be high. At the point of greatest concentration at Scott Creek, the water table was nearly six feet below the surface of the bar. This means that the concentrated water must be practically stationary.

One has little basis for applying these conclusions on a larger scale. However, it does seem that the theoretical relationships of salt and fresh water may be controverted by the fact that one is not dealing with water masses but rather with minute units in the interstices of the Earth. If this be so, limitation of fluctuation of water levels may be more significant in the control of salt water invasion than the mere height of the water table.

References

Hubbert, M. K., 1940, The theory of ground-water motion: Jour. Geology, v. 48, p. 785-944.

Lyman, John, and Fleming, R. H., 1940, Composition of sea water: Jour. Marine Research, v. 3, p. 134-146.

Perlmutter, N. M., Geraghty, J. J., and Upson, J. E., 1959, The relation between fresh and salty ground water in southern Nassau and southeastern Queens Counties, Long Island, New York: Econ. Geology, v. 54, p. 416-435.

REVIEWS

The Morphology and Anatomy of American Species of the Genus Psaronius; by JEANNE MORGAN. P. 108. Urbana, 1959 (University of Illinois Press, Illinois Biological Monographs No. 27, paperbound, $3.00; clothbound, $4.00).—The appearance of this monograph of the Paleozoic arborescent fern genus *Psaronius* in the Western Hemisphere fulfills a longstanding need for such a comprehensive study. Although this book is based on extensive American collections, the morphological conclusions are valid for the genus as a whole. Credible answers to some perplexing morphological problems have been presented in this well illustrated monograph. Of interest to all should be the impressive frontispiece, which represents a reconstruction of a *Psaronius* tree, one of the conspicuous members of late Paleozoic landscapes.

THEODORE DELEVORYAS

Principles of Paleobotany, 2nd ed.; by WILLIAM C. DARRAH. P. 295; 63 figs. New York, 1960 (The Ronald Press Company, $6.50).—There is a noticeable improvement in this, a second edition, over the first appearance of *Principles of Paleobotany* in 1939. In the preface, Professor Darrah indicates that "the book is intended as a text in one-semester and one-quarter undergraduate and graduate courses in paleobotany, plant evolution, and phylogeny, and as supplementary reading in courses in plant morphology."

It is possible to organize a paleobotany text in one of various ways, depending upon the audience. This book has introductory chapters on principles, aims, and techniques, followed by chapters on the various groups of fossil plants. Such a presentation is probably the best for the botanical reader. The geologist is also accommodated by interspersed chapters on floras of the Carboniferous, Mesozoic, Upper Cretaceous, and Cenozoic.

The book is a compact one and gives a creditable summary of paleobotanical findings. There are some unfortunate shortcomings, however, which greatly restrict its usefulness and accuracy.

First of all, for a first exposure to paleobotany, it lacks sufficient illustrative material to clarify the descriptions. In fact, many of the descriptions are so terse that a non-specialist would have no idea of the concepts which the author wishes to portray. Furthermore, the quality of illustrations is not consistent. Many are expertly done, while others look crude and hurriedly executed.

A second, and even more serious shortcoming, is the fact that there are very few references to work done in 1950 or after. Paleobotany has made great strides since 1950, and the author, in spite of his intended emphasis on "classic" papers, would suggest that nothing since 1950 is of any great significance.

In spite of this reviewer's reservations, it must be admitted that the book serves a purpose. It is a concise guide to many of the fossil groups for students wishing to know something of fossil plants other than what is included in texts on historical geology or general botany.

THOEDORE DELEVORYAS

VOL. 258 No. 8, 1960

American Journal of Science

OCTOBER 1960

CONTENTS

Regressions of Physical Properties on the Compositions of Clinopyroxenes I. Lattice Constants ..... *Horace Winchell and Robert Tilling* 529

Si-Al Relation in Clinopyroxenes from Igneous Rocks ..... *Ikuo Kushiro* 548

Jadeite-rocks and Glaucophane-schists from Angel Island, San Francisco Bay, California ..... *T. W. Bloxam* 555

Systems S—Na_2O—H_2O and S—H_2O: Application to the Mode of Origin of Natural Alkaline Polysulfide and Thiosulfate Solutions *R. W. Arntson, F. W. Dickson, and George Tunell* 574

Argon Diffusion in Glauconite, Microcline, Sanidine, Leucite and Phlogopite *J. F. Evernden, G. H. Curtis, R. W. Kistler, and J. Obradovich* 583

Salt- and Fresh Water Relationships in Two Terminal Stream Bars *James P. Heath* 605

REVIEWS

The Morphology and Anatomy of American Species of the Genus Psaronius; by Jeanne Morgan ..... *Theodore Delevoryas* 608

Principles of Paleobotany, 2nd ed.; by William C. Darrah ..... *Theodore Delevoryas* 608